(19) Europäisches Patentamt
European Patent Office
Office européen des brevets

(11) EP 0 816 890 A2

(12) EUROPEAN PATENT APPLICATION

(43) Date of publication:
07.01.1998 Bulletin 1998/02

(51) Int. Cl.[6]: **G02B 13/00**

(21) Application number: **97115262.4**

(22) Date of filing: **25.02.1994**

(84) Designated Contracting States:
DE FR GB

(30) Priority: **26.02.1993 JP 38532/93**
18.11.1993 JP 289231/93
18.11.1993 JP 289232/93

(62) Document number(s) of the earlier application(s) in accordance with Art. 76 EPC:
94102915.9 / 0 613 035

(71) Applicant:
FUJI PHOTO FILM CO., LTD.
Kanagawa-ken (JP)

(72) Inventors:
- **Noguchi, Masaru,**
  c/o Fuji Photo Film Co. Ltd.
  Ashigarakami-gun, Kanagawa-ken (JP)
- **Shimada, Katsumi**
  c/o Fuji Photo Film Co., Ltd
  Ashigarakami-gun, Kanagawa-ken (JP)

(74) Representative:
Klunker . Schmitt-Nilson . Hirsch
Winzererstrasse 106
80797 München (DE)

Remarks:
This application was filed on 03 - 09 - 1997 as a divisional application to the application mentioned under INID code 62.

(54) F-theta lens

(57) An fθ lens includes first and second lens groups arranged in this order from the entrance pupil side. The first lens group consists of a first lens having a negative or positive refracting power. The second lens group consists of a second lens having a positive refracting power and a third lens having a negative refracting power with the second and third lenses being cemented together. The second lens group has a positive refracting power as a whole. The following formulae (1) to (4) are satisfied.

$$12 \leqq \nu_{d2} - \nu_{d3} \quad (1)$$

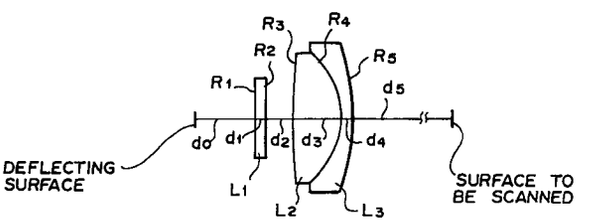
$$-0.035 \leqq \Sigma(\phi_i / \nu_{di}) \leqq 0.005 \quad (2)$$

$$0.7 \leqq \phi_{23} \leqq 2.0 \quad (3)$$

$$0.03 \leqq d_{12} \leqq 0.20 \quad (4)$$

wherein ϕ_i represents the power of i-th lens as numbered from the entrance pupil side standardized on the basis of the power of the whole system, ϕ_{23} represents the power of the second lens group standardized on the basis of the power of the whole system, ν_{di} represents the Abbe's number for the sodium d-line of i-th lens as numbered from the entrance pupil side and d_{12} represents the surface separation between the first and second lens groups standardized on the basis of the focal length of the whole system.

FIG.2A



EP 0 816 890 A2

Description

BACKGROUND OF THE INVENTION

Field of the Invention

This invention relates to an fθ lens for a scanning optical system, and more particularly to an fθ lens suitable for use in a scanning optical system in which a plurality of laser beams having different wavelengths are used.

Description of the Prior Art

Recently there has been put into wide use various instruments such as a laser beam printer in which a laser beam scanning optical system is used. In such an optical system, an fθ lens is used to cause a laser beam, which is deflected by a rotary polygonal mirror or the like, to scan the surface of a medium at a constant speed. The fθ lens is a lens which satisfies a condition that $Y=f\theta$ wherein θ represents the incident angle of the laser beam to the lens, f represents the focal length of the lens and Y represents the height of the image formed.

Conventionally the fθ lens is designed on the assumption that a monochromatic or single wavelength laser beam is used and accordingly the color aberration causes no problem and correction of the color aberration has been unnecessary heretofore.

However, for instance, in a laser recording system in which color images are recorded on silver salt film by use of a plurality of laser beams having different wavelengths, e.g., red, green and blue laser beams, the problem of color aberration must be taken into account. As is well known in the art, the color aberration includes the axial color aberration and the lateral color aberration. The axial color aberration shifts the position of the image in the direction of the optical axis depending on the wavelength and practically does not cause a serious problem since the focal depth of the laser beam is sufficiently large. However, the lateral color aberration causes the position of the image to shift in the direction perpendicular to the optical axis depending on the wavelength, and accordingly, the beam is shifted in the scanning direction by different distance depending on the wavelength, which makes it impossible to precisely superimpose the spots of the respective colors one on another and adversely affects the quality of images.

Though this problem may be overcome by operating the laser beams of the respective colors in different timings, this approach requires complicated control and is not suitable for high-speed scanning.

In Japanese Patent Publication No. 61(1986)-51289, there is disclosed a technique for correcting lateral color aberration. However this technique can correct lateral color aberration only by a wavelength of 20nm and is originally developed to correct color aberration due to fluctuation in wavelength of a semiconductor laser. Accordingly it cannot be applied to a multiple wavelength scanning optical system for color image recording.

An fθ lens disclosed in Japanese Unexamined Patent Publication No. 62(1987)-262812 can correct the lateral color aberration for two or more laser beams with a high accuracy under predetermined conditions. However the fθ lens comprises four elements in three lens groups. When the number of lens elements is large, the manufacturing cost increases, and at the same time, errors in processing the lens elements and assembly of the same can accumulate. Further in order to satisfy the disclosed conditions, the material for the lens elements must be selected within a narrow range.

SUMMARY OF THE INVENTION

In view of the foregoing observations and description, the primary object of the present invention is to provide an fθ lens which can correct the color aberration with a high accuracy over a wide wavelength range, and coisists of a small number of lens elements to permit reduction of the size of the optical system, the manufacturing cost and the error in assembly.

In accordance with a first aspect of the present invention, there is provided an fθ lens comprising a first lens group which consists of a first lens having a negative or positive refracting power, and a second lens group which consists of a second lens having a positive refracting power and a third lens having a negative refracting power, the second and third lenses being cemented together, the second lens group having a positive refracting power as a whole, and the first and second lens groups being arranged in this order from the entrance pupil (deflecting surface) side and satisfying the following formulae (1) to (4),

$$12 \leqq \nu_{d2} - \nu_{d3} \tag{1}$$

$$-0.035 \leqq \Sigma(\phi_i/\nu_{di}) \leqq 0.005 \tag{2}$$

$$0.7 \leqq \phi_{23} \leqq 2.0 \quad (3)$$

$$0.03 \leqq d_{12} \leqq 0.20 \quad (4)$$

wherein ϕ_i represents the power of i-th lens as numbered from the entrance pupil side standardized on the basis of the power of the whole system, ϕ_{23} represents the power of the second lens group standardized on the basis of the power of the whole system, ν_{di} represents the Abbe's number for the sodium d-line of i-th lens as numbered from the entrance pupil side and d_{12} represents the surface separation between the first and second lens groups standardized on the basis of the focal length of the whole system.

In accordance with a second aspect of the present invention, there is provided an fθ lens comprising first and second lens groups arranged in this order from the entrance pupil (deflecting surface) side, the first lens group consisting of first and second lenses cemented together, the refracting powers of the first and second lenses being one of the combinations of negative and positive, positive and positive, and positive and negative, the second lens group consisting of a third lens having a positive or negative refracting power, and the first and second lens groups satisfying the following formulae (5) to (9),

$$2 \leqq |\nu_{d1} - \nu_{d2}| \quad (5)$$

$$-0.020 \leqq \Sigma(\phi_i / \nu_{di}) \leqq 0.005 \quad (6)$$

$$35 \leqq \nu_{dL} \quad (7)$$

$$1.0 \leqq \phi_{12} \leqq 2.5 \quad (8)$$

$$0.01 \leqq d_{12} \leqq 0.22 \quad (9)$$

wherein ϕ_i represents the power of i-th lens as numbered from the entrance pupil side standardized on the basis of the power of the whole system, ϕ_{12} represents the power of the first lens group standardized on the basis of the power of the whole system, ν_{di} represents the Abbe's number for the sodium d-line of i-th lens as numbered from the entrance pupil side, ν_{dL} represents the Abbe's number for the sodium d-line of one of the first and second lenses having the smaller dispersive power than the other and d_{12} represents the surface separation between the first and second lens groups standardized on the basis of the focal length of the whole system.

In accordance with a third aspect of the present invention, there is provided an fθ lens for scanning light emanating from a deflecting point comprising a first lens having a positive refracting power and second lens having a negative refracting power, the first and second lenses being cemented together with the first lens positioned on the entrance pupil side (deflecting point side) and satisfying the following formulae (10) to (12),

$$n_{d1} < n_{d2} \quad (10)$$

$$0.4 \leqq \nu_{d2} / \nu_{d1} \leqq 0.8 \quad (11)$$

$$1.5 \leqq \phi_1 \leqq 4.7 \quad (12)$$

wherein n_{d1} and n_{d2} respectively represent the refractive indices for the sodium d-line of the first and second lenses, ν_{d1} and ν_{d2} respectively represent the Abbe's numbers for the sodium d-line of the first and second lenses, and ϕ_1 represents the power of the first lens standardized on the basis of the power of the whole system, said fθ lens being used in a position where the distance between the deflecting point and the entrance pupil side surface of the first lens standardized on the basis of the focal length of the whole system is in the range of 0.1 to 0.4 inclusive (either of these values being standardized on the basis of the focal length of the whole system).

The lens elements of the fθ lens in accordance with the first to third aspects of the present invention need not be limited to spherical lenses but may be aspheric lenses.

The fθ lens in accordance with the first aspect of the present invention comprises only three lens elements in two lens groups and simple in structure.

Further when the formulae (1) to (4) are satisfied, the color aberration can be corrected over a wide wavelength range.

The formula (1) limits the relation between the Abbe's numbers of the second and third lenses of the second lens group, which is a cemented lens. The difference between the Abbe's numbers governs the amount of color aberration generated at the interface between the second and third lenses. When the difference between the Abbe's numbers of

the second and third lenses is smaller than 12, the negative color aberration generated at the interface is reduced and the positive color aberration increases as a whole.

The formula (2) relates to correction of the axial color aberration in paraxial theory and in order to correct the axial color aberration, the value of $\Sigma(\phi_i/\nu_{di})$ must be substantially 0. Further in order to correct the lateral color aberration, the axial color aberration must be small to a certain extent. In accordance with the first aspect of the present invention, the relation between the power of each lens and the Abbe's number thereof is limited by the formula (2) in order to correct the lateral color aberration. When the value of $\Sigma(\phi_i/\nu_{di})$ is smaller than the lower limit, the negative lateral color aberration increases and when the value of $\Sigma(\phi_i/\nu_{di})$ is larger than the upper limit, the positive lateral color aberration increases.

The formula (3) relates to the Petzval sum and limits the amount of curvature of field. That is, when the power of the second lens group standardized on the basis of the power of the whole system is larger than the upper limit, the fθ characteristic becomes too large in the positive direction to correct, and at the same time, the amount of curvature of field in the three-dimensional meridional image surface becomes too large in the negative direction to correct. On the other hand, when it is smaller than the lower limit, the amount of curvature of field in the three-dimensional meridional image surface becomes too large in the positive direction to correct.

Further, since the fθ characteristic depends on the distance from the entrance pupil, the position of the first and second lens groups relative to the entrance pupil must be limited in order to correct the fθ characteristic. However since the position of the first lens group is more restricted by the system in which the fθ lens is employed and accordingly it is preferable to limit the position of the second lens system. That is, the formula (4) limits the position of the second lens group by limiting the distance between the first and second lens groups. When the distance between the first and second lens groups is smaller than the lower limit, the fθ characteristic becomes too large in the positive direction to correct, and when it is larger than the upper limit, the size of the second lens group increases, which adds to the manufacturing cost of the fθ lens.

The fθ lens in accordance with the second aspect of the present invention comprises only three lens elements in two lens groups and simple in structure.

Further when the formulae (5) to (9) are satisfied, the color aberration can be corrected over a wide wavelength range.

The formula (5) limits the relation between the Abbe's numbers of the first and second lenses of the first lens group, which is a cemented lens. The difference between the Abbe's numbers governs the amount of color aberration generated at the interface between the first and second lenses. When the difference between the Abbe's numbers of the first and second lenses is smaller than 2, correction of color aberration becomes difficult and at the same time, the power of the first lens group, which is a cemented lens, becomes too large (irrespective of whether it has a positive refractive power or a negative refractive power) and both the curvature of field and the fθ characteristic deteriorate.

The formula (6) relates to correction of the axial color aberration in paraxial theory and in order to correct the axial color aberration, the value of $\Sigma(\phi_i/\nu_{di})$ must be substantially 0. Further in order to correct the lateral color aberration, the axial color aberration must be small to a certain extent. In accordance with the second aspect of the present invention, the relation between the power of each lens and the Abbe's number thereof is limited by the formula (6) in order to correct the lateral color aberration. When the value of $\Sigma(\phi_i/\nu_{di})$ is smaller than the lower limit, the negative lateral color aberration increases and when the value of $\Sigma(\phi_i/\nu_{di})$ is larger than the upper limit, the positive lateral color aberration increases.

The formula (7) defines the lower limit of the Abbe's number for the sodium d-line of one of the first and second lenses having the smaller dispersive power than the other. From the viewpoint of the achromatism, the more this value is, the better. When this value is smaller than the lower limit, the Abbe's number for the sodium d-line of the other lens must be smaller than that of said one lens. In such a case, said the other lens must be formed from SF glass. However the SF glass has a large refractive index, which results in a large Petzval sum and makes difficult correction of the curvature of field.

The formula (8) relates to the Petzval sum and limits the amount of curvature of field. That is, when the power of the first lens group standardized on the basis of the power of the whole system is larger than the upper limit, the second lens group (the third lens) becomes a negative lens and the power of the negative lens becomes so strong that the fθ characteristic sharply deteriorates at the edge of the angle of view when the curvature of field and the color aberration are corrected. On the other hand, when the power of the first lens group is smaller than the lower limit, the power of the second lens group must be strong in the positive direction and accordingly the second lens group must be a meniscus lens having a small radius of curvature which is difficult to manufacture. Further it gives rise to a problem that the curvature of field becomes large and fluctuation of the lateral color aberration with change of the angle of view becomes large.

Further, since the fθ characteristic depends on the distance from the entrance pupil as described above, the position of the first and second lens groups relative to the entrance pupil must be limited in order to correct the fθ characteristic. However since the position of the first lens group is more restricted by the system in which the fθ lens is

employed and accordingly it is preferable to limit the position of the second lens system. That is, the formula (9) limits the position of the second lens group by limiting the distance between the first and second lens groups. When the distance between the first and second lens groups is smaller than the lower limit, the fθ characteristic becomes too large in the positive direction to correct, and when it is larger than the upper limit, the fθ characteristic becomes too large in the negative direction to correct and the size of the second lens group increases, which adds to the manufacturing cost of the fθ lens.

The fθ lens in accordance with the third aspect of the present invention comprises only two lens elements in a single lens group and simple in structure.

Further when the formulae (10) to (12) are satisfied and the fθ lens being used in a position where the distance between the deflecting point and the entrance pupil side surface of the first lens standardized on the basis of the focal length of the whole system is in the range of 0.1 to 0.4 inclusive, the color aberration can be corrected over a wide wavelength range.

The formula (10) limits the relation between the refractive indices for the sodium d-line of the first and second lenses. When the refractive index of the first lens is not smaller than that of the second lens, the color aberration becomes too large in the positive direction and at the same time, the amount of curvature of field in the three-dimensional meridional image surface becomes too large in the negative direction, whereby it becomes difficult to correct both the color aberration and the curvature of field.

The formula (11) limits the relation between the Abbe's numbers of the first and second lenses forming a cemented lens group. The ratio of the Abbe's numbers governs the amount of color aberration generated at the interface between the first and second lenses. When the ratio of the Abbe's numbers of the first and second lenses is larger than 0.8, the color aberration generated at the interface in the negative direction becomes small and the color aberration in the positive direction increases as a whole, which results in under correction. On the other hand, when the ratio of the Abbe's numbers of the first and second lenses is smaller than 0.4, the color aberration generated at the interface in the negative direction becomes large and the color aberration in the negative direction increases as a whole, which results in over correction.

The formula (12) relates to the Petzval sum and limits the amount of curvature of field. That is, when the power of the first lens standardized on the basis of the power of the whole system is larger than the upper limit 4.7, the fθ characteristic becomes too large in the positive direction to correct and at the same time, the amount of curvature of field in the three-dimensional meridional image surface becomes too large in the negative direction to correct. On the other hand, when the power of the first lens is smaller than the lower limit 1.5, the amount of curvature of field in the three-dimensional meridional image surface becomes too large in the positive direction to correct.

Further, since the fθ characteristic depends on the distance from the entrance pupil as described above, the distance between the deflecting point (the intersection of the deflecting surface and the optical axis) and the surface of the first lens must be in a predetermined range. When the distance between the deflecting point and the surface of the first lens standardized on the basis of the focal length of the whole system is smaller than the lower limit 0.1, the fθ characteristic becomes too large in the positive direction to correct, and when it is larger than the upper limit 0.4, the fθ characteristic becomes too large in the negative direction to correct and at the same time, the size of the second lens group increases, which adds to the manufacturing cost of the fθ lens. Further when the distance is smaller than the lower limit, the amount of curvature of field in the three-dimensional meridional image surface becomes too large in the negative direction to correct and when the distance is larger than the upper limit, the amount of curvature of field in the three-dimensional meridional image surface becomes too large in the positive direction to correct.

BRIEF DESCRIPTION OF THE DRAWINGS

Figure 1A is a view showing the arrangement of the lens elements in an fθ lens of a first embodiment in accordance with the first aspect of the present invention,

Figure 1B is a graph showing the lateral color aberration of the fθ lens shown in Figure 1A for three wavelengths W1, W2 and W3,

Figure 1C is a graph showing the astigmatic field curves (curvature of field) of the fθ lens shown in Figure 1A for the three wavelengths W1, W2 and W3,

Figure 1D is a graph showing the linearity (fθ characteristic) of the fθ lens shown in Figure 1A for the three wavelengths W1, W2 and W3,

Figure 2A is a view showing the arrangement of the lens elements in an fθ lens of a second embodiment in accordance with the first aspect of the present invention,

Figure 2B is a graph showing the lateral color aberration of the fθ lens shown in Figure 2A for three wavelengths W1, W2 and W3,

Figure 2C is a graph showing the astigmatic field curves (curvature of field) of the fθ lens shown in Figure 2A for the three wavelengths W1, W2 and W3,

Figure 2D is a graph showing the linearity (fθ characteristic) of the fθ lens shown in Figure 2A for the three wavelengths W1, W2 and W3,

Figure 3A is a view showing the arrangement of the lens elements in an fθ lens of a third embodiment in accordance with the first aspect of the present invention,

Figure 3B is a graph showing the lateral color aberration of the fθ lens shown in Figure 3A for three wavelengths W1, W2 and W3,

Figure 3C is a graph showing the astigmatic field curves (curvature of field) of the fθ lens shown in Figure 3A for the three wavelengths W1, W2 and W3,

Figure 3D is a graph showing the linearity (fθ characteristic) of the fθ lens shown in Figure 3A for the three wavelengths W1, W2 and W3,

Figure 4A is a view showing the arrangement of the lens elements in an fθ lens of a fourth embodiment in accordance with the first aspect of the present invention,

Figure 4B is a graph showing the lateral color aberration of the fθ lens shown in Figure 4A for three wavelengths W1, W2 and W3,

Figure 4C is a graph showing the astigmatic field curves (curvature of field) of the fθ lens shown in Figure 4A for the three wavelengths W1, W2 and W3,

Figure 4D is a graph showing the linearity (fθ characteristic) of the fθ lens shown in Figure 4A for the three wavelengths W1, W2 and W3,

Figure 5A is a view showing the arrangement of the lens elements in an fθ lens of a fifth embodiment in accordance with the first aspect of the present invention,

Figure 5B is a graph showing the lateral color aberration of the fθ lens shown in Figure 5A for three wavelengths W1, W2 and W3,

Figure 5C is a graph showing the astigmatic field curves (curvature of field) of the fθ lens shown in Figure 5A for the three wavelengths W1, W2 and W3,

Figure 5D is a graph showing the linearity (fθ characteristic) of the fθ lens shown in Figure 5A for the three wavelengths W1, W2 and W3,

Figure 6A is a view showing the arrangement of the lens elements in an fθ lens of a sixth embodiment in accordance with the first aspect of the present invention,

Figure 6B is a graph showing the lateral color aberration of the fθ lens shown in Figure 6A for three wavelengths W1, W2 and W3,

Figure 6C is a graph showing the astigmatic field curves (curvature of field) of the fθ lens shown in Figure 6A for the three wavelengths W1, W2 and W3,

Figure 6D is a graph showing the linearity (fθ characteristic) of the fθ lens shown in Figure 6A for the three wavelengths W1, W2 and W3,

Figure 7A is a view showing the arrangement of the lens elements in an fθ lens of a seventh embodiment in accordance with the first aspect of the present invention,

Figure 7B is a graph showing the lateral color aberration of the fθ lens shown in Figure 7A for three wavelengths W1, W2 and W3,

Figure 7C is a graph showing the astigmatic field curves (curvature of field) of the fθ lens shown in Figure 7A for the three wavelengths W1, W2 and W3,

Figure 7D is a graph showing the linearity (fθ characteristic) of the fθ lens shown in Figure 7A for the three wavelengths W1, W2 and W3,

Figure 8A is a view showing the arrangement of the lens elements in an fθ lens of an eighth embodiment in accordance with the first aspect of the present invention,

Figure 8B is a graph showing the lateral color aberration of the fθ lens shown in Figure 8A for three wavelengths W1, W2 and W3,

Figure 8C is a graph showing the astigmatic field curves (curvature of field) of the fθ lens shown in Figure 8A for the three wavelengths W1, W2 and W3,

Figure 8D is a graph showing the linearity (fθ characteristic) of the fθ lens shown in Figure 8A for the three wavelengths W1, W2 and W3,

Figure 9A is a view showing the arrangement of the lens elements in an fθ lens of a ninth embodiment in accordance with the first aspect of the present invention,

Figure 9B is a graph showing the lateral color aberration of the fθ lens shown in Figure 9A for three wavelengths W1, W2 and W3,

Figure 9C is a graph showing the astigmatic field curves (curvature of field) of the fθ lens shown in Figure 9A for the three wavelengths W1, W2 and W3,

Figure 9D is a graph showing the linearity (fθ characteristic) of the fθ lens shown in Figure 9A for the three wavelengths W1, W2 and W3,

Figure 10A is a view showing the arrangement of the lens elements in an fθ lens of a tenth embodiment in accordance with the first aspect of the present invention,

Figure 10B is a graph showing the lateral color aberration of the fθ lens shown in Figure 10A for three wavelengths W1, W2 and W3,

Figure 10C is a graph showing the astigmatic field curves (curvature of field) of the fθ lens shown in Figure 10A for the three wavelengths W1, W2 and W3,

Figure 10D is a graph showing the linearity (fθ characteristic) of the fθ lens shown in Figure 10A for the three wavelengths W1, W2 and W3,

Figure 11A is a view showing the arrangement of the lens elements in an fθ lens of an eleventh embodiment in accordance with the first aspect of the present invention,

Figure 11B is a graph showing the lateral color aberration of the fθ lens shown in Figure 11A for three wavelengths W1, W2 and W3,

Figure 11C is a graph showing the astigmatic field curves (curvature of field) of the fθ lens shown in Figure 11A for the three wavelengths W1, W2 and W3,

Figure 11D is a graph showing the linearity (fθ characteristic) of the fθ lens shown in Figure 11A for the three wavelengths W1, W2 and W3,

Figure 12A is a view showing the arrangement of the lens elements in an fθ lens of an twelfth embodiment in accordance with the first aspect of the present invention,

Figure 12B is a graph showing the lateral color aberration of the fθ lens shown in Figure 12A for three wavelengths W1, W2 and W3,

Figure 12C is a graph showing the astigmatic field curves (curvature of field) of the fθ lens shown in Figure 12A for the three wavelengths W1, W2 and W3,

Figure 12D is a graph showing the linearity (fθ characteristic) of the fθ lens shown in Figure 12A for the three wavelengths W1, W2 and W3,

Figure 13A is a view showing the arrangement of the lens elements in an fθ lens of an thirteenth embodiment in accordance with the first aspect of the present invention,

Figure 13B is a graph showing the lateral color aberration of the fθ lens shown in Figure 13A for three wavelengths W1, W2 and W3,

Figure 13C is a graph showing the astigmatic field curves (curvature of field) of the fθ lens shown in Figure 13A for the three wavelengths W1, W2 and W3,

Figure 13D is a graph showing the linearity (fθ characteristic) of the fθ lens shown in Figure 13A for the three wavelengths W1, W2 and W3,

Figure 14A is a view showing the arrangement of the lens elements in an fθ lens of a first embodiment in accordance with the second aspect of the present invention,

Figure 14B is a graph showing the lateral color aberration of the fθ lens shown in Figure 14A for three wavelengths W1, W2 and W3,

Figure 14C is a graph showing the astigmatic field curves (curvature of field) of the fθ lens shown in Figure 14A for the three wavelengths W1, W2 and W3,

Figure 14D is a graph showing the linearity (fθ characteristic) of the fθ lens shown in Figure 14A for the three wavelengths W1, W2 and W3,

Figure 15A is a view showing the arrangement of the lens elements in an fθ lens of a second embodiment in accordance with the second aspect of the present invention,

Figure 15B is a graph showing the lateral color aberration of the fθ lens shown in Figure 15A for three wavelengths W1, W2 and W3,

Figure 15C is a graph showing the astigmatic field curves (curvature of field) of the fθ lens shown in Figure 15A for the three wavelengths W1, W2 and W3,

Figure 15D is a graph showing the linearity (fθ characteristic) of the fθ lens shown in Figure 15A for the three wavelengths W1, W2 and W3,

Figure 16A is a view showing the arrangement of the lens elements in an fθ lens of a third embodiment in accordance with the second aspect of the present invention,

Figure 16B is a graph showing the lateral color aberration of the fθ lens shown in Figure 16A for three wavelengths W1, W2 and W3,

Figure 16C is a graph showing the astigmatic field curves (curvature of field) of the fθ lens shown in Figure 16A for the three wavelengths W1, W2 and W3,

Figure 16D is a graph showing the linearity (fθ characteristic) of the fθ lens shown in Figure 16A for the three wavelengths W1, W2 and W3,

Figure 17A is a view showing the arrangement of the lens elements in an fθ lens of a fourth embodiment in accordance with the second aspect of the present invention,

Figure 17B is a graph showing the lateral color aberration of the fθ lens shown in Figure 17A for three wavelengths W1, W2 and W3,

Figure 17C is a graph showing the astigmatic field curves (curvature of field) of the fθ lens shown in Figure 17A for the three wavelengths W1, W2 and W3,

Figure 17D is a graph showing the linearity (fθ characteristic) of the fθ lens shown in Figure 17A for the three wavelengths W1, W2 and W3,

Figure 18A is a view showing the arrangement of the lens elements in an fθ lens of a fifth embodiment in accordance with the second aspect of the present invention,

Figure 18B is a graph showing the lateral color aberration of the fθ lens shown in Figure 18A for three wavelengths W1, W2 and W3,

Figure 18C is a graph showing the astigmatic field curves (curvature of field) of the fθ lens shown in Figure 18A for the three wavelengths W1, W2 and W3,

Figure 18D is a graph showing the linearity (fθ characteristic) of the fθ lens shown in Figure 18A for the three wavelengths W1, W2 and W3,

Figure 19A is a view showing the arrangement of the lens elements in an fθ lens of a sixth embodiment in accordance with the second aspect of the present invention,

Figure 19B is a graph showing the lateral color aberration of the fθ lens shown in Figure 19A for three wavelengths W1, W2 and W3,

Figure 19C is a graph showing the astigmatic field curves (curvature of field) of the fθ lens shown in Figure 19A for the three wavelengths W1, W2 and W3,

Figure 19D is a graph showing the linearity (fθ characteristic) of the fθ lens shown in Figure 19A for the three wavelengths W1, W2 and W3,

Figure 20A is a view showing the arrangement of the lens elements in an fθ lens of a seventh embodiment in accordance with the second aspect of the present invention,

Figure 20B is a graph showing the lateral color aberration of the fθ lens shown in Figure 20A for three wavelengths W1, W2 and W3,

Figure 20C is a graph showing the astigmatic field curves (curvature of field) of the fθ lens shown in Figure 20A for the three wavelengths W1, W2 and W3,

Figure 20D is a graph showing the linearity (fθ characteristic) of the fθ lens shown in Figure 20A for the three wavelengths W1, W2 and W3,

Figure 21A is a view showing the arrangement of the lens elements in an fθ lens of an eighth embodiment in accordance with the second aspect of the present invention,

Figure 21B is a graph showing the lateral color aberration of the fθ lens shown in Figure 21A for three wavelengths W1, W2 and W3,

Figure 21C is a graph showing the astigmatic field curves (curvature of field) of the fθ lens shown in Figure 21A for the three wavelengths W1, W2 and W3,

Figure 21D is a graph showing the linearity (fθ characteristic) of the fθ lens shown in Figure 21A for the three wavelengths W1, W2 and W3,

Figure 22A is a view showing the arrangement of the lens elements in an fθ lens of a ninth embodiment in accordance with the second aspect of the present invention,

Figure 22B is a graph showing the lateral color aberration of the fθ lens shown in Figure 22A for three wavelengths W1, W2 and W3,

Figure 22C is a graph showing the astigmatic field curves (curvature of field) of the fθ lens shown in Figure 22A for the three wavelengths W1, W2 and W3,

Figure 22D is a graph showing the linearity (fθ characteristic) of the fθ lens shown in Figure 22A for the three wavelengths W1, W2 and W3,

Figure 23A is a view showing the arrangement of the lens elements in an fθ lens of a tenth embodiment in accordance with the second aspect of the present invention,

Figure 23B is a graph showing the lateral color aberration of the fθ lens shown in Figure 23A for three wavelengths W1, W2 and W3,

Figure 23C is a graph showing the astigmatic field curves (curvature of field) of the fθ lens shown in Figure 23A for the three wavelengths W1, W2 and W3,

Figure 23D is a graph showing the linearity (fθ characteristic) of the fθ lens shown in Figure 23A for the three wavelengths W1, W2 and W3,

Figure 24A is a view showing the arrangement of the lens elements in an fθ lens of an eleventh embodiment in accordance with the second aspect of the present invention,

Figure 24B is a graph showing the lateral color aberration of the fθ lens shown in Figure 24A for three wavelengths W1, W2 and W3,

Figure 24C is a graph showing the astigmatic field curves (curvature of field) of the fθ lens shown in Figure 24A for the three wavelengths W1, W2 and W3,

Figure 24D is a graph showing the linearity (fθ characteristic) of the fθ lens shown in Figure 24A for the three wavelengths W1, W2 and W3,

Figure 25A is a view showing the arrangement of the lens elements in an fθ lens of a first embodiment in accordance with the third aspect of the present invention,

Figure 25B is a graph showing the lateral color aberration of the fθ lens shown in Figure 25A for three wavelengths W1, W2 and W3,

Figure 25C is a graph showing the astigmatic field curves (curvature of field) of the fθ lens shown in Figure 25A for the three wavelengths W1, W2 and W3,

Figure 25D is a graph showing the linearity (fθ characteristic) of the fθ lens shown in Figure 25A for the three wavelengths W1, W2 and W3,

Figure 26A is a view showing the arrangement of the lens elements in an fθ lens of a second embodiment in accordance with the third aspect of the present invention,

Figure 26B is a graph showing the lateral color aberration of the fθ lens shown in Figure 26A for three wavelengths W1, W2 and W3,

Figure 26C is a graph showing the astigmatic field curves (curvature of field) of the fθ lens shown in Figure 26A for the three wavelengths W1, W2 and W3,

Figure 26D is a graph showing the linearity (fθ characteristic) of the fθ lens shown in Figure 26A for the three wavelengths W1, W2 and W3,

Figure 27A is a view showing the arrangement of the lens elements in an fθ lens of a third embodiment in accordance with the third aspect of the present invention,

Figure 27B is a graph showing the lateral color aberration of the fθ lens shown in Figure 27A for three wavelengths W1, W2 and W3,

Figure 27C is a graph showing the astigmatic field curves (curvature of field) of the fθ lens shown in Figure 27A for the three wavelengths W1, W2 and W3,

Figure 27D is a graph showing the linearity (fθ characteristic) of the fθ lens shown in Figure 27A for the three wavelengths W1, W2 and W3,

Figure 28A is a view showing the arrangement of the lens elements in an fθ lens of a fourth embodiment in accordance with the third aspect of the present invention,

Figure 28B is a graph showing the lateral color aberration of the fθ lens shown in Figure 28A for three wavelengths W1, W2 and W3,

Figure 28C is a graph showing the astigmatic field curves (curvature of field) of the fθ lens shown in Figure 28A for the three wavelengths W1, W2 and W3, Figure 28D is a graph showing the linearity (fθ characteristic) of the fθ lens shown in Figure 28A for the three wavelengths W1, W2 and W3,

Figure 29A is a view showing the arrangement of the lens elements in an fθ lens of a fifth embodiment in accordance with the third aspect of the present invention,

Figure 29B is a graph showing the lateral color aberration of the fθ lens shown in Figure 29A for three wavelengths W1, W2 and W3,

Figure 29C is a graph showing the astigmatic field curves (curvature of field) of the fθ lens shown in Figure 29A for the three wavelengths W1, W2 and W3,

Figure 29D is a graph showing the linearity (fθ characteristic) of the fθ lens shown in Figure 29A for the three wavelengths W1, W2 and W3,

Figure 30A is a view showing the arrangement of the lens elements in an fθ lens of a sixth embodiment in accordance with the third aspect of the present invention,

Figure 30B is a graph showing the lateral color aberration of the fθ lens shown in Figure 30A for three wavelengths W1, W2 and W3,

Figure 30C is a graph showing the astigmatic field curves (curvature of field) of the fθ lens shown in Figure 30A for the three wavelengths W1, W2 and W3,

Figure 30D is a graph showing the linearity (fθ characteristic) of the fθ lens shown in Figure 30A for the three wavelengths W1, W2 and W3,

Figure 31A is a view showing the arrangement of the lens elements in an fθ lens of a seventh embodiment in accordance with the third aspect of the present invention,

Figure 31B is a graph showing the lateral color aberration of the fθ lens shown in Figure 31A for three wavelengths W1, W2 and W3,

Figure 31C is a graph showing the astigmatic field curves (curvature of field) of the fθ lens shown in Figure 31A for the three wavelengths W1, W2 and W3,

Figure 31D is a graph showing the linearity (fθ characteristic) of the fθ lens shown in Figure 31A for the three wave-

lengths W1, W2 and W3,

Figure 32A is a view showing the arrangement of the lens elements in an fθ lens of an eighth embodiment in accordance with the third aspect of the present invention,

Figure 32B is a graph showing the lateral color aberration of the fθ lens shown in Figure 32A for three wavelengths W1, W2 and W3,

Figure 32C is a graph showing the astigmatic field curves (curvature of field) of the fθ lens shown in Figure 32A for the three wavelengths W1, W2 and W3,

Figure 32D is a graph showing the linearity (fθ characteristic) of the fθ lens shown in Figure 32A for the three wavelengths W1, W2 and W3,

Figure 33A is a view showing the arrangement of the lens elements in an fθ lens of a ninth embodiment in accordance with the third aspect of the present invention,

Figure 33B is a graph showing the lateral color aberration of the fθ lens shown in Figure 33A for three wavelengths W1, W2 and W3,

Figure 33C is a graph showing the astigmatic field curves (curvature of field) of the fθ lens shown in Figure 33A for the three wavelengths W1, W2 and W3,

Figure 33D is a graph showing the linearity (fθ characteristic) of the fθ lens shown in Figure 33A for the three wavelengths W1, W2 and W3,

Figure 34A is a view showing the arrangement of the lens elements in an fθ lens of a tenth embodiment in accordance with the third aspect of the present invention,

Figure 34B is a graph showing the lateral color aberration of the fθ lens shown in Figure 34A for three wavelengths W1, W2 and W3,

Figure 34C is a graph showing the astigmatic field curves (curvature of field) of the fθ lens shown in Figure 34A for the three wavelengths W1, W2 and W3,

Figure 34D is a graph showing the linearity (fθ characteristic) of the fθ lens shown in Figure 34A for the three wavelengths W1, W2 and W3,

Figure 35A is a view showing the arrangement of the lens elements in an fθ lens of a eleventh embodiment in accordance with the third aspect of the present invention,

Figure 35B is a graph showing the lateral color aberration of the fθ lens shown in Figure 35A for three wavelengths W1, W2 and W3,

Figure 35C is a graph showing the astigmatic field curves (curvature of field) of the fθ lens shown in Figure 35A for the three wavelengths W1, W2 and W3, and

Figure 35D is a graph showing the linearity (fθ characteristic) of the fθ lens shown in Figure 35A for the three wavelengths W1, W2 and W3.

DESCRIPTION OF THE PREFERRED EMBODIMENTS

fθ lenses of thirteen embodiments in accordance with the first aspect of the present invention will be described with reference to Figures 1 (1A to 1D) to 13 (13A to 13D) and tables 1 to 13, hereinbelow. Figures 1A to 13A respectively show the arrangements of the lens elements of the fθ lenses of first to thirteenth embodiments, and Figures 1B, 1C and 1D to 13B, 13C and 13D respectively show the lateral color aberration, the astigmatic field curves (curvature of field) and the linearity (fθ characteristic) of the fθ lenses of the first to thirteenth embodiments when three laser beams having different wavelengths W1, W2 and W3 used in a scanning optical system enter the respective fθ lenses. The values of the wavelengths W1, W2 and W3 are shown on the top of the tables corresponding to the fθ lenses.

Each fθ lens comprises a first lens group which consists of a single first lens L1 having a negative or positive refracting power, and a second lens group which consists of a second lens L2 having a positive refracting power and a third lens L3 having a negative refracting power. The second and third lenses L2 and L3 are cemented together and the second lens group has a positive refracting power as a whole. The first and second lens groups are arranged in this order from the entrance pupil (deflecting surface) side and satisfies the following formulae (1) to (4),

$$12 \leqq \nu_{d2} - \nu_{d3} \tag{1}$$

$$-0.035 \leqq \Sigma(\phi_i / \nu_{di}) \leqq 0.005 \tag{2}$$

$$0.7 \leqq \phi_{23} \leqq 2.0 \tag{3}$$

$$0.03 \leqq d_{12} \leqq 0.20 \tag{4}$$

wherein ϕ_i represents the power of i-th lens as numbered from the entrance pupil side standardized on the basis of the

power of the whole system, ϕ_{23} represents the power of the second lens group standardized on the basis of the power of the whole system, ν_{di} represents the Abbe's number for the sodium d-line of i-th lens as numbered from the entrance pupil side and d_{12} represents the air separation between the first and second lens groups standardized on the basis of the focal length of the whole system.

In the first embodiment shown in Figure 1A, the factors limited by the formulae (2) to (4) are set substantially at the middle of the ranges defined by the formulae. The radii of curvature R of the refracting surfaces, the axial surface separations d, and the refractive indexes n_d and the Abbe's numbers ν_d of the lenses for the sodium d-line in the fθ lens of this embodiment are shown in table 1. The radii of curvature R of the refracting surfaces and the axial surface separations d are in the values standardized on the basis of the focal length of the whole system. (the same for all the embodiments including the embodiments in accordance with the second and third aspects of the present invention described later) The numbers in the leftmost column of table 1 designate the numbers of the symbols R, d, n_d and ν_d as numbered from the entrance pupil (deflecting surface) side. (the same for all the tables in this specification)

Table1

wavelength W1;810nm, W2;750nm, W3;680nm, angle of view 62.5°

i	Ri	di	n_d	ν_d
OBJ	-	infinity		
0	infinity	0.10391		
1	-1.76735	0.02474	n_{d1} 1.48749	ν_{d1} 70.4
2	18.24431	0.07422		
3	2.39800	0.09896	n_{d2} 1.63930	ν_{d2} 45.1
4	-0.21884	0.02474	n_{d3} 1.80518	ν_{d3} 25.5
5	-0.46351	1.03924		
surface scanned	infinity	-		

$\nu_{d2}-\nu_{d3}=19.6$
$\Sigma(\phi i/\nu_{di})=-0.007$
$\phi_{23}=1.24$
$d_{12}=0.07422$

lateral color aberration 0.049x10^{-3}
curvature of field 0.016
fθ characteristic 1.16%

Figures 1B to 1D respectively show the lateral color aberration, the astigmatic field curves (curvature of field) in the scanning direction and the linearity (fθ characteristic) of the fθ lens of the first embodiment when laser beams having wavelengths of 810nm (W1), 750nm (W2) and 680nm (W3) enter the fθ lens. In Figures 1C and 1D, the astigmatic field curves and the linearity for the wavelengths W1, W2 and W3 are respectively shown by the solid line, the fine broken line and the rough broken line, but when one or both of the broken lines coincide with the solid line, the broken line is not shown. (the same for all the embodiments including the embodiments in accordance with the second and third aspects of the present invention described later)

As can be understood from Figures 1B to 1D, in the fθ lens of this embodiment, the lateral color aberration is well corrected for the respective wavelengths in spite of a simple structure consisting of only three lens elements in two lens groups.

In the second embodiment shown in Figure 2A, the difference between the Abbe's numbers of the second lens L2 and the third lens L3 is set to a value close to the lower limit of the range defined by the formula (1). The radii of curvature R of the refracting surfaces, the axial surface separations d, and the refractive indexes n_d and the Abbe's numbers

ν_d of the lenses for the sodium d-line in the fθ lens of this embodiment are shown in table 2.

Table2

wavelength W1;810nm, W2;750nm, W3;680nm, angle of view 62.5°

i	Ri	di	n_d	ν_d
OBJ	-	infinity		
0	infinity	0.10390		
1	-1.19973	0.02474	n_{d1} 1.80518	ν_{d1} 25.5
2	7.58872	0.05332		
3	2.00978	0.09895	n_{d2} 1.72342	ν_{d2} 38.0
4	-0.17854	0.02474	n_{d3} 1.80518	ν_{d3} 25.5
5	-0.46377	1.08380		
surface scanned	infinity	-		

ν_{d2}-ν_{d3}=12.5
$\Sigma(\phi i/\nu_{di})$=-0.020
ϕ_{23}=1.61
d_{12}=0.05332

lateral color aberration 0.039x10^{-3}
curvature of field 0.014
fθ characteristic 2.39%

Figures 2B to 2D respectively show the lateral color aberration, the astigmatic field curves in the scanning direction and the linearity of the fθ lens of the second embodiment when laser beams having wavelengths of 810nm (W1), 750nm (W2) and 680nm (W3) enter the fθ lens.

As can be understood from Figures 2B to 2D, in the fθ lens of this embodiment, the lateral color aberration is well corrected for the respective wavelengths in spite of a simple structure consisting of only three lens elements in two lens groups.

In the third embodiment shown in Figure 3A, the surface separation d_{12} between the first and second lens groups is set to a value close to the lower limit of the range defined by the formula (4). The radii of curvature R of the refracting surfaces, the axial surface separations d, and the refractive indexes n_d and the Abbe's numbers ν_d of the lenses for the sodium d-line in the fθ lens of this embodiment are shown in table 3.

Table3

wavelength W1;810nm, W2;750nm, W3;680nm, angle of view 62.5°

i	Ri	di	n_d	ν_d
OBJ	-	infinity		
0	infinity	0.10393		
1	-14.8476	0.02475	n_{d1} 1.80518	ν_{d1} 25.5
2	0.73495	0.03228		
3	0.94676	0.09898	n_{d2} 1.62012	ν_{d2} 49.8
4	-0.17322	0.02475	n_{d3} 1.64769	ν_{d3} 33.8
5	-0.42690	1.07406		
surface scanned	infinity			

$\nu_{d2}-\nu_{d3}=16.0$

$\Sigma(\phi i/\nu_{di})=-0.025$

$\phi_{23}=1.94$

$d_{12}=0.03228$

lateral color aberration 0.074x10^{-3}

curvature in field 0.016

fθ characteristic 3.04%

Figures 3B to 3D respectively show the lateral color aberration, the astigmatic field curves in the scanning direction and the linearity of the fθ lens of the third embodiment when laser beams having wavelengths of 810nm (W1), 750nm (W2) and 680nm (W3) enter the fθ lens.

As can be understood from Figures 3B to 3D, in the fθ lens of this embodiment, the lateral color aberration is well corrected for the respective wavelengths in spite of a simple structure consisting of only three lens elements in two lens groups.

In the fourth embodiment shown in Figure 4A, the first lens L1 has a negative refracting power and the surface separation d_{12} between the first and second lens groups is set to a relatively large value in the range defined by the formula (4). The radii of curvature R of the refracting surfaces, the axial surface separations d, and the refractive indexes n_d and the Abbe's numbers ν_d of the lenses for the sodium d-line in the fθ lens of this embodiment are shown in table 4.

Table4

wavelength W1;810nm, W2;750nm, W3;680nm, angle of view 62.5°

i	Ri	di	n_d	ν_d
OBJ	-	infinity		
0	infinity	0.10390		
1	-0.45615	0.02474	n_{d1} 1.51680	ν_{d1} 64.2
2	-0.48189	0.14842		
3	8.15793	0.11379	n_{d2} 1.66672	ν_{d2} 48.3
4	-0.28119	0.02474	n_{d3} 1.80518	ν_{d3} 25.5
5	-0.56734	1.02736		
surface scanned	infinity	-		

$\nu_{d2}-\nu_{d3}=22.8$

$\Sigma(\phi i/\nu_{di})=-0.004$

$\phi_{23}=1.01$

$d_{12}=0.14842$

lateral color aberration 0.055x10^{-3}

curvature of field 0.015

fθ characteristic 1.03%

Figures 4B to 4D respectively show the lateral color aberration, the astigmatic field curves in the scanning direction and the linearity of the fθ lens of the fourth embodiment when laser beams having wavelengths of 810nm (W1), 750nm (W2) and 680nm (W3) enter the fθ lens.

As can be understood from Figures 4B to 4D, in the fθ lens of this embodiment, the lateral color aberration is well corrected for the respective wavelengths in spite of a simple structure consisting of only three lens elements in two lens groups.

In the fifth embodiment shown in Figure 5A, the first lens L1 has a positive refracting power. The radii of curvature R of the refracting surfaces, the axial surface separations d, and the refractive indexes n_d and the Abbe's numbers ν_d of the lenses for the sodium d-line in the fθ lens of this embodiment are shown in table 5.

Table5

wavelength W1;810nm, W2;750nm, W3;680nm, angle of view 62.5°

i	Ri	di	n_d	ν_d
OBJ	-	infinity		
0	infinity	0.10390		
1	-0.14842	0.02474	n_{d1} 1.51680	ν_{d1} 64.2
2	-0.14564	0.13018		
3	1.25361	0.09895	n_{d2} 1.53172	ν_{d2} 48.8
4	-0.30864	0.02474	n_{d3} 1.80518	ν_{d3} 25.5
5	-0.67737	0.97906		
surface scanned	infinity	-		

ν_{d2}-ν_{d3}=23.3
$\Sigma(\phi i/\nu_{di})$=-0.006
ϕ_{23}=0.73
d_{12}=0.13018

lateral color aberration 0.034x10^{-3}
curvature of field 0.011
$f\theta$ characteristic 2.52%

Figures 5B to 5D respectively show the lateral color aberration, the astigmatic field curves in the scanning direction and the linearity of the fθ lens of the fifth embodiment when laser beams having wavelengths of 810nm (W1), 750nm (W2) and 680nm (W3) enter the fθ lens.

As can be understood from Figures 5B to 5D, in the fθ lens of this embodiment, the lateral color aberration is well corrected for tee respective wavelengths in spite of a simple structure consisting of only three lens elements in two lens groups.

In the sixth embodiment shown in Figure 6A, the factors limited by the formulae (2) to (4) are set substantially at the middle of the ranges defined by the formulae. The radii of curvature R of the refracting surfaces, the axial surface separations d, and the refractive indexes n_d and the Abbe's numbers ν_d of the lenses for the sodium d-line in the fθ lens of this embodiment are shown in table 6.

Table6

wavelength W1;870nm, W2;810nm, W3;750nm, angle of view 62.5°

i	Ri	di	n_d	ν_d
OBJ	-	infinity		
0	infinity	0.10390		
1	-0.69730	0.02474	n_{d1} 1.51680	ν_{d1} 64.2
2	-4.91198	0.07766		
3	3.12259	0.09895	n_{d2} 1.65844	ν_{d2} 50.9
4	-0.18906	0.02474	n_{d3} 1.72825	ν_{d3} 28.3
5	-0.44235	1.09609		
surface scanned	infinity	-		

$\nu_{d2}-\nu_{d3}=22.6$
$\Sigma(\phi i/\nu_{di})=-0.012$
$\phi_{23}=1.48$
$d_{12}=0.07766$

lateral color aberration 0.041x10^{-3}
curvature of field 0.015
fθ characteristic 1.88%

Figures 6B to 6D respectively show the lateral color aberration, the astigmatic field curves in the scanning direction and the linearity of the fθ lens of the sixth embodiment when laser beams having wavelengths of 870nm (W1), 810nm (W2) and 750nm (W3) enter the fθ lens.

As can be understood from Figures 6B to 6D, in the fθ lens of this embodiment, the lateral color aberration is well corrected for the respective wavelengths in spite of a simple structure consisting of only three lens elements in two lens groups.

In the seventh embodiment shown in Figure 7A, the factors limited by the formulae (2) to (4) are set substantially at the middle of the ranges defined by the formulae. The radii of curvature R of the refracting surfaces, the axial surface separations d, and the refractive indexes n_d and the Abbe's numbers ν_d of the lenses for the sodium d-line in the fθ lens of this embodiment are shown in table 7.

Table7

wavelength W1;890nm, W2;830nm, W3;780nm, angle of view 62.5°

i	Ri	di	n_d	ν_d
OBJ	-	infinity		
0	infinity	0.10390		
1	-0.57722	0.02474	n_{d1} 1.56732	ν_{d1} 42.8
2	-1.68735	0.08847		
3	4.06146	0.09895	n_{d2} 1.62299	ν_{d2} 58.1
4	-0.20052	0.02474	n_{d3} 1.72825	ν_{d3} 28.3
5	-0.39721	1.11410		
surface scanned	infinity	-		

$\nu_{d2}-\nu_{d3}=29.8$ lateral color aberration 0.029×10^{-3}

$\Sigma(\phi i/\nu_{di})=-0.019$ curvature of field 0.013

$\phi_{23}=1.46$ $f\theta$ characteristic 1.75%

$d_{12}=0.08847$

Figures 7B to 7D respectively show the lateral color aberration, the astigmatic field curves in the scanning direction and the linearity of the fθ lens of the seventh embodiment when laser beams having wavelengths of 890nm (W1), 830nm (W2) and 780nm (W3) enter the fθ lens.

As can be understood from Figures 7B to 7D, in the fθ lens of this embodiment, the lateral color aberration is well corrected for the respective wavelengths in spite of a simple structure consisting of only three lens elements in two lens groups.

In the eighth embodiment shown in Figure 8A, the first lens L1 has a negative refracting power and the difference between the longest and the shortest of the wavelengths W1 to W3 of the laser beams entering the fθ lens is enlarged. The radii of curvature R of the refracting surfaces, the axial surface separations d, and the refractive indexes n_d and the Abbe's numbers ν_d of the lenses for the sodium d-line in the fθ lens of this embodiment are shown in table 8.

Table8

wavelength W1;680nm, W2;532nm, W3;473nm, angle of view 55.7°

i	Ri	di	n_d	ν_d
OBJ	-	infinity		
0	infinity	0.14278		
1	-1.61585	0.02380	n_{d1} 1.60000	ν_{d1} 42.5
2	1.80042	0.04427		
3	1.08641	0.09519	n_{d2} 1.49700	ν_{d2} 81.6
4	-0.18913	0.01904	n_{d3} 1.64844	ν_{d3} 50.9
5	-0.32890	1.06515		
surface scanned	infinity	-		

ν_{d2}-ν_{d3}=30.7
$\Sigma(\phi i/\nu_{di})$=-0.007
ϕ_{23}=1.58
d_{12}=0.04427

lateral color aberration 0.071x10^{-3}
curvature of field 0.002
fθ characteristic 1.44%

Figures 8B to 8D respectively show the lateral color aberration, the astigmatic field curves in the scanning direction and the linearity of the fθ lens of the eighth embodiment when laser beams having wavelengths of 680nm (W1), 532nm (W2) and 473nm (W3) enter the fθ lens.

As can be understood from Figures 8B to 8D, in the fθ lens of this embodiment, the lateral color aberration is well corrected for the respective wavelengths in spite of a simple structure consisting of only three lens elements in two lens groups.

In the ninth embodiment shown in Figure 9A, the first lens L1 has a positive refracting power and the difference between the longest and the shortest of the wavelengths W1 to W3 of the laser beams entering the fθ lens is enlarged. The radii of curvature R of the refracting surfaces, the axial surface separations d, and the refractive indexes n_d and the Abbe's numbers ν_d of the lenses for the sodium d-line in the fθ lens of this embodiment are shown in table 9.

Table9

wavelength W1;680nm, W2;532nm, W3;473nm, angle of view 55.7°

i	Ri	di	n_d	ν_d
OBJ	-	infinity		
0	infinity	0.09518		
1	-0.16194	0.01666	n_{d1} 1.65844	ν_{d1} 50.9
2	-0.16505	0.09968		
3	1.37817	0.07138	n_{d2} 1.49700	ν_{d2} 81.6
4	-0.21639	0.02855	n_{d3} 1.67003	ν_{d3} 47.2
5	-0.50462	1.01642		
surface scanned	infinity	-		

$\nu_{d2}-\nu_{d3}=34.4$
$\Sigma(\phi i/\nu_{di})=-0.002$
$\phi_{23}=0.89$
$d_{12}=0.09968$

lateral color aberration 0.071x10^{-3}
curvature of field 0.011
fθ characteristic 0.69%

Figures 9B to 9D respectively show the lateral color aberration, the astigmatic field curves in the scanning direction and the linearity of the fθ lens of the ninth embodiment when laser beams having wavelengths of 680nm (W1), 532nm (W2) and 473nm (W3) enter the fθ lens.

As can be understood from Figures 9B to 9D, in the fθ lens of this embodiment, the lateral color aberration is well corrected for the respective wavelengths in spite of a simple structure consisting of only three lens elements in two lens groups.

As can be understood from the description above, in the fθ lens in accordance with the first aspect of the present invention, the color aberration can be corrected with a high accuracy over a wide wavelength range, and accordingly, the error in super imposing the beam spots can be reduced in the scanning optical system or the like using a plurality of laser beams having different wavelengths. Further since being simple in structure, the fθ lens in accordance with the first aspect of the present invention can be manufactured at low cost.

The fθ lens in accordance with the first aspect of the present invention need not be limited to those described above but may be variously modified so long as the formulae (1) to (4) are satisfied.

The fθ lenses of tenth to thirteenth embodiments shown in Figures 10A to 13A comprise an aspheric lense.

In the tenth embodiment shown in Figure 10A, the first surface of the first lens L1 (the entrance surface) is an aspheric surface as shown in table 10 and the factors limited by the formulae (2) to (4) are set substantially at the middle of the ranges defined by the formulae. The radii of curvature R of the refracting surfaces, the axial surface separations d, and the refractive indexes n_d and the Abbe's numbers ν_d of the lenses for the sodium d-line in the fθ lens of this embodiment are shown in table 10.

In table 10, the value designated by ★ represents the radius of curvature on the optical axis (at the vertex of the aspheric surface) and means that the aspheric surface has a shape defined by the following formula (13). (the same in tables 11 to 13, 21 to 24, 34 and 35)

$$x=ch^2/[1+\{1-(1+k)c^2h^2\}^{1/2}]+a_1h^4+a_2h^6+a_3h^8+a_4h^{10} \quad (13)$$

wherein x represents the length of a perpendicular line between a point on an aspheric plane at a height of h above the optical axis and a plane tangent to the aspheric plane (a plane perpendicular to the optical axis) (as standardized on the basis of the focal length of the whole system), h represents the height above the optical axis (as standardized on the basis of the focal length of the whole system), c represents the curvature at the vertex of the aspheric plane (the reciprocal of the radius of curvature =I/R), k represents a conic constant, and a_1 to a_4 respectively represents four-dimensional, six-dimensional, eight-dimensional and ten-dimensional aspheric coefficients.

Table10

wavelength W1;810nm, W2;750nm, W3;680nm, angle of view 62.5°

i	Ri	di	n_d	ν_d
OBJ	-	infinity		
0	infinity	0.11999		
1	-1.65445★	0.02475	n_{d1} 1.48749	ν_{d1} 70.4
2	26.55325	0.07455		
3	2.88037	0.09941	n_{d2} 1.63930	ν_{d2} 45.1
4	-0.21440	0.02485	n_{d3} 1.80518	ν_{d3} 25.5
5	-0.44731	1.04490		
surface scanned	infinity	-		

ν_{d2}-ν_{d3}=19.6 lateral color aberration 0.038x10^{-3}

$\Sigma(\phi i/\nu_{di})$=-0.007 curvature of field 0.001

ϕ_{23}=1.25 fθ characteristic 0.89%

d_{12}=0.07455

k=-7.7304 a_1=0.2513 a_2=1.4333x10^2 a_3=0 a_4=0

Figures 10B to 10D respectively show the lateral color aberration, the astigmatic field curves in the scanning direction and the linearity of the fθ lens of the tenth embodiment when laser beams having wavelengths of 810nm (W1), 750nm (W2) and 680nm (W3) enter the fθ lens.

As can be understood from Figures 10B to 10D, in the fθ lens of this embodiment, the lateral color aberration is well corrected for the respective wavelengths in spite of a simple structure consisting of only three lens elements in two lens groups.

In the eleventh embodiment shown in Figure 11A, the second surface of the first lens L1 (the exit surface) is an aspheric surface as shown in table 11 and the factors limited by the formulae (2) to (4) are set substantially at the middle of the ranges defined by the formulae. The radii of curvature R of the refracting surfaces, the axial surface separations d, and the refractive indexes n_d and the Abbe's numbers ν_d of the lenses for the sodium d-line in the fθ lens of this embodiment are shown in table 11.

Table11

wavelength W1;870nm, W2;810nm, W3;750nm, angle of view 62.5°

i	Ri	di	n_d	ν_d
OBJ	-	infinity		
0	infinity	0.07950		
1	-0.71770	0.02484	n_{d1} 1.51680	ν_{d1} 64.2
2	-6.02623★	0.08604		
3	5.67504	0.09937	n_{d2} 1.65844	ν_{d2} 50.9
4	-0.17857	0.02484	n_{d3} 1.72825	ν_{d3} 28.3
5	-0.41850	1.10872		
surface scanned	infinity	-		

ν_{d2}-ν_{d3}=22.6
$\Sigma(\phi i/\nu_{di})$=-0.014
ϕ_{23}=1.46
d_{12}=0.08604
k=4383.87 a_1=0.8706
a_3=3.5625x10^4

lateral color aberration 0.036x10^{-3}
curvature of field 0.002
fθ characteristic 0.82%

a_2=-1.0612x10^2
a_4=0

Figures 11B to 11D respectively show the lateral color aberration, the astigmatic field curves in the scanning direction and the linearity of the fθ lens of the eleventh embodiment when laser beams having wavelengths of 870nm (W1), 810nm (W2) and 750nm (W3) enter the fθ lens.

As can be understood from Figures 11B to 11D, in the fθ lens of this embodiment, the lateral color aberration is well corrected for the respective wavelengths in spite of a simple structure consisting of only three lens elements in two lens groups.

In the twelfth embodiment shown in Figure 12A, the first surface of the second lens L2 (the entrance surface) is an aspheric surface as shown in table 12, the first lens L1 has a positive refracting power and the difference between the longest and the shortest of the wavelengths W1 to W3 of the laser beams entering the fθ lens is enlarged. The radii of curvature R of the refracting surfaces, the axial surface separations d, and the refractive indexes n_d and the Abbe's numbers ν_d of the lenses for the sodium d-line in the fθ lens of this embodiment are shown in table 12.

Table 12

wavelength W1;680nm, W2;532nm, W3;473nm, angle of view 55.7°

i	Ri	di	n_d	ν_d
OBJ	-	infinity		
0	infinity	0.07613		
1	-0.16136	0.01665	n_{d1} 1.65844	ν_{d1} 50.9
2	-0.16480	0.11960		
3	1.69737★	0.07137	n_{d2} 1.49700	ν_{d2} 81.6
4	-0.21108	0.02855	n_{d3} 1.67003	ν_{d3} 47.2
5	-0.47179	1.02119		
surface scanned	infinity	-		

$\nu_{d2}-\nu_{d3}=34.4$ lateral color aberration 0.057×10^{-3}

$\Sigma(\phi i/\nu_{di})=-0.002$ curvature of field 0.005

$\phi_{23}=0.90$ fθ characteristic 0.69%

$d_{12}=0.11960$

$k=30.6572$ $a_1=-0.4346$ $a_2=-2.5820$ $a_3=0$ $a_4=0$

Figures 12B to 12D respectively show the lateral color aberration, the astigmatic field curves in the scanning direction and the linearity of the fθ lens of the twelfth embodiment when laser beams having wavelengths of 680nm (W1), 532nm (W2) and 473nm (W3) enter the fθ lens.

As can be understood from Figures 12B to 12D, in the fθ lens of this embodiment, the lateral color aberration is well corrected for the respective wavelengths in spite of a simple structure consisting of only three lens elements in two lens groups.

In the thirteenth embodiment shown in Figure 13A, the second surface of the third lens L3 (the exit surface) is an aspheric surface as shown in table 13 and the difference between the longest and the shortest of the wavelengths W1 to W3 of the laser beams entering the fθ lens is enlarged. The radii of curvature R of the refracting surfaces, the axial surface separations d, and the refractive indexes n_d and the Abbe's numbers ν_d of the lenses for the sodium d-line in the fθ lens of this embodiment are shown in table 13.

Table 13

wavelength W1;680nm, W2;532nm, W3;473nm, angle of view 55.7°

i	Ri	di	n_d	ν_d
OBJ	-	infinity		
0	infinity	0.15546		
1	0.77803	0.02380	n_{d1} 1.60000	ν_{d1} 42.5
2	0.48766	0.05440		
3	1.53489	0.09520	n_{d2} 1.49700	ν_{d2} 81.6
4	-0.18752	0.01904	n_{d3} 1.65844	ν_{d3} 50.9
5	-0.34026★	1.03201		
surface scanned	infinity	-		

$\nu_{d2}-\nu_{d3}=30.7$ lateral color aberration 0.057×10^{-3}

$\Sigma(\phi i/\nu_{di})=-0.004$ curvature of field 0.001

$\phi_{23}=1.39$ $f\theta$ characteristic 0.82%

$d_{12}=0.05440$

$k=0.5643$ $a_1=0.4421$ $a_2=-1.7884$

$a_3=-5.1822\times10$ $a_4=-1.9613\times10^3$

Figures 13B to 13D respectively show the lateral color aberration, the astigmatic field curves in the scanning direction and the linearity of the fθ lens of the thirteenth embodiment when laser beams having wavelengths of 680nm (W1), 532nm (W2) and 473nm (W3) enter the fθ lens.

As can be understood from Figures 13B to 13D, in the fθ lens of this embodiment, the lateral color aberration is well corrected for the respective wavelengths in spite of a simple structure consisting of only three lens elements in two lens groups.

fθ lenses of eleven embodiments in accordance with the second aspect of the present invention will be described with reference to Figures 14 (14A to 14D) to 24 (24A to 24D) and tables 14 to 24, hereinbelow. Figures 14A to 24A respectively show the arrangements of the lens elements of the fθ lenses of first to eleventh embodiments, and Figures 14B, 14C and 14D to 24B, 24C and 24D respectively show the lateral color aberration, the astigmatic field curves (curvature of field) and the linearity (fθ characteristic) of the fθ lenses of the first to eleventh embodiments when three laser beams having different wavelengths W1, W2 and W3 used in a scanning optical system enter the respective fθ lenses. The values of the wavelengths W1, W2 and W3 are shown on the top of the tables corresponding to the fθ lenses.

Each fθ lens comprises first and second lens groups arranged in this order from the entrance pupil (deflecting surface) side. The first lens group consists of first and second lenses L1' and L2' cemented together, the refracting powers of the first and second lenses L1' and L2' being one of the combinations of negative and positive, positive and positive, and positive and negative. The second lens group consists of a third lens L3' having a positive or negative refracting power. The first and second lens groups satisfies the following formulae (5) to (9),

$$2 \leqq |\nu_{d1}-\nu_{d2}| \quad (5)$$

$$-0.020 \leqq \Sigma(\phi_i/\nu_{di}) \leqq 0.005 \quad (6)$$

$$35 \leqq \nu_{dL} \tag{7}$$

$$1.0 \leqq \phi_{12} \leqq 2.5 \tag{8}$$

$$0.01 \leqq d_{12} \leqq 0.22 \tag{9}$$

wherein ϕ_i represents the power of i-th lens as numbered from the entrance pupil side standardized on the basis of the power of the whole system, ϕ_{12} represents the power of the first lens group standardized on the basis of the power of the whole system, ν_{di} represents the Abbe's number for the sodium d-line of i-th lens as numbered from the entrance pupil side, ν_{dL} represents the Abbe's number for the sodium d-line of one of the first and second lenses having the smaller dispersive power than the other and d_{12} represents the surface separation between the first and second lens groups standardized on the basis of the focal length of the whole system.

In the first embodiment of the second aspect of the present invention shown in Figure 14A, the first lens L1' has a positive refracting power, the second lens L2' has a negative refracting power and the power of the first lens group is set close to the upper limit of the range defined by the formula (8). The radii of curvature R of the refracting surfaces, the axial surface separations d, and the refractive indexes n_d and the Abbe's numbers ν_d of the lenses for the sodium d-line in the fθ lens of this embodiment are shown in table 14.

Table14

wavelength W1;680nm, W2;532nm, W3;473nm, angle of view 55.7°

i	Ri	di	n_d	ν_d
OBJ	-	infinity		
0	infinity	0.14220		
1	0.68707	0.09480	n_{d1} 1.62280	ν_{d1} 56.9
2	-0.12788	0.01896	n_{d2} 1.54041	ν_{d2} 51.0
3	-0.59246	0.03447		
4	-0.16691	0.02370	n_{d3} 1.57845	ν_{d3} 41.7
5	-0.31521	0.85500		
surface scanned	infinity	-		

$|\nu_{d1}-\nu_{d2}| = 5.9$
$\Sigma(\phi i/\nu_{di}) = -0.004$
$\nu_{dL} = 56.9$
$\phi_{12} = 2.37$
$d_{12} = 0.03447$

lateral color aberration	0.067×10^{-3}
curvature of field	0.023
fθ characteristic	1.28%

Figures 14B to 14D respectively show the lateral color aberration, the astigmatic field curves in the scanning direction and the linearity of the fθ lens of the first embodiment when laser beams having wavelengths of 680nm (W1), 532nm (W2) and 473nm (W3) enter the fθ lens.

As can be understood from Figures 14B to 14D, in the fθ lens of this embodiment, the lateral color aberration is well corrected for the respective wavelengths in spite of a simple structure consisting of only three lens elements in two lens groups.

In the second embodiment shown in Figure 15A, the first lens L1' has a negative refracting power, the second lens

L2' has a positive refracting power and the power of the first lens group is set substantially at the middle of the range defined by the formula (8). The radii of curvature R of the refracting surfaces, the axial surface separations d, and the refractive indexes n_d and the Abbe's numbers ν_d of the lenses for the sodium d-line in the fθ lens of this embodiment are shown in table 15.

Table15

wavelength W1;680nm, W2;532nm, W3;473nm, angle of view 55.7°

i	Ri	di	n_d	ν_d
OBJ	-	infinity		
0	infinity	0.14220		
1	0.96791	0.01905	n_{d1} 1.48749	ν_{d1} 70.4
2	0.22673	0.09524	n_{d2} 1.49700	ν_{d2} 81.6
3	-0.36345	0.02250		
4	-0.20429	0.02370	n_{d3} 1.80450	ν_{d3} 39.6
5	-0.27455	0.94015		
surface scanned	infinity	-		

$|\nu_{d1}-\nu_{d2}|=11.2$
$\Sigma(\phi i/\nu_{di})=-0.004$
$\nu_{dL}=81.6$
$\phi_{12}=1.86$
$d_{12}=0.02250$

lateral color aberration 0.037x10^{-3}
curvature of field 0.023
fθ characteristic 1.35%

Figures 15B to 15D respectively show the lateral color aberration, the astigmatic field curves in the scanning direction and the linearity of the fθ lens of the second embodiment when laser beams having wavelengths of 680nm (W1), 532nm (W2) and 473nm (W3) enter the fθ lens.

As can be understood from Figures 15B to 15D, in the fθ lens of this embodiment, the lateral color aberration is well corrected for the respective wavelengths in spite of a simple structure consisting of only three lens elements in two lens groups.

In the third embodiment shown in Figure 16A, the first lens L1' has a positive refracting power, the second lens L2' has a negative refracting power and the third lend L3' has a positive refracting power. Further the sum of the values obtained by dividing the powers of the respective lenses by the Abbe's numbers of the respective lenses is set close to the lower limit of the range defined by the formula (6) and the power of the first lens group is set close to the lower limit of the range defined by the formula (8). The radii of curvature R of the refracting surfaces, the axial surface separations d, and the refractive indexes n_d and the Abbe's numbers ν_d of the lenses for the sodium d-line in the fθ lens of this embodiment are shown in table 16.

Table 16

wavelength W1;680nm, W2;532nm, W3;473nm, angle of view 55.7°

i	Ri	di	n_d	ν_d
OBJ	-	infinity		
0	infinity	0.14220		
1	1.65490	0.09480	n_{d1} 1.49700	ν_{d1} 81.6
2	-0.12295	0.01896	n_{d2} 1.62012	ν_{d2} 49.8
3	-0.34948	0.05834		
4	-0.14919	0.02370	n_{d3} 1.80610	ν_{d3} 33.3
5	-0.15976	0.97879		
surface scanned	infinity	-		

$|\nu_{d1}-\nu_{d2}|=31.8$
$\Sigma(\phi i/\nu_{di})=-0.011$
$\nu_{dL}=81.6$
$\phi_{12}=1.07$
$d_{12}=0.05834$

lateral color aberration 0.046x10^{-3}
curvature of field 0.023
fθ characteristic 0.92%

Figures 16B to 16D respectively show the lateral color aberration, the astigmatic field curves in the scanning direction and the linearity of the fθ lens of the third embodiment when laser beams having wavelengths of 680nm (W1), 532nm (W2) and 473nm (W3) enter the fθ lens.

As can be understood from Figures 16B to 16D, in the fθ lens of this embodiment, the lateral color aberration is well corrected for the respective wavelengths in spite of a simple structure consisting of only three lens elements in two lens groups.

In the fourth embodiment shown in Figure 17A, the first lens L1' has a positive refracting power, the second lens L2' has a negative refracting power and the surface separation d_{12} between the first and second lens groups is set close to the upper limit of the range defined by the formula (9). The radii of curvature R of the refracting surfaces, the axial surface separations d, and the refractive indexes n_d and the Abbe's numbers ν_d of the lenses for the sodium d-line in the fθ lens of this embodiment are shown in table 17.

Table 17

wavelength W1;680nm, W2;532nm, W3;473nm, angle of view 55.7°

i	Ri	di	n_d	ν_d
OBJ	-	infinity		
0	infinity	0.14220		
1	1.21407	0.09480	n_{d1} 1.49700	ν_{d1} 81.6
2	-0.11808	0.18960	n_{d2} 1.53996	ν_{d2} 59.7
3	-0.49715	0.21251		
4	-0.16849	0.02370	n_{d3} 1.56873	ν_{d3} 63.1
5	-0.18138	0.75813		
surface scanned	infinity	-		

$|\nu_{d1}-\nu_{d2}|=21.9$
$\Sigma(\phi i/\nu_{di})=-0.004$
$\nu_{dL}=81.6$
$\phi_{12}=1.11$
$d_{12}=0.21251$

lateral color aberration 0.018x10^{-3}
curvature of field 0.026
$f\theta$ characteristic 1.40%

Figures 17B to 17D respectively show the lateral color aberration, the astigmatic field curves in the scanning direction and the linearity of the fθ lens of the fourth embodiment when laser beams having wavelengths of 680nm (W1), 532nm (W2) and 473nm (W3) enter the fθ lens.

As can be understood from Figures 17B to 17D, in the fθ lens of this embodiment, the lateral color aberration is well corrected for the respective wavelengths in spite of a simple structure consisting of only three lens elements in two lens groups.

In the fifth embodiment shown in Figure 18A, both the first and second lenses L1' and L2' have positive refracting powers, the difference in the Abbe's number between the first and second lenses is set close to the upper limit of the range which is defined by the formula (5) and determined from the practical viewpoints such as manufacturing cost and the like. The radii of curvature R of the refracting surfaces, the axial surface separations d, and the refractive indexes n_d and the Abbe's numbers ν_d of the lenses for the sodium d-line in the fθ lens of this embodiment are shown in table 18.

Table 18

wavelength W1;680nm, W2;532nm, W3;473nm, angle of view 55.7°

i	Ri	di	n_d	ν_d
OBJ	-	infinity		
0	infinity	0.14220		
1	0.77508	0.09480	n_{d1} 1.45650	ν_{d1} 90.8
2	-0.46275	0.18960	n_{d2} 1.80518	ν_{d2} 25.5
3	-0.37110	0.02889		
4	-0.21405	0.02370	n_{d3} 1.80518	ν_{d3} 25.5
5	-0.30344	0.92581		
surface scanned	infinity	-		

$|\nu_{d1}-\nu_{d2}|=65.3$
$\Sigma(\phi i/\nu_{di})=-0.001$
$\nu_{dL}=90.8$
$\phi_{12}=1.97$
$d_{12}=0.02889$

lateral color aberration 0.066x10^{-3}
curvature of field 0.026
$f\theta$ characteristic 1.44%

Figures 18B to 18D respectively show the lateral color aberration, the astigmatic field curves in the scanning direction and the linearity of the fθ lens of the fifth embodiment when laser beams having wavelengths of 680nm (W1), 532nm (W2) and 473nm (W3) enter the fθ lens.

As can be understood from Figures 18B to 18D, in the fθ lens of this embodiment, the lateral color aberration is well corrected for the respective wavelengths in spite of a simple structure consisting of only three lens elements in two lens groups.

In the sixth embodiment shown in Figure 19A, the first lens L1' has a positive refracting power and the second lens L2' has a negative refracting power. Further the sum of the values obtained by dividing the powers of the respective lenses by the Abbe's numbers of the respective lenses is set close to the upper limit of the range defined by the formula (6). The radii of curvature R of the refracting surfaces, the axial surface separations d, and the refractive indexes n_d and the Abbe's numbers ν_d of the lenses for the sodium d-line in the fθ lens of this embodiment are shown in table 19.

Table19

wavelength W1;680nm, W2;532nm, W3;473nm, angle of view 55.7°

i	Ri	di	n_d	ν_d
OBJ	-	infinity		
0	infinity	0.14220		
1	0.99859	0.09480	n_{d1} 1.49700	ν_{d1} 81.6
2	-0.13870	0.01896	n_{d2} 1.50378	ν_{d2} 66.9
3	-0.32198	0.01262		
4	-0.21507	0.02370	n_{d3} 1.60729	ν_{d3} 49.3
5	-0.34034	0.94833		
surface scanned	infinity	-		

$|\nu_{d1}-\nu_{d2}|=14.7$

$\Sigma(\phi i/\nu_{di})=-0.001$

$\nu_{dL}=81.6$

$\phi_{12}=1.96$

$d_{12}=0.01262$

lateral color aberration 0.025x10^{-3}

curvature of field 0.023

$f\theta$ characteristic 2.04%

Figures 19B to 19D respectively show the lateral color aberration, the astigmatic field curves in the scanning direction and the linearity of the fθ lens of the sixth embodiment when laser beams having wavelengths of 680nm (W1), 532nm (W2) and 473nm (W3) enter the fθ lens.

As can be understood from Figures 19B to 19D, in the fθ lens of this embodiment, the lateral color aberration is well corrected for the respective wavelengths in spite of a simple structure consisting of only three lens elements in two lens groups.

In the seventh embodiment shown in Figure 20A, the first lens L1' has a positive refracting power and the second lens L2' has a negative refracting power. Further the difference in the Abbe's number between the first and second lenses is set close to the lower limit of the range defined by the formula (5) and the Abbe's number ν_{dL} for the sodium d-line of one of the first and second lenses having the smaller dispersive power than the other is set close to the lower limit of the range defined by the formula (7). The radii of curvature R of the refracting surfaces, the axial surface separations d, and the refractive indexes n_d and the Abbe's numbers ν_d of the lenses for the sodium d-line in the fθ lens of this embodiment are shown in table 20.

Table20

wavelength W1;680nm, W2;532nm, W3;473nm, angle of view 55.7°

i	Ri	di	n_d	ν_d
OBJ	-	infinity		
0	infinity	0.14220		
1	0.63606	0.09480	n_{d1} 1.66446	ν_{d1} 35.9
2	-0.11059	0.01896	n_{d2} 1.64769	ν_{d2} 33.8
3	-0.52266	0.05358		
4	-0.18894	0.02370	n_{d3} 1.78470	ν_{d3} 26.1
5	-0.32143	0.81368		
surface scanned	infinity	-		

$|\nu_{d1}-\nu_{d2}|=2.1$

$\Sigma(\phi i/\nu_{di})=-0.008$

$\nu_{dL}=35.9$

$\phi_{12}=2.35$

$d_{12}=0.05358$

lateral color aberration 0.091×10^{-3}

curvature of field 0.023

$f\theta$ characteristic 1.47%

Figures 20B to 20D respectively show the lateral color aberration, the astigmatic field curves in the scanning direction and the linearity of the fθ lens of the seventh embodiment when laser beams having wavelengths of 680nm (W1), 532nm (W2) and 473nm (W3) enter the fθ lens.

As can be understood from Figures 20B to 20D, in the fθ lens of this embodiment, the lateral color aberration is well corrected for the respective wavelengths in spite of a simple structure consisting of only three lens elements in two lens groups.

As can be understood from the description above, in the fθ lens in accordance with the second aspect of the present invention, the color aberration can be corrected with a high accuracy over a wide wavelength range, and accordingly, the error in superimposing the beam spots can be reduced in the scanning optical system or the like using a plurality of laser beams having different wavelengths. Further since being simple in structure, the fθ lens in accordance with the second aspect of the present invention can be manufactured at low cost.

The fθ lens in accordance with the second aspect of the present invention need not be limited to those described above but may be variously modified so long as the formulae (5) to (9) are satisfied.

The fθ lenses of eighth to eleventh embodiments shown in Figures 21A to 24A comprise an aspheric lens represented by the formula (13).

In the eighth embodiment shown in Figure 21A, the first surface of the first lens L1' (the entrance surface) is an aspheric surface as shown in table 21 and the first lens has a positive refracting power. The second lens L2' has a negative refracting power. Further the power of the first lens group is set close to the upper limit of the range defined by the formula (8) and the surface separation d_{12} between the first and second lens groups is set substantially at the middle of the range defined by the formula (9). The radii of curvature R of the refracting surfaces, the axial surface separations d, and the refractive indexes n_d and the Abbe's numbers ν_d of the lenses for the sodium d-line in the fθ lens of this embodiment are shown in table 21.

Table 21

wavelength W1;680nm, W2;532nm, W3;473nm, angle of view 55.7°

i	Ri	di	n_d	ν_d
OBJ	-	infinity		
0	infinity	0.19093		
1	0.60502★	0.09489	n_{d1} 1.62280	ν_{d1} 56.9
2	-0.15804	0.01898	n_{d2} 1.54041	ν_{d2} 51.0
3	-1.04490	0.09063		
4	-0.24204	0.02372	n_{d3} 1.57845	ν_{d3} 41.7
5	-0.55340	0.73573		
surface scanned	infinity	-		

$|\nu_{d1}-\nu_{d2}|=5.9$ lateral color aberration 0.067×10^{-3}

$\Sigma(\phi i/\nu_{di})=-0.005$ curvature of field 0.011

$\nu_{dL}=56.9$ $f\theta$ characteristic 1.01%

$\phi_{12}=2.01$

$d_{12}=0.09063$

$k=-1.9206$ $a_1=-3.3812$ $a_2=1.6691$ $a_3=0$ $a_4=0$

Figures 21B to 21D respectively show the lateral color aberration, the astigmatic field curves in the scanning direction and the linearity of the fθ lens of the eighth embodiment when laser beams having wavelengths of 680nm (W1), 532nm (W2) and 473nm (W3) enter the fθ lens.

As can be understood from Figures 21B to 21D, in the fθ lens of this embodiment, the lateral color aberration is well corrected for the respective wavelengths in spite of a simple structure consisting of only three lens elements in two lens groups.

In the ninth embodiment shown in Figure 22A, the second surface of the second lens L2' (the exit surface) is an aspheric surface as shown in table 22 and the second lens L2' has a positive refracting power. The first lens L1' has a negative refracting power. The radii of curvature R of the refracting surfaces, the axial surface separations d, and the refractive indexes n_d and the Abbe's numbers ν_d of the lenses for the sodium d-line in the fθ lens of this embodiment are shown in table 22.

Table 22

wavelength W1;680nm, W2;532nm, W3;473nm, angle of view 55.7°

i	Ri	di	n_d	ν_d
OBJ	-	infinity		
0	infinity	0.20745		
1	9.65432	0.01905	n_{d1} 1.48749	ν_{d1} 70.4
2	0.38653	0.09525	n_{d2} 1.49700	ν_{d2} 81.6
3	-0.26969★	0.06585		
4	-0.17725	0.02381	n_{d3} 1.80450	ν_{d3} 39.6
5	-0.23743	0.89559		
surface scanned	infinity	-		

$|\nu_{d1}-\nu_{d2}|=11.2$ lateral color aberration 0.048×10^{-3}

$\Sigma(\phi i/\nu_{di})=-0.005$ curvature of field 0.001

$\nu_{dL}=81.6$ $f\theta$ characteristic 0.85%

$\phi_{12}=1.92$

$d_{12}=0.06585$

$k=1.1996$ $a_1=0.7967$ $a_2=3.8706$ $a_3=0$ $a_4=0$

Figures 22B to 22D respectively show the lateral color aberration, the astigmatic field curves in the scanning direction and the linearity of the fθ lens of the ninth embodiment when laser beams having wavelengths of 680nm (W1), 532nm (W2) and 473nm (W3) enter the fθ lens.

As can be understood from Figures 22B to 22D, in the fθ lens of this embodiment, the lateral color aberration is well corrected for the respective wavelengths in spite of a simple structure consisting of only three lens elements in two lens groups.

In the tenth embodiment shown in Figure 23A, the first surface of the third lens L3' (the entrance surface) is an aspheric surface as shown in table 23. The power of the first lens group is set to the upper limit of the range defined by the formula (8). The radii of curvature R of the refracting surfaces, the axial surface separations d, and the refractive indexes n_d and the Abbe's numbers ν_d of the lenses for the sodium d-line in the fθ lens of this embodiment are shown in table 23.

Table 23

wavelength W1;680nm, W2;532nm, W3;473nm, angle of view 55.7°

i	Ri	di	n_d	ν_d
OBJ	-	infinity		
0	infinity	0.16651		
1	-1.43764	0.09515	n_{d1} 1.49700	ν_{d1} 81.6
2	-0.12062	0.01903	n_{d2} 1.50378	ν_{d2} 66.9
3	-0.17870	0.05837		
4	-0.13985★	0.02368	n_{d3} 1.60729	ν_{d3} 49.3
5	-0.23434	0.90103		
surface scanned	infinity	-		

$|\nu_{d1}-\nu_{d2}| = 14.7$ lateral color aberration 0.048×10^{-3}

$\Sigma(\phi i/\nu_{di}) = -0.003$ curvature of field 0.002

$\nu_{dL} = 81.6$ $f\theta$ characteristic 0.72%

$\phi_{12} = 2.50$

$d_{12} = 0.05837$

$k = -0.2987$ $a_1 = -1.1856$ $a_2 = -61.0250$ $a_3 = 0$ $a_4 = 0$

Figures 23B to 23D respectively show the lateral color aberration, the astigmatic field curves in the scanning direction and the linearity of the fθ lens of the tenth embodiment when laser beams having wavelengths of 680nm (W1), 532nm (W2) and 473nm (W3) enter the fθ lens.

As can be understood from Figures 23B to 23D, in the fθ lens of this embodiment, the lateral color aberration is well corrected for the respective wavelengths in spite of a simple structure consisting of only three lens elements in two lens groups.

In the eleventh embodiment shown in Figure 24A, the second surface (the exit surface) of the third lend L3' is an aspheric surface as shown in table 24. Further the sum of the values obtained by dividing the powers of the respective lenses by the Abbe's numbers of the respective lenses is set substantially at the middle of the range defined by the formula (6) and the power of the first lens group is set close to the lower limit of the range defined by the formula (8). The radii of curvature R of the refracting surfaces, the axial surface separations d, and the refractive indexes n_d and the Abbe's numbers ν_d of the lenses for the sodium d-line in the fθ lens of this embodiment are shown in table 24.

Table 24

wavelength W1;680nm, W2;532nm, W3;473nm, angle of view 55.7°

i	Ri	di	n_d	ν_d
OBJ	-	infinity		
0	infinity	0.14195		
1	-42.5251	0.09463	n_{d1} 1.49700	ν_{d1} 81.6
2	-0.12060	0.01893	n_{d2} 1.62012	ν_{d2} 49.8
3	-0.28146	0.04029		
4	-0.16066	0.02366	n_{d3} 1.80610	ν_{d3} 33.3
5	-0.17571★	1.01298		
surface scanned	infinity	-		

$|\nu_{d1}-\nu_{d2}|=31.8$ lateral color aberration 0.048x10^{-3}

$\Sigma(\phi i/\nu_{di})=-0.010$ curvature of field 0.008

$\nu_{dL}=81.6$ fθ characteristic 0.55%

$\phi_{12}=1.20$

$d_{12}=0.04029$

$k=0.0608$ $a_1=-0.1573$ $a_2=9.2171$ $a_3=0$ $a_4=0$

Figures 24B to 24D respectively show the lateral color aberration, the astigmatic field curves in the scanning direction and the linearity of the fθ lens of the eleventh embodiment when laser beams having wavelengths of 680nm (W1), 532nm (W2) and 473nm (W3) enter the fθ lens.

As can be understood from Figures 24B to 24D, in the fθ lens of this embodiment, the lateral color aberration is well corrected for the respective wavelengths in spite of a simple structure consisting of only three lens elements in two lens groups.

fθ lenses of eleven embodiments in accordance with the third aspect of the present invention will be described with reference to Figures 25 (25A to 25D) to 35 (35A to 35D) and tables 25 to 35, hereinbelow. Figures 25A to 35A respectively show the arrangements of the lens elements of the fθ lenses of first to eleventh embodiments, and Figures 25B, 25C and 25D to 35B, 35C and 35D respectively show the lateral color aberration, the astigmatic field curves (curvature of field) and the linearity (fθ characteristic) of the fθ lenses of the first to eleventh embodiments when three laser beams having different wavelengths W1, W2 and W3 used in a scanning optical system enter the respective fθ lenses. The values of the wavelengths W1, W2 and W3 are shown on the top of the tables corresponding to the fθ lenses.

Each of the fθ lenses in accordance with the third aspect of the present invention is for scanning light emanating from a deflecting point and comprises a first lens L1" having a positive refracting power and second lens L2" having a negative refracting power, the first and second lenses L1" and L2" being cemented together with the first lens L1" positioned on the entrance pupil side (deflecting point side). The fθ lens satisfies the following formulae (10) to (12),

$$n_{d1}<n_{d2} \tag{10}$$

$$0.4\leqq\nu_{d2}/\nu_{d1}\leqq0.8 \tag{11}$$

$$1.5\leqq\phi_1\leqq4.7 \tag{12}$$

wherein n_{d1} and n_{d2} respectively represent the refractive indexes for the sodium d-line of the first and second lenses L1" and L2", ν_{d1} and ν_{d2} respectively represent the Abbe's numbers for the sodium d-line of the first and second lenses L1" and L2", and ϕ_1 represents the power of the first lens L1" standardized on the basis of the power of the whole system. The fθ lens is used in a position where the distance d_0 between the deflecting point and the entrance pupil side surface of the first lens L1" standardized on the basis of the focal length of the whole system is in the range of 0.1 to 0.4 inclusive ($0.1 \leqq d_0 \leqq 0.4$;either of these values being standardized on the basis of the focal length of the whole system).

In the first embodiment shown in Figure 25A, the factors respectively limited by the formulae (11) and (12) are set close to the lower limits of the ranges respectively defined by the formulae (11) and (12) and the distance d_0 is set close to the upper limit. The radii of curvature R of the refracting surfaces, the axial surface separations d, and the refractive indexes n_d and the Abbe's numbers ν_d of the lenses for the sodium d-line in the fθ lens of this embodiment are shown in table 25.

Table 25

wavelength W1;680nm, W2;532nm, W3;473nm, angle of view 55.7°

i	Ri	di	n_d	ν_d
OBJ	-	infinity		
0	infinity	0.30415		
1	3.22923	0.10930	n_{d1} 1.49700	ν_{d1} 81.6
2	-0.27449	0.02376	n_{d2} 1.72342	ν_{d2} 38.0
3	-0.43441	0.99803		
surface scanned	infinity	-		

$n_{d1}=1.497$, $n_{d2}=1.723$
$\nu_{d1}/\nu_{d2}=0.47$
$\phi_1=1.95$
$d_0=0.30415$

lateral color aberration	0.138×10^{-3}
curvature of field	0.011
$f\theta$ characteristic	0.43%

Figures 25B to 25D respectively show the lateral color aberration, the astigmatic field curves in the scanning direction and the linearity of the fθ lens of the first embodiment when laser beams having wavelengths of 680nm (W1), 532nm (W2) and 473nm (W3) enter the fθ lens.

As can be understood from Figures 25B to 25D, in the fθ lens of this embodiment, the lateral color aberration is well corrected for the respective wavelengths in spite of a very simple structure consisting of only two lens elements in one lens group.

In the second embodiment shown in Figure 26A, the ratio of the Abbe's number of the first lens to that of the second lend is set close to the lower limit of the range defined by the formula (11). The radii of curvature R of the refracting surfaces, the axial surface separations d, and the refractive indexes n_d and the Abbe's numbers ν_d of the lenses for the sodium d-line in the fθ lens of this embodiment are shown in table 26.

Table 26

wavelength W1;680nm, W2;532nm, W3;473nm, angle of view 55.7°

i	Ri	di	n_d	ν_d
OBJ	-	infinity		
0	infinity	0.26657		
1	2.79072	0.09520	n_{d1} 1.48749	ν_{d1} 70.4
2	-0.26207	0.02380	n_{d2} 1.80610	ν_{d2} 33.3
3	-0.39849	1.00254		
surface scanned	infinity	-		

$n_{d1}=1.487$, $n_{d2}=1.806$
$\nu_{d1}/\nu_{d2}=0.47$
$\phi_1=2.02$
$d_0=0.26657$

lateral color aberration 0.143x10^{-3}
curvature of field 0.011
fθ characteristic 0.77%

Figures 26B to 26D respectively show the lateral color aberration, the astigmatic field curves in the scanning direction and the linearity of the fθ lens of the second embodiment when laser beams having wavelengths of 680nm (W1), 532nm (W2) and 473nm (W3) enter the fθ lens.

As can be understood from Figures 25B to 25D, in the fθ lens of this embodiment, the lateral color aberration is well corrected for the respective wavelengths in spite of a very simple structure consisting of only two lens elements in one lens group.

In the third embodiment shown in Figure 27A, the distance d_0 is set close to the lower limit. The radii of curvature R of the refracting surfaces, the axial surface separations d, and the refractive indexes n_d and the Abbe's numbers ν_d of the lenses for the sodium d-line in the fθ lens of this embodiment are shown in table 27.

Table 27

wavelength W1;680nm, W2;532nm, W3;473nm, angle of view 55.7°

i	Ri	di	n_d	ν_d
OBJ	-	infinity		
0	infinity	0.14865		
1	1.09840	0.06713	n_{d1} 1.51680	ν_{d1} 64.2
2	-0.14539	0.01918	n_{d2} 1.67003	ν_{d2} 47.2
3	-0.42289	0.98566		
surface scanned	infinity	-		

$n_{d1}=1.517$, $n_{d2}=1.670$
$\nu_{d1}/\nu_{d2}=0.74$
$\phi_1=3.97$
$d_0=0.14865$

lateral color aberration 0.115×10^{-3}
curvature of field 0.027
$f\theta$ characteristic 2.90%

Figures 27B to 27D respectively show the lateral color aberration, the astigmatic field curves in the scanning direction and the linearity of the fθ lens of the third embodiment when laser beams having wavelengths of 680nm (W1), 532nm (W2) and 473nm (W3) enter the fθ lens.

As can be understood from Figures 27B to 27D, in the fθ lens of this embodiment, the lateral color aberration is well corrected for the respective wavelengths in spite of a very simple structure consisting of only two lens elements in one lens group.

In the fourth embodiment shown in Figure 28A, the factors respectively limited by the formulae (11) and (12) are set close to the upper limits of the ranges respectively defined by the formulae (11) and (12). The radii of curvature R of the refracting surfaces, the axial surface separations d, and the refractive indexes n_d and the Abbe's numbers ν_d of the lenses for the sodium d-line in the fθ lens of this embodiment are shown in table 28.

Table 28

wavelength W1;680nm, W2;532nm, W3;473nm, angle of view 55.7°

i	Ri	di	n_d	ν_d
OBJ	-	infinity		
0	infinity	0.15435		
1	1.33208	0.05788	n_{d1} 1.56883	ν_{d1} 56.0
2	-0.14870	0.01929	n_{d2} 1.72000	ν_{d2} 42.0
3	-0.45323	0.99074		
surface scanned	infinity	-		

$n_{d1}=1.569$, $n_{d2}=1.720$
$\nu_{d1}/\nu_{d2}=0.75$
$\phi_1=4.21$
$d_0=0.15435$

lateral color aberration 0.106x10^{-3}
curvature of field 0.027
fθ characteristic 3.00%

Figures 28B to 28D respectively show the lateral color aberration, the astigmatic field curves in the scanning direction and the linearity of the fθ lens of the fourth embodiment when laser beams having wavelengths of 680nm (W1), 532nm (W2) and 473nm (W3) enter the fθ lens.

As can be understood from Figures 28B to 28D, in the fθ lens of this embodiment, the lateral color aberration is well corrected for the respective wavelengths in spite of a very simple structure consisting of only two lens elements in one lens group.

In the fifth embodiment shown in Figure 29A, the Abbe's number ν_{d1} of the first lens L1" is smaller than that in the other embodiments. The radii of curvature R of the refracting surfaces, the axial surface separations d, and the refractive indexes n_d and the Abbe's numbers ν_d of the lenses for the sodium d-line in the fθ lens of this embodiment are shown in table 29.

Table 29

wavelength W1;680nm, W2;532nm, W3;473nm, angle of view 55.7°

i	Ri	di	n_d	ν_d
OBJ	-	infinity		
0	infinity	0.16754		
1	1.62437	0.06702	n_{d1} 1.59270	ν_{d1} 35.5
2	-0.17459	0.01436	n_{d2} 1.80518	ν_{d2} 25.5
3	-0.43526	0.99134		
surface scanned	infinity	-		

$n_{d1}=1.593$, $n_{d2}=1.805$
$\nu_{d1}/\nu_{d2}=0.72$
$\phi_1=3.74$
$d_0=0.16754$

lateral color aberration 0.143×10^{-3}
curvature of field 0.022
$f\theta$ characteristic 2.41%

Figures 29B to 29D respectively show the lateral color aberration, the astigmatic field curves in the scanning direction and the linearity of the fθ lens of the fifth embodiment when laser beams having wavelengths of 680nm (W1), 532nm (W2) and 473nm (W3) enter the fθ lens.

As can be understood from Figures 29B to 29D, in the fθ lens of this embodiment, the lateral color aberration is well corrected for the respective wavelengths in spite of such a small Abbe's number of the first lens L1" as shown in table 29 and in spite of a very simple structure consisting of only two lens elements in one lens group.

In the sixth embodiment shown in Figure 30A, the refractive index n_{d1} of the first lens L1" is higher than that in the other embodiments. The radii of curvature R of the refracting surfaces, the axial surface separations d, and the refractive indexes n_d and the Abbe's numbers ν_d of the lenses for the sodium d-line in the fθ lens of this embodiment are shown in table 30.

Table30

wavelength W1;680nm, W2;532nm, W3;473nm, angle of view 55.7°

i	Ri	di	n_d	ν_d
OBJ	-	infinity		
0	infinity	0.20070		
1	3.17313	0.07168	n_{d1} 1.72000	ν_{d1} 50.3
2	-0.19268	0.01911	n_{d2} 1.83400	ν_{d2} 37.3
3	-0.61013	0.99436		
surface scanned	infinity	-		

$n_{d1}=1.720$, $n_{d2}=1.834$
$\nu_{d1}/\nu_{d2}=0.74$
$\phi_1=3.95$
$d_0=0.20070$

lateral color aberration 0.143x10-3
curvature of field 0.018
$f\theta$ characteristic 2.06%

Figures 30B to 30D respectively show the lateral color aberration, the astigmatic field curves in the scanning direction and the linearity of the fθ lens of the sixth embodiment when laser beams having wavelengths of 680nm (W1), 532nm (W2) and 473nm (W3) enter the fθ lens.

As can be understood from Figures 30B to 30D, in the fθ lens of this embodiment, the lateral color aberration is well corrected for the respective wavelengths in spite of such a high refractive index of the first lens L1" as shown in table 30 and in spite of a very simple structure consisting of only two lens elements in one lens group.

In the seventh embodiment shown in Figure 31A, the factors respectively limited by the formulae (11) and (12) are set substantially at the middle of the ranges respectively defined by the formulae (11) and (12). The radii of curvature R of the refracting surfaces, the axial surface separations d, and the refractive indexes n_d and the Abbe's numbers ν_d of the lenses for the sodium d-line in the fθ lens of this embodiment are shown in table 31.

Table 31

wavelength W1;810nm, W2;750nm, W3;680nm, angle of view 62.5°

i	Ri	di	n_d	ν_d
OBJ	-	infinity		
0	infinity	0.19948		
1	1.90834	0.08976	n_{d1} 1.51680	ν_{d1} 64.2
2	-0.20983	0.01995	n_{d2} 1.71852	ν_{d2} 33.5
3	-0.42608	0.99160		
surface scanned	infinity	-		

$n_{d1}=1.517$, $n_{d2}=1.719$
$\nu_{d1}/\nu_{d2}=0.52$
$\phi_1=2.67$
$d_0=0.19948$

lateral color aberration 0.071×10^{-3}
curvature of field 0.024
$f\theta$ characteristic 1.49%

Figures 31B to 31D respectively show the lateral color aberration, the astigmatic field curves in the scanning direction and the linearity of the fθ lens of the seventh embodiment when laser beams having wavelengths of 810nm (W1), 750nm (W2) and 680nm (W3) which are different from those of the laser beams used in the first to sixth embodiments enter the fθ lens.

As can be understood from Figures 31B to 31D, in the fθ lens of this embodiment, the lateral color aberration is well corrected irrespective of wavelength in spite of a very simple structure consisting of only two lens elements in one lens group.

In the eighth embodiment shown in Figure 32A, the factors respectively limited by the formulae (11) and (12) are set substantially at the middle of the ranges respectively defined by the formulae (11) and (12) as in the seventh embodiment. The radii of curvature R of the refracting surfaces, the axial surface separations d, and the refractive indexes n_d and the Abbe's numbers ν_d of the lenses for the sodium d-line in the fθ lens of this embodiment are shown in table 32.

Table 32

wavelength W1;870nm, W2;810nm, W3;750nm, angle of view 62.5°

i	Ri	di	n_d	ν_d
OBJ	-	infinity		
0	infinity	0.19905		
1	1.64325	0.08957	n_{d1} 1.51742	ν_{d1} 52.2
2	-0.20875	0.01991	n_{d2} 1.72825	ν_{d2} 28.3
3	-0.43041	0.98895		
surface scanned	infinity	-		

$n_{d1}=1.517$, $n_{d2}=1.728$
$\nu_{d1}/\nu_{d2}=0.54$
$\phi_1=2.71$
$d_0=0.19905$

lateral color aberration 0.064x10^{-3}
curvature of field 0.024
$f\theta$ characteristic 1.05%

Figures 32B to 32D respectively show the lateral color aberration, the astigmatic field curves in the scanning direction and the linearity of the fθ lens of the eighth embodiment when laser beams having wavelengths of 870nm (W1), 810nm (W2) and 750nm (W3) which are different from those of the laser beams used in the first to seventh embodiments enter the fθ lens.

As can be understood from Figures 32B to 32D, in the fθ lens of this embodiment, the lateral color aberration is well corrected irrespective of wavelength in spite of a very simple structure consisting of only two lens elements in one lens group.

In the ninth embodiment shown in Figure 33A, the factors respectively limited by the formulae (11) and (12) are set substantially at the middle of the ranges respectively defined by the formulae (11) and (12) as in the seventh and eighth embodiments. The radii of curvature R of the refracting surfaces, the axial surface separations d, and the refractive indexes n_d and the Abbe's numbers ν_d of the lenses for the sodium d-line in the fθ lens of this embodiment are shown in table 33.

Table 33

wavelength W1;890nm, W2;830nm, W3;780nm, angle of view 62.5°

i	Ri	di	n_d	ν_d
OBJ	-	infinity		
0	infinity	0.19915		
1	1.74894	0.08962	n_{d1} 1.51742	ν_{d1} 52.2
2	-0.21778	0.01991	n_{d2} 1.80518	ν_{d2} 25.5
3	-0.40058	0.99321		
surface scanned	infinity	-		

$n_{d1}=1.517$, $n_{d2}=1.805$
$\nu_{d1}/\nu_{d2}=0.49$
$\phi_1=2.59$
$d_0=0.19915$

lateral color aberration 0.028×10^{-3}
curvature of field 0.022
$f\theta$ characteristic 1.13%

Figures 33B to 33D respectively show the lateral color aberration, the astigmatic field curves in the scanning direction and the linearity of the fθ lens of the ninth embodiment when laser beams having wavelengths of 890nm (W1), 830nm (W2) and 780nm (W3) which are different from those of the laser beams used in the first to eighth embodiments enter the fθ lens.

As can be understood from Figures 33B to 33D, in the fθ lens of this embodiment, the lateral color aberration is well corrected irrespective of wavelength in spite of a very simple structure consisting of only two lens elements in one lens group.

As can be understood from the description above, in the fθ lens in accordance with the third aspect of the present invention, the color aberration can be corrected with a high accuracy over a wide wavelength range, and accordingly, the error in superimposing the beam spots can be reduced in the scanning optical system or the like using a plurality of laser beams having different wavelengths. Further since being very simple in structure, the fθ lens in accordance with the third aspect of the present invention can be manufactured at low cost, and at the same time, the scanning optical system can be small in size, assembly of the fθ lens is facilitated and the error in assembly can be reduced.

The fθ lens in accordance with the third aspect of the present invention need not be limited to those described above but may be variously modified so long as the formulae (10) to (12) are satisfied.

The fθ lenses of tenth and eleventh embodiments shown in Figures 34A and 35A comprise an aspheric lens represented by the formula (13).

In the tenth embodiment shown in Figure 34A, the second surface of the second lens L2" (the exit surface) is an aspheric surface as shown in table 34. Further, the factors respectively limited by the formulae (11) and (12) are set substantially at the middle of the ranges respectively defined by the formulae (11) and (12). The radii of curvature R of the refracting surfaces, the axial surface separations d, and the refractive indexes n_d and the Abbe's numbers ν_d of the lenses for the sodium d-line in the fθ lens of this embodiment are shown in table 34.

Table 34

wavelength W1;680nm, W2;532nm, W3;473nm, angle of view 55.7°

i	Ri	di	n_d	ν_d
OBJ	-	infinity		
0	infinity	0.21449		
1	1.58428	0.08580	n_{d1} 1.49700	ν_{d1} 81.6
2	-0.19942	0.02383	n_{d2} 1.65844	ν_{d2} 50.9
3	-0.43956★	0.98901		
surface scanned	infinity	-		

$n_{d1}=1.497$, $n_{d2}=1.658$ lateral color aberration 0.057×10^{-3}

$\nu_{d1}/\nu_{d2}=0.62$ curvature of field 0.003

$\phi_1=2.77$ $f\theta$ characteristic 1.00%

$d_0=0.21449$

$k=1.02636$ $a_1=1.74145$ $a_2=-0.88321$

$a_3=0.41777\times10^3$ $a_4=-0.61915\times10^4$

Figures 34B to 34D respectively show the lateral color aberration, the astigmatic field curves in the scanning direction and the linearity of the fθ lens of the tenth embodiment when laser beams having wavelengths of 680nm (W1), 532nm (W2) and 473nm (W3) enter the fθ lens.

As can be understood from Figures 34B to 34D, in the fθ lens of this embodiment, the lateral color aberration is well corrected for the respective wavelengths irrespective of a very simple structure consisting of only two lens elements in one lens group.

In the eleventh embodiment shown in Figure 35A, the first surface of the first lens L1" (the entrance surface) is an aspheric surface as shown in table 35. Further, the factors respectively limited by the formulae (11) and (12) are set substantially at the middle of the ranges respectively defined by the formulae (11) and (12). The radii of curvature R of the refracting surfaces, the axial surface separations d, and the refractive indexes n_d and the Abbe's numbers ν_d of the lenses for the sodium d-line in the fθ lens of this embodiment are shown in table 35.

Table 35

wavelength W1;680nm, W2;532nm, W3;473nm, angle of view 55.7°

i	Ri	di	n_d	ν_d
OBJ	-	infinity		
0	infinity	0.18333		
1	0.89104★	0.09532	n_{d1} 1.48749	ν_{d1} 70.4
2	-0.20918	0.01906	n_{d2} 1.74400	ν_{d2} 44.7
3	-0.44194	0.97190		
surface scanned	infinity	-		

$n_{d1}=1.487$, $n_{d2}=1.744$ lateral color aberration 0.095×10^{-3}

$\nu_{d1}/\nu_{d2}=0.63$ curvature of field 0.005

$\phi_1=2.81$ $f\theta$ characteristic 1.02%

$d_0=0.18333$

$k=-18.4838$ $a_1=0.3965$ $a_2=35.0041$ $a_3=0$ $a_4=0$

Figures 35B to 35D respectively show the lateral color aberration, the astigmatic field curves in the scanning direction and the linearity of the fθ lens of the eleventh embodiment when laser beams having wavelengths of 680nm (W1), 532nm (W2) and 473nm (W3) enter the fθ lens.

As can be understood from Figures 35B to 35D, in the fθ lens of this embodiment, the lateral color aberration is well corrected for the respective wavelengths irrespective of a very simple structure consisting of only two lens elements in one lens group.

Claims

1. An fθ lens comprising first and second lens groups arranged in this order from the entrance pupil side, the first lens group consisting of first and second lenses cemented together, the refracting powers of the first and second lenses being one of the combinations of negative and positive, positive and positive, and positive and negative, the second lens group consisting of a third lens having a positive or negative refracting power, and the first and second lens groups satisfying the following formulae (5) to (9),

$$2 \leqq |\nu_{d1}-\nu_{d2}| \quad (5)$$

$$-0.020 \leqq \Sigma(\phi_i/\nu_{di}) \leqq 0.005 \quad (6)$$

$$35 \leqq \nu_{dL} \quad (7)$$

$$1.0 \leqq \phi_{12} \leqq 2.5 \quad (8)$$

$$0.01 \leqq d_{12} \leqq 0.22 \quad (9)$$

wherein ϕ_i represents the power of i-th lens as numbered from the entrance pupil side standardized on the basis of the power of the whole system, ϕ_{12} represents the power of the first lens group standardized on the basis of the

power of the whole system, ν_{di} represents the Abbe's number for the sodium d-line of i-th lens as numbered from the entrance pupil side, ν_{dL} represents the Abbe's number for the sodium d-line of one of the first and second lenses having the smaller dispersive power than the other and d_{12} represents the surface separation between the first and second lens groups standardized on the basis of the focal length of the whole system.

FIG.1A

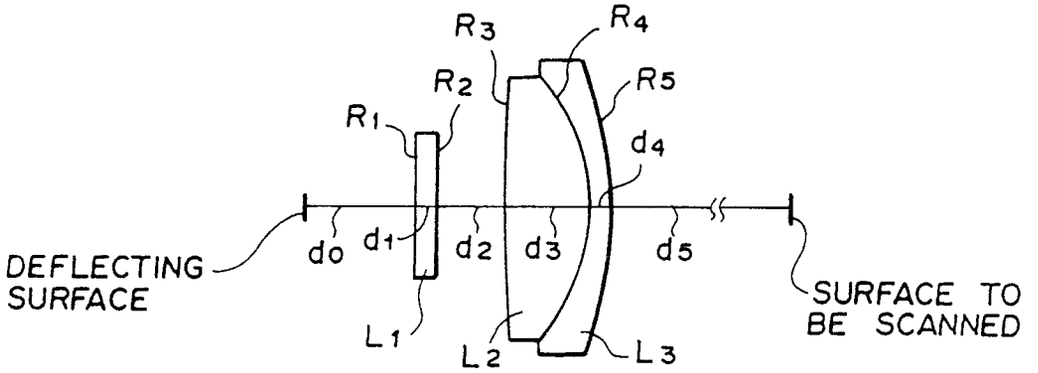


FIG.1B

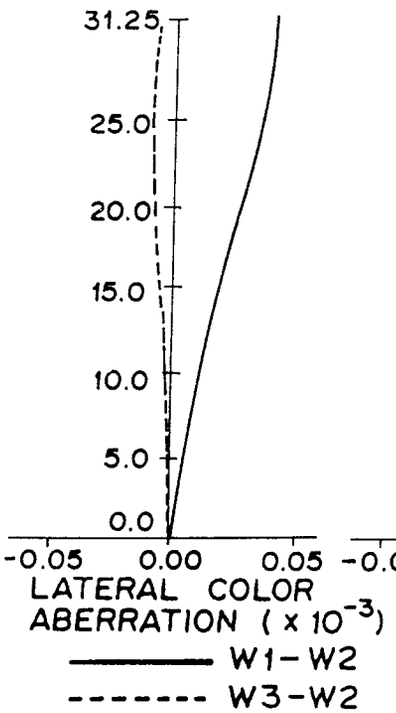


FIG.1C

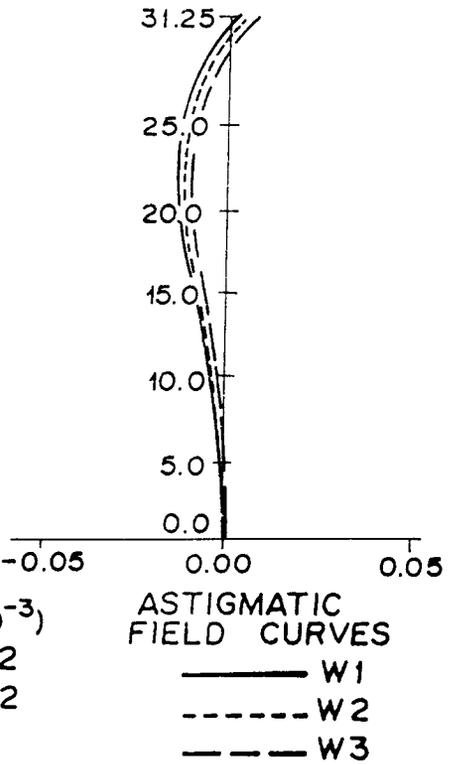


FIG.1D

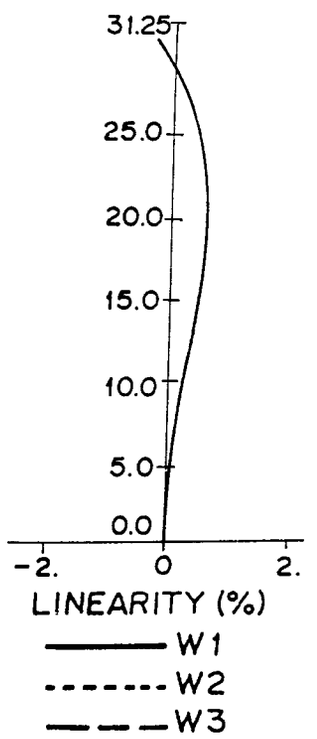


FIG.2A

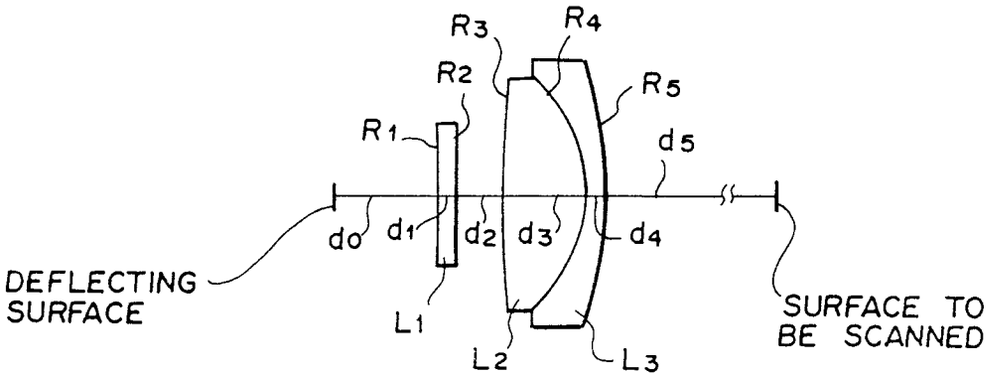


FIG.2B

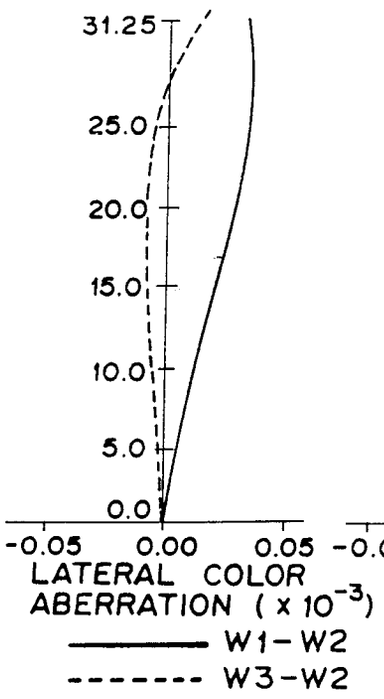


FIG.2C

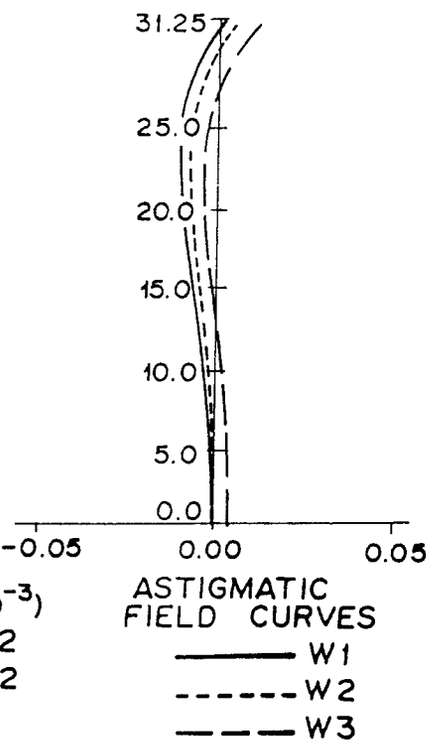


FIG.2D

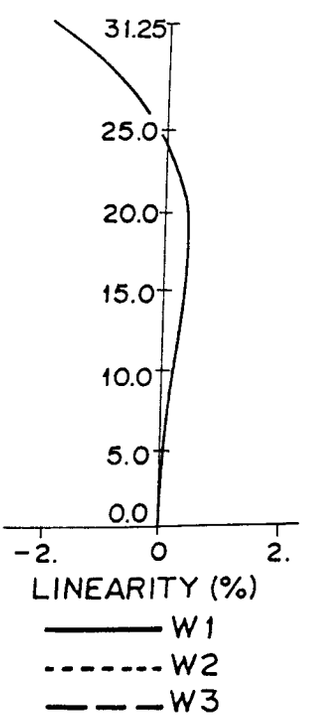


FIG.3A

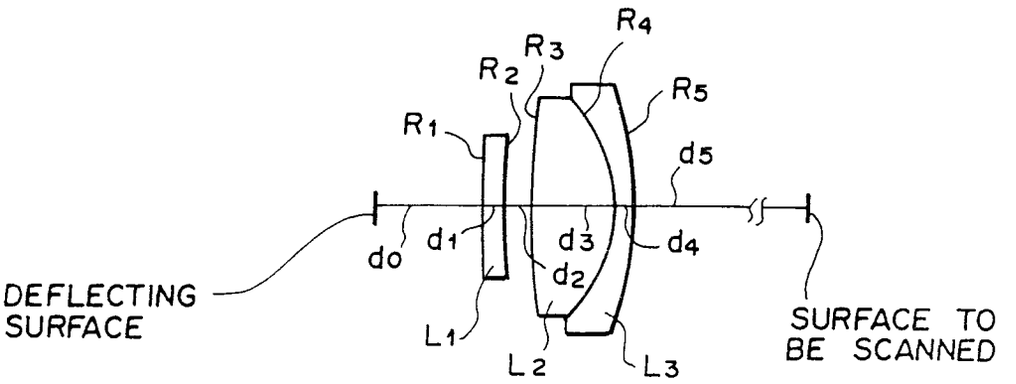


FIG.3B

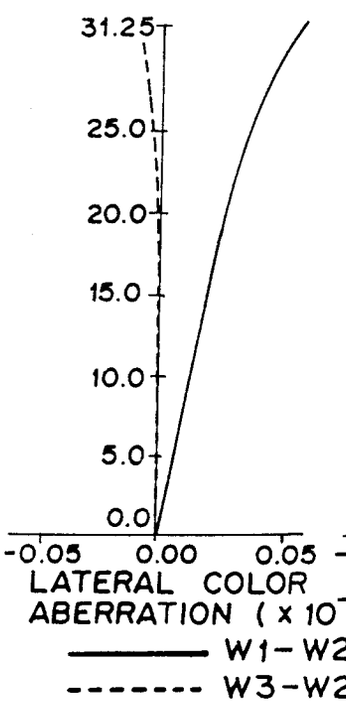


FIG.3C

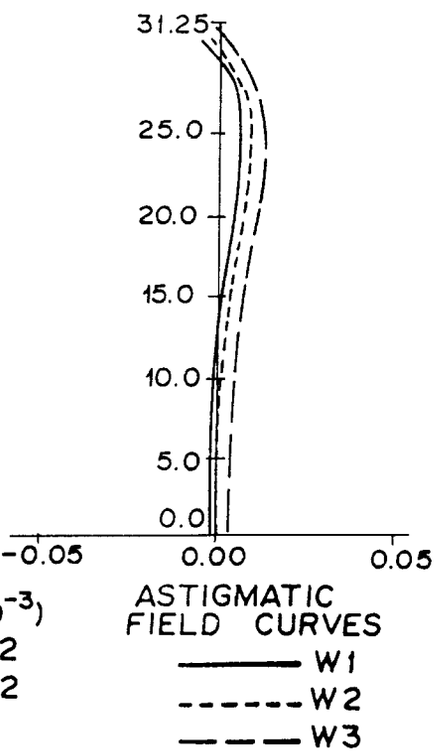


FIG.3D

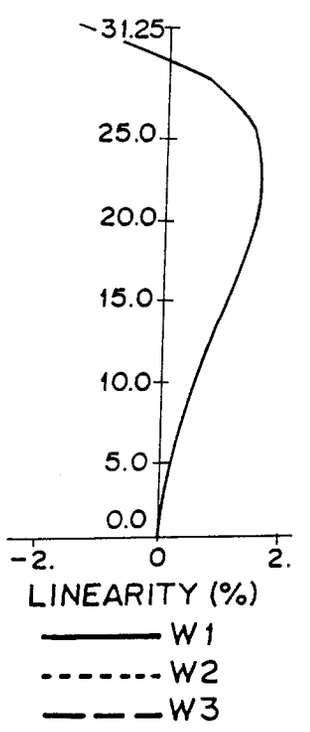


FIG. 4A

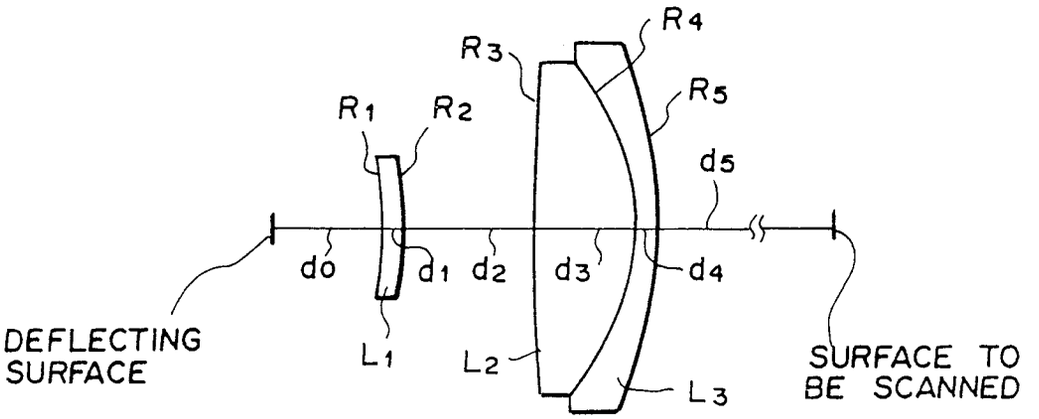


FIG. 4B

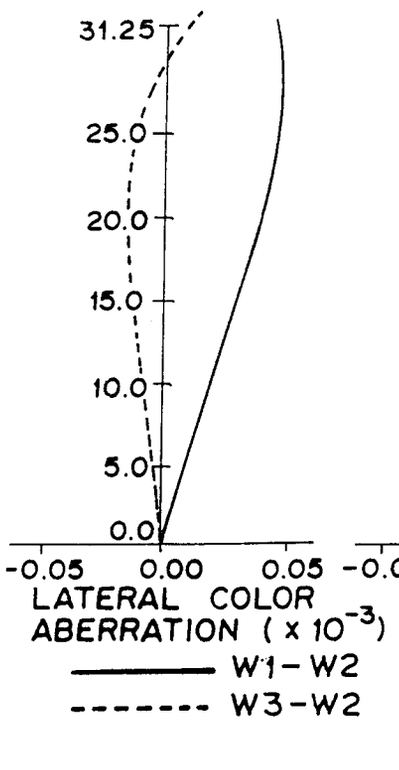


FIG. 4C

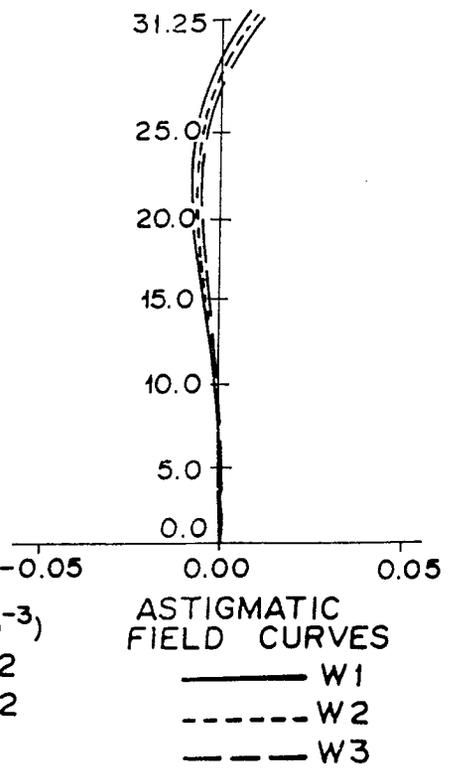


FIG. 4D

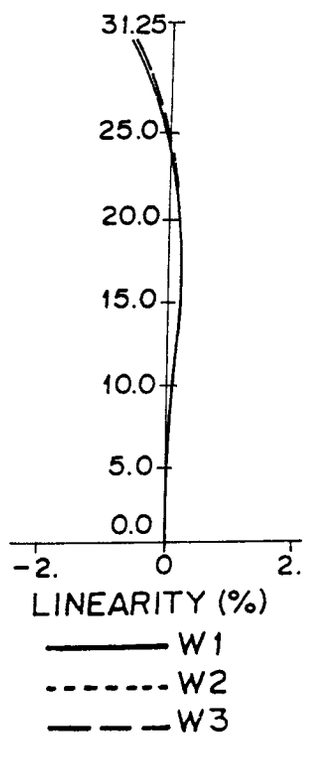


FIG. 5A

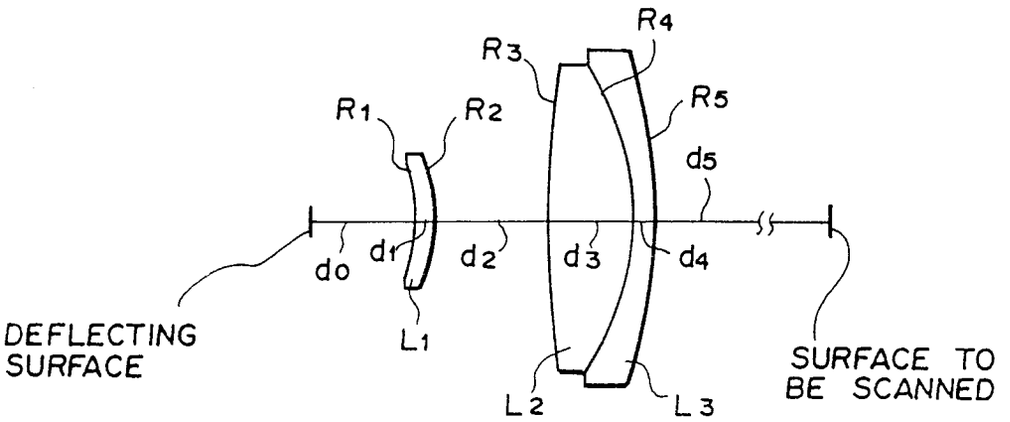


FIG. 5B

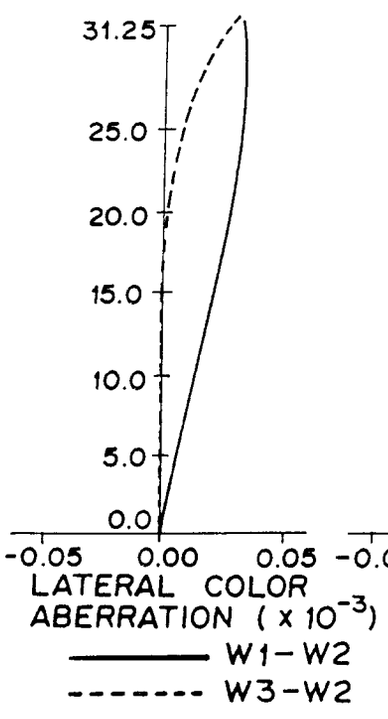


FIG. 5C

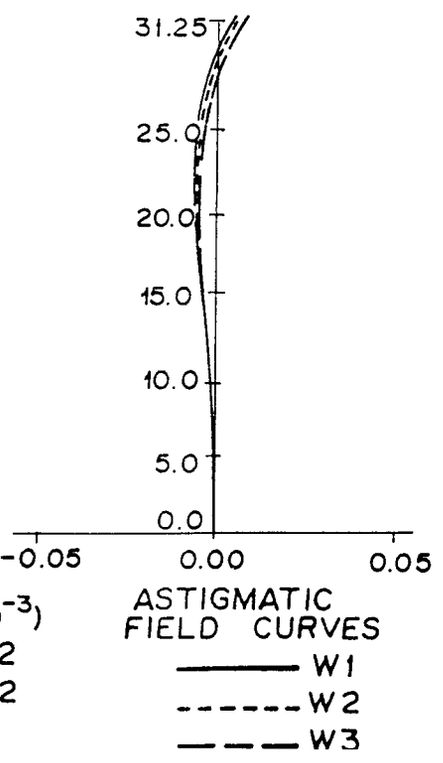


FIG. 5D

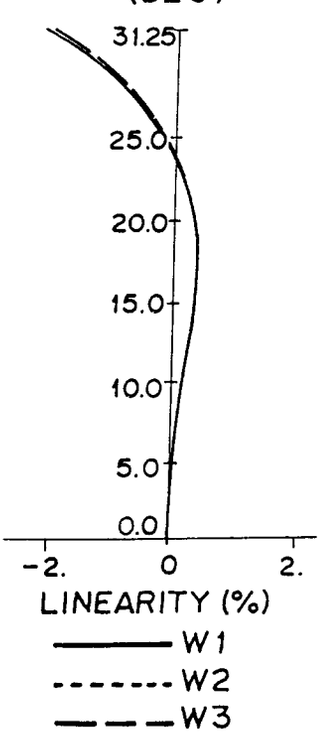


FIG. 6A

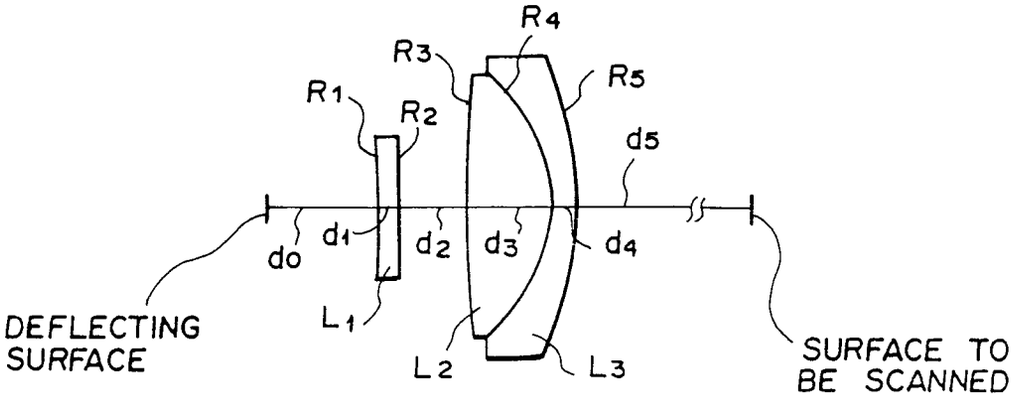


FIG. 6B

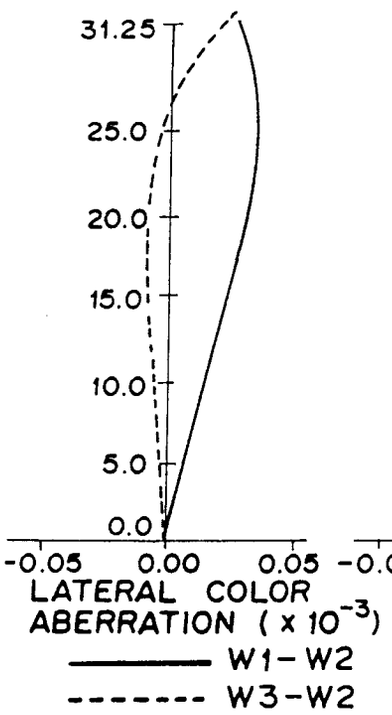


FIG. 6C

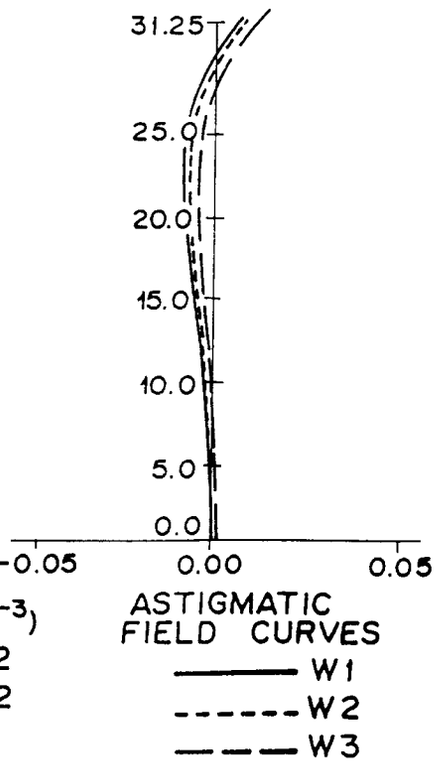


FIG. 6D

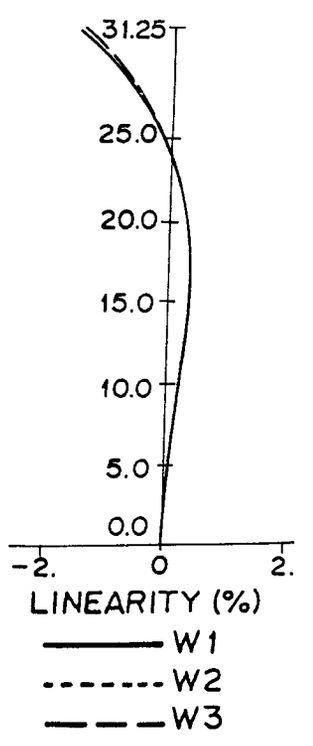


FIG. 7A

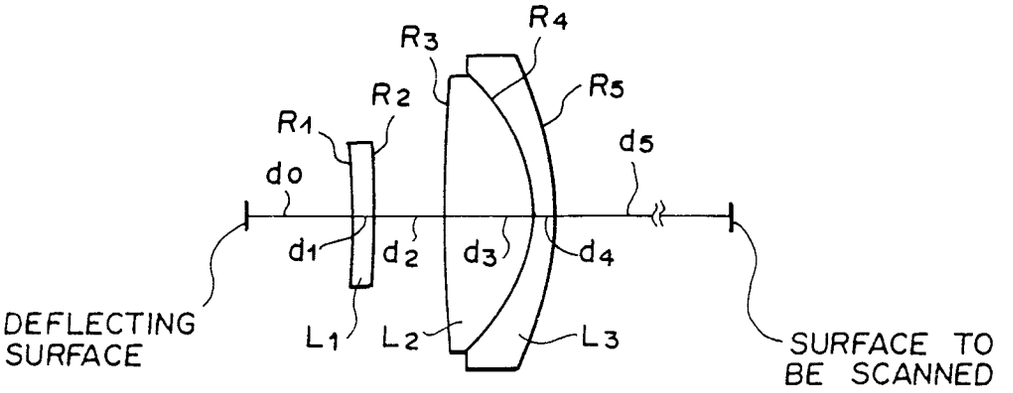


FIG. 7B

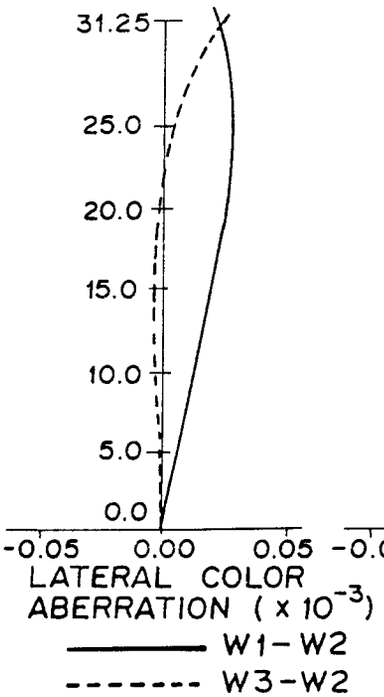


FIG. 7C

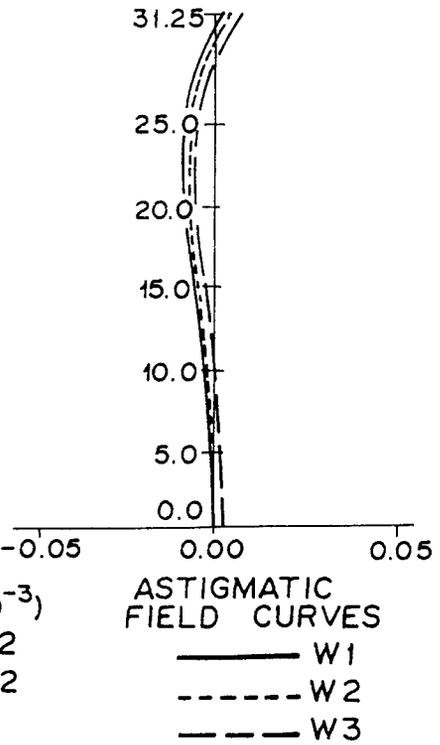


FIG. 7D

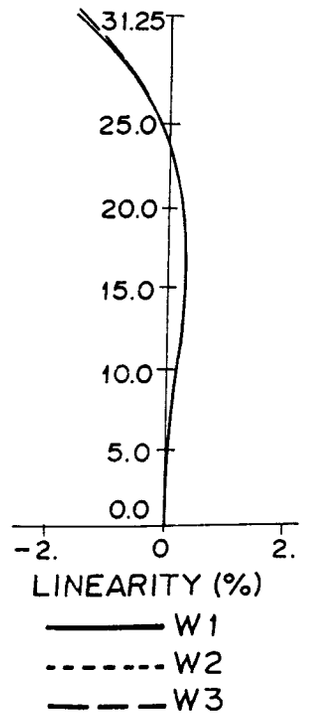


FIG. 8A

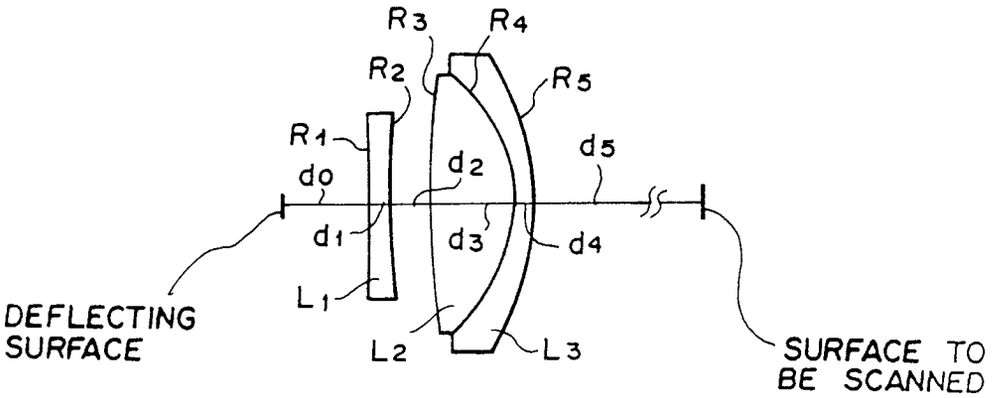


FIG. 8B

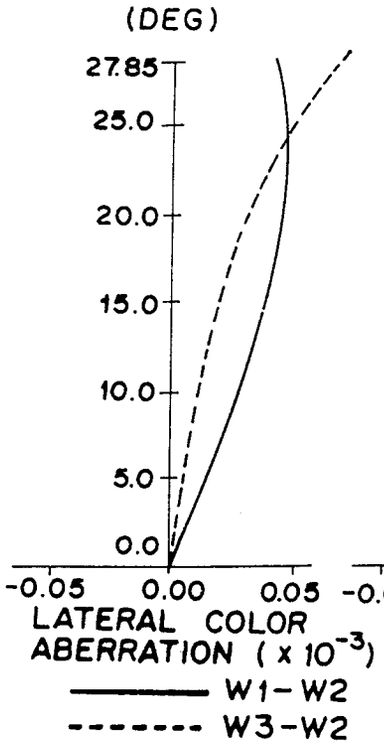


FIG. 8C

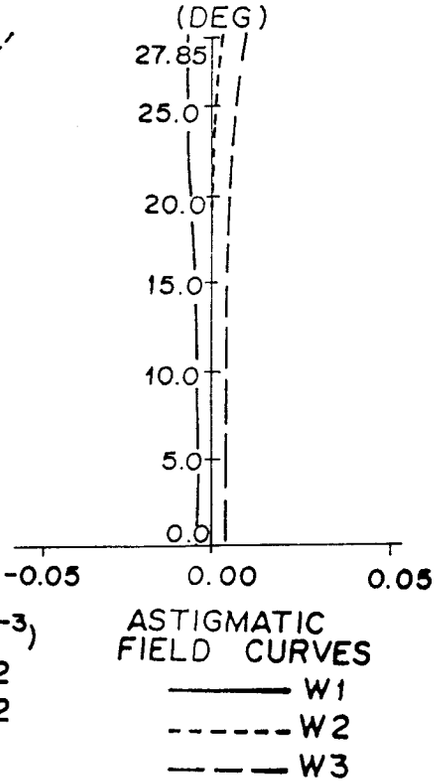


FIG. 8D

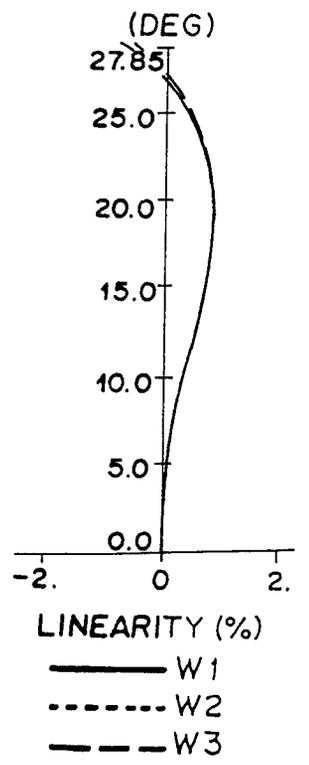


FIG. 9A

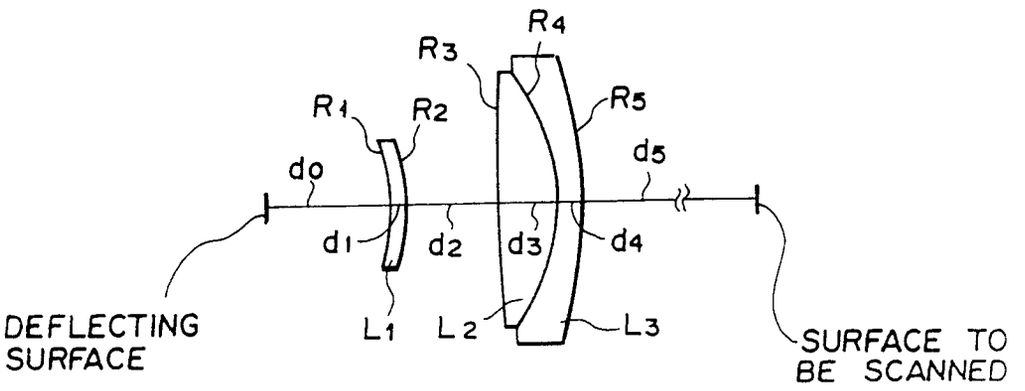


FIG. 9B

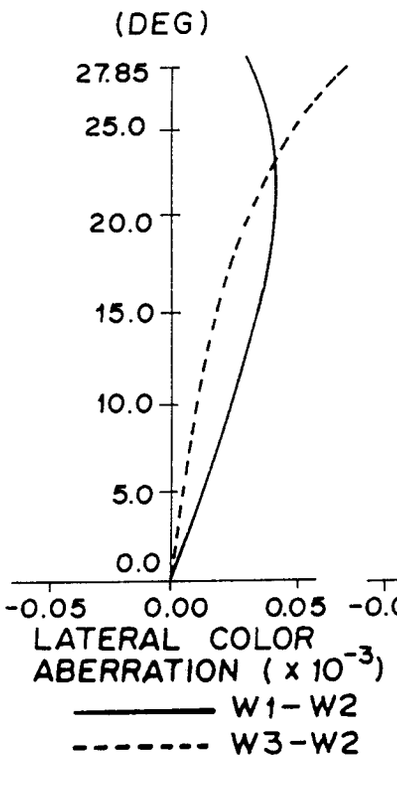


FIG. 9C

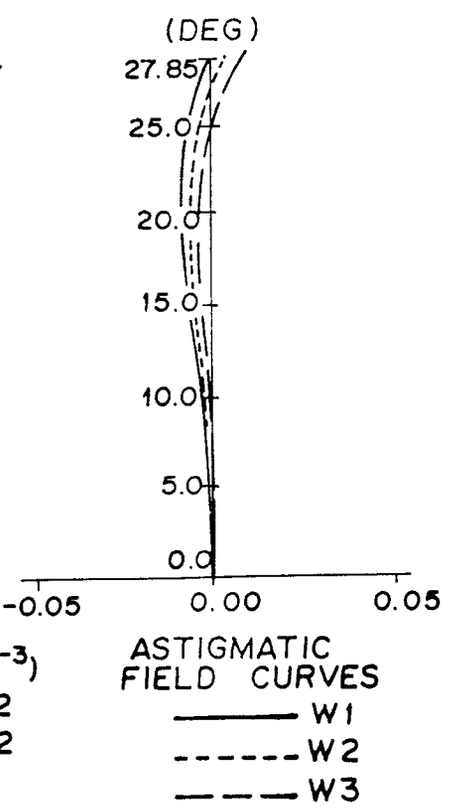


FIG. 9D

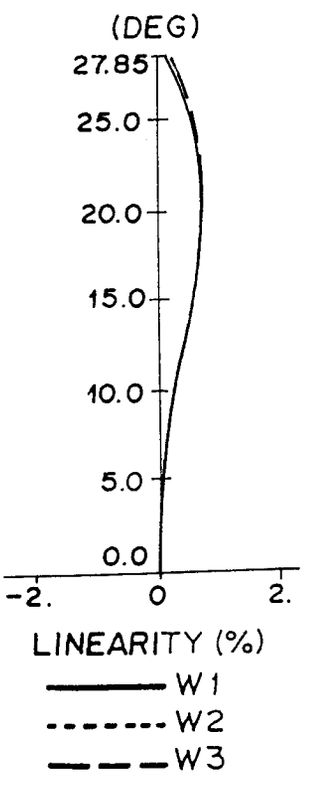


FIG.10A

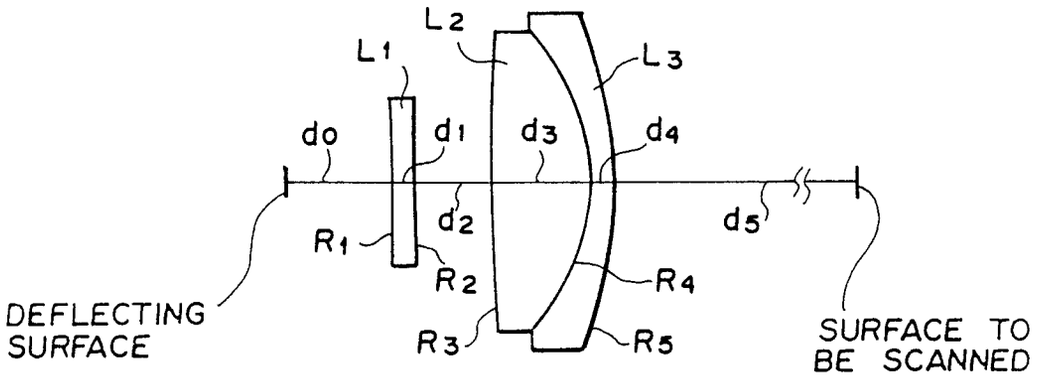


FIG.10B

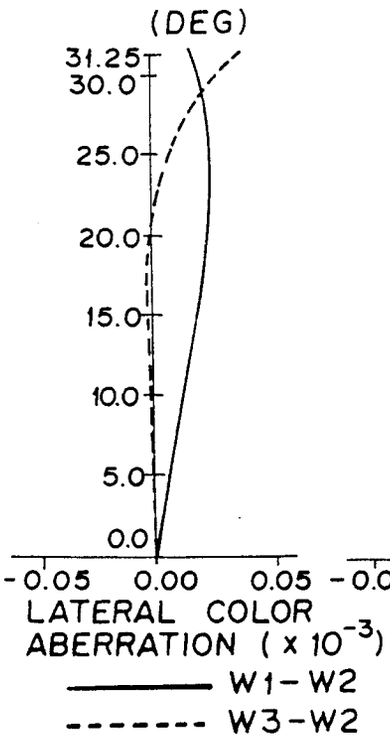


FIG.10C

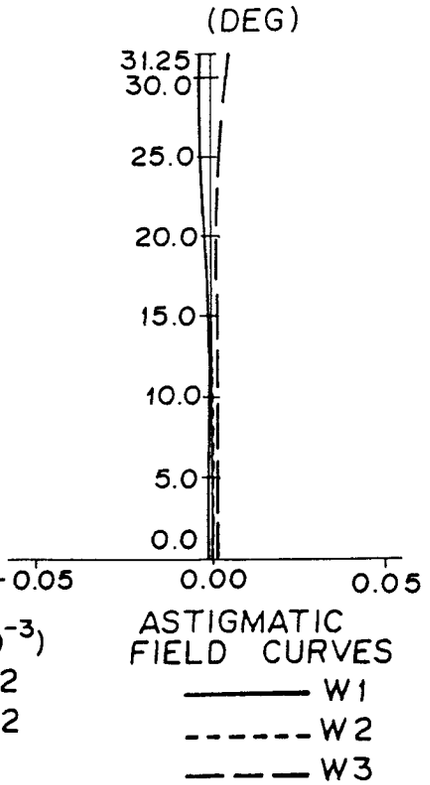


FIG.10D

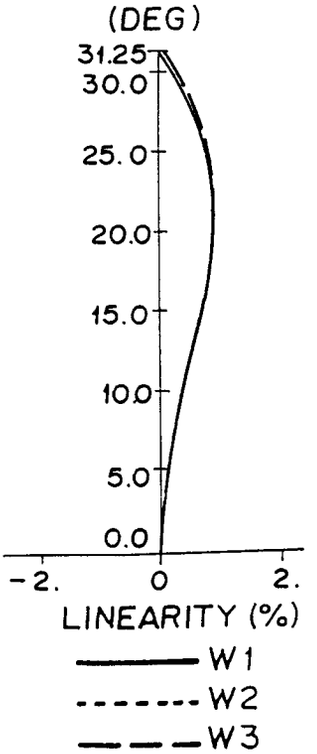


FIG.11A

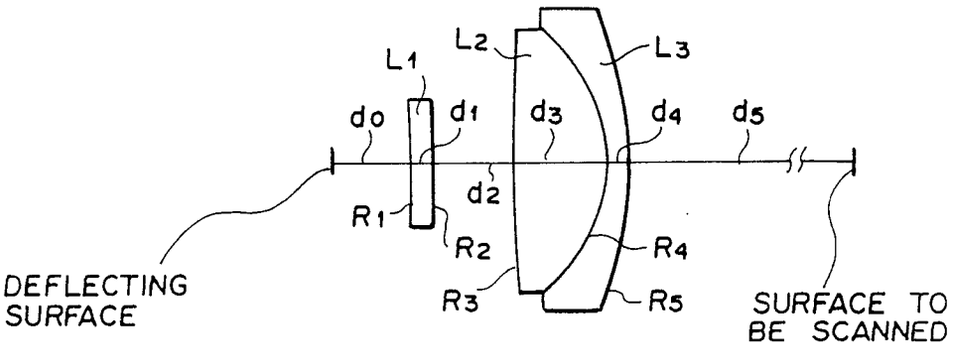


FIG.11B

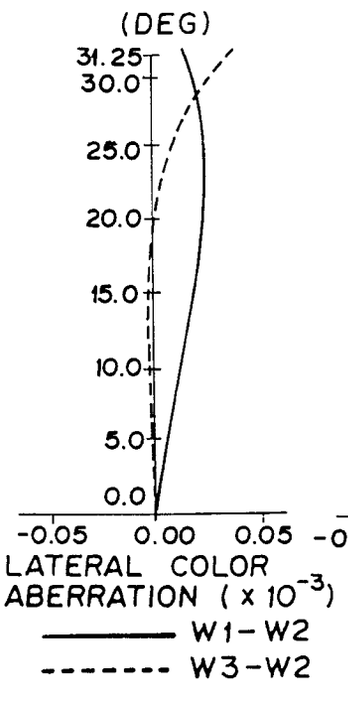


FIG.11C

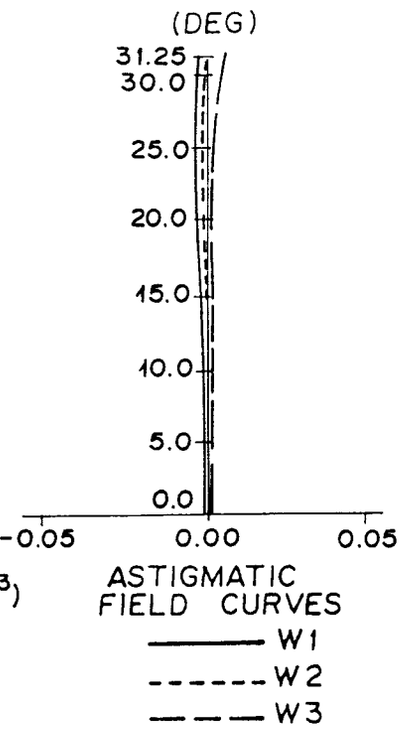


FIG.11D

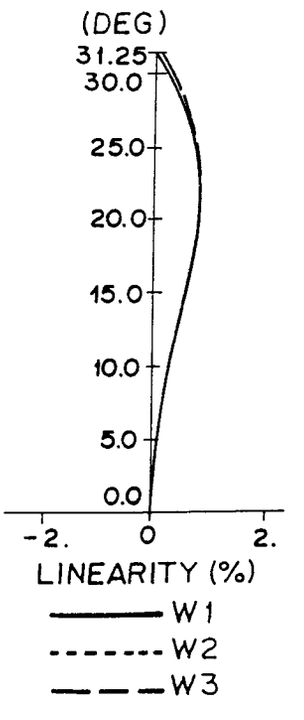


FIG.12A

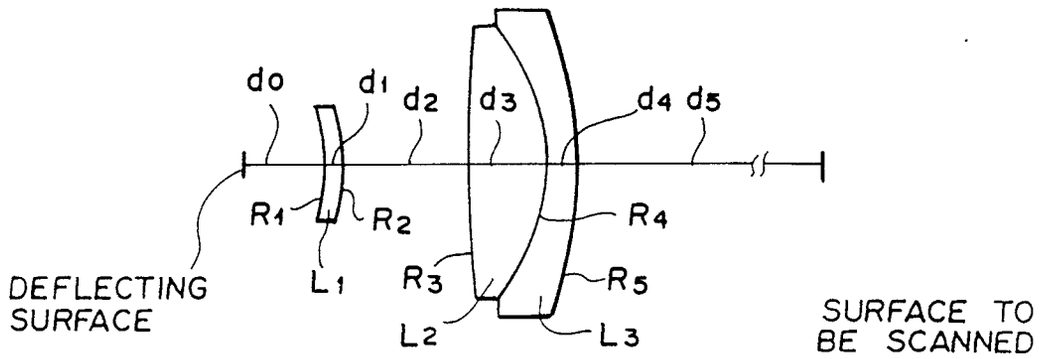


FIG.12B

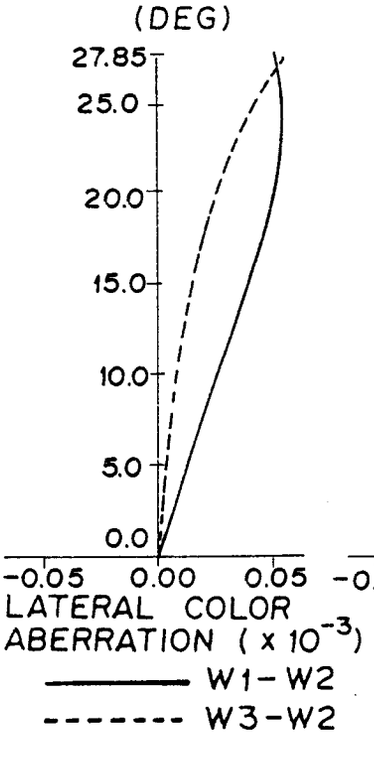


FIG.12C

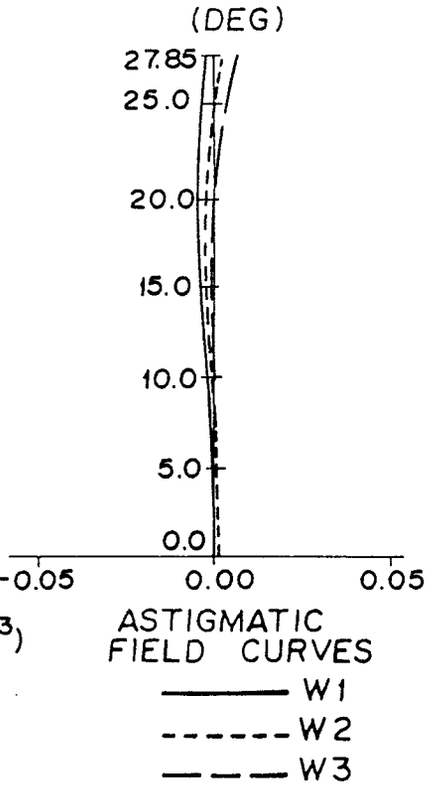


FIG.12D

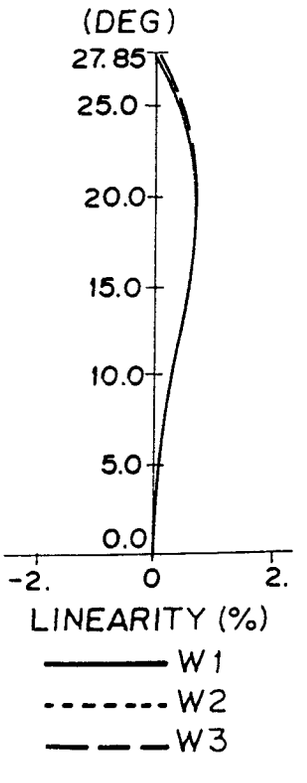


FIG.13A

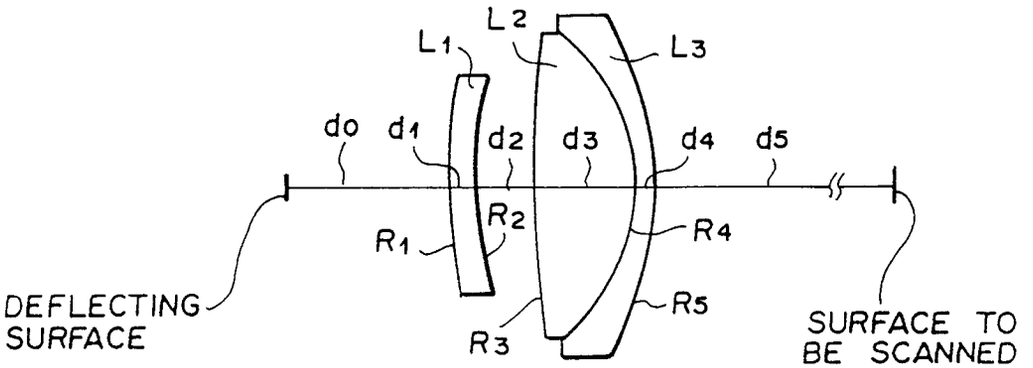


FIG.13B

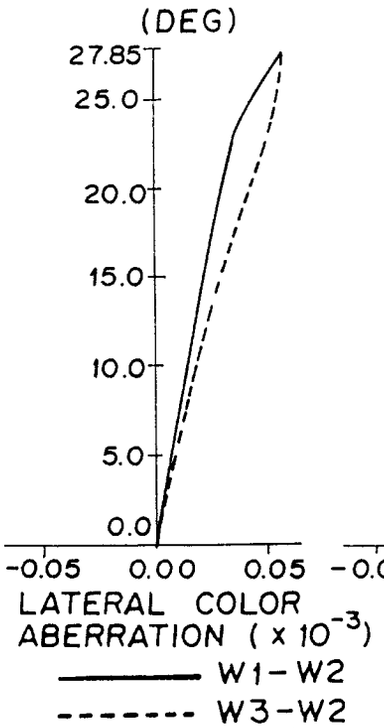


FIG.13C

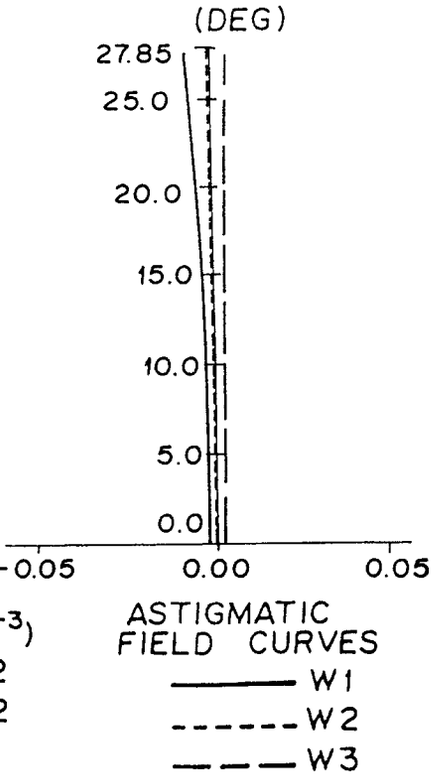


FIG.13D

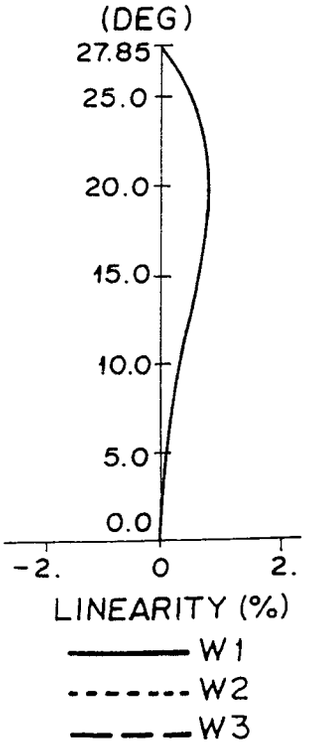


FIG.14A

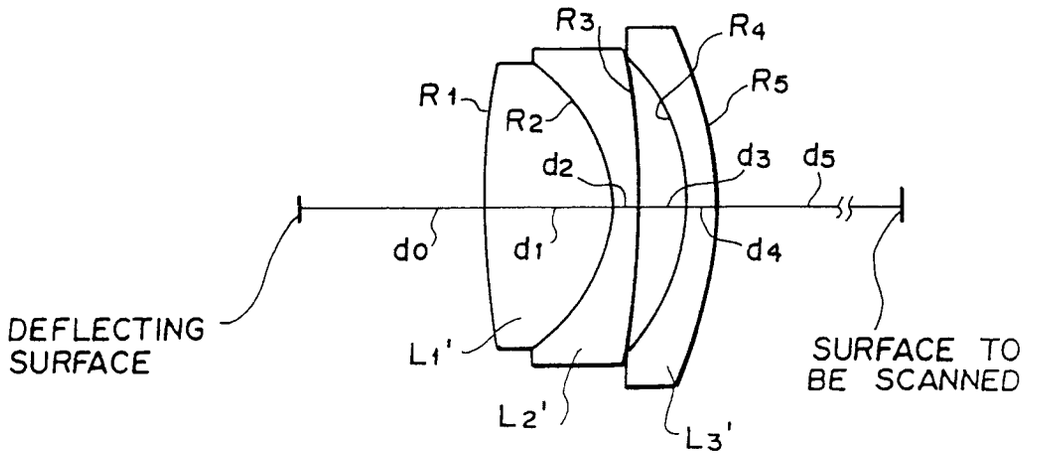


FIG.14B

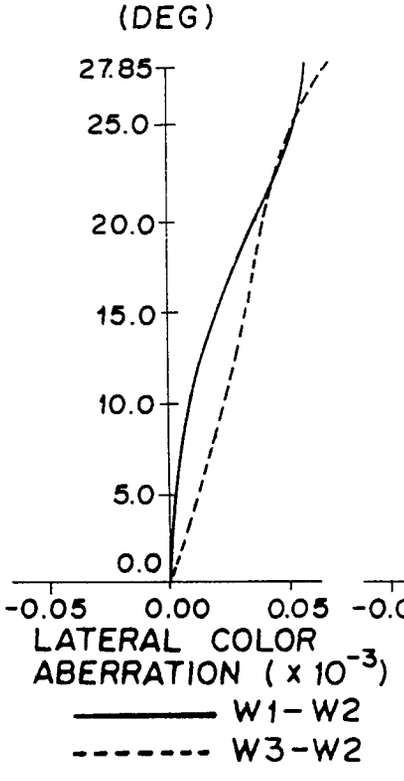


FIG.14C

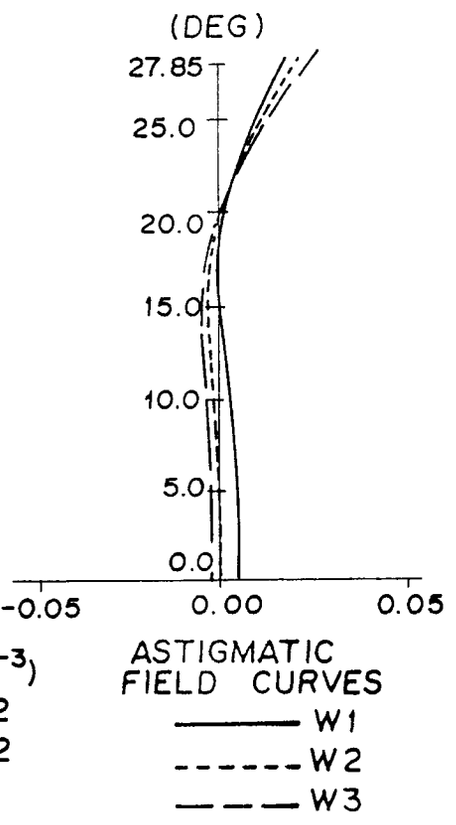


FIG.14D

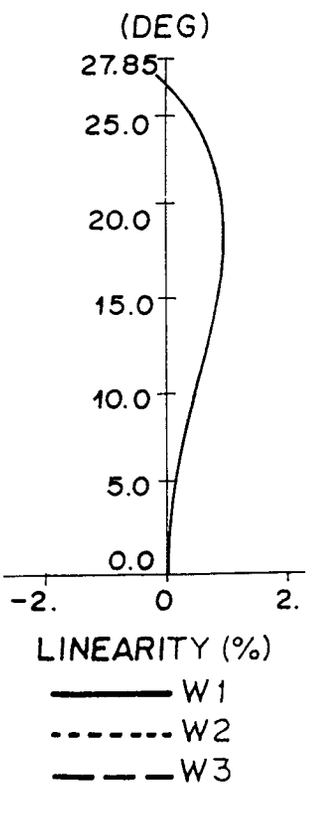


FIG.15A

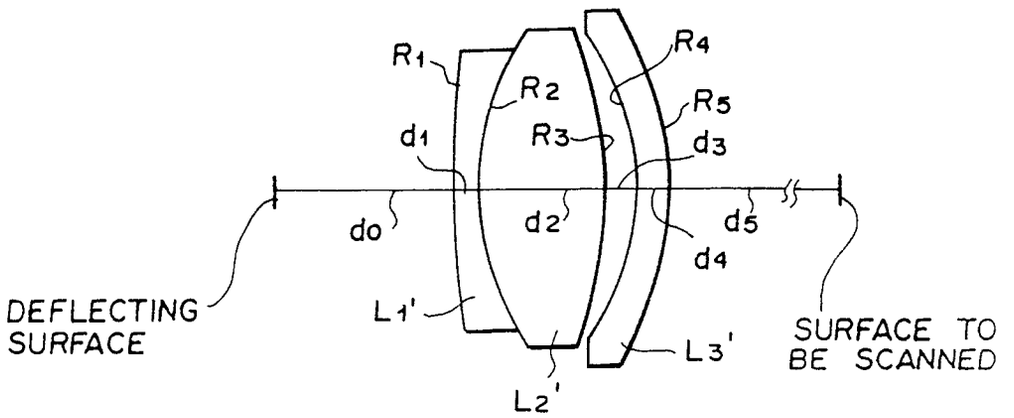


FIG.15B

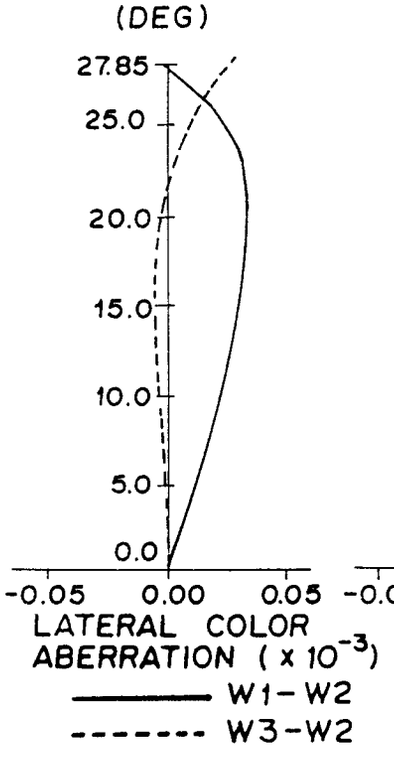


FIG.15C

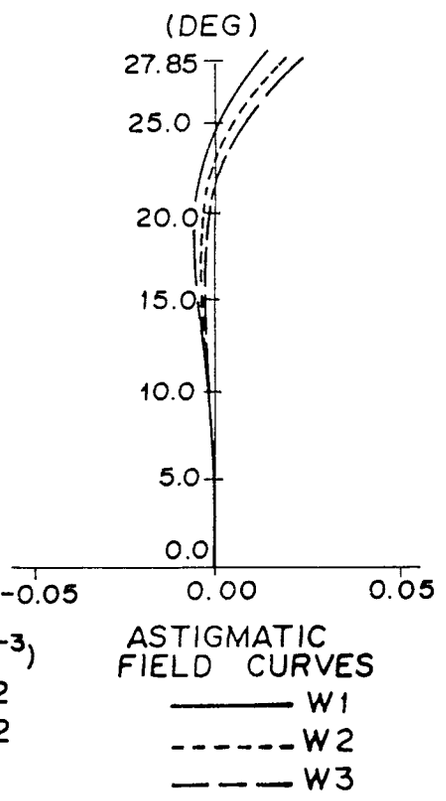


FIG.15D

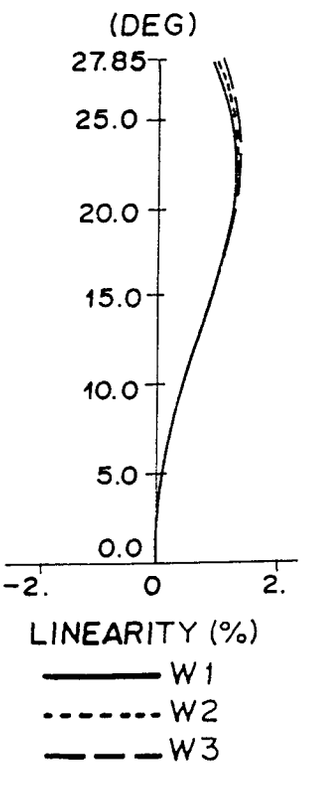


FIG.16A

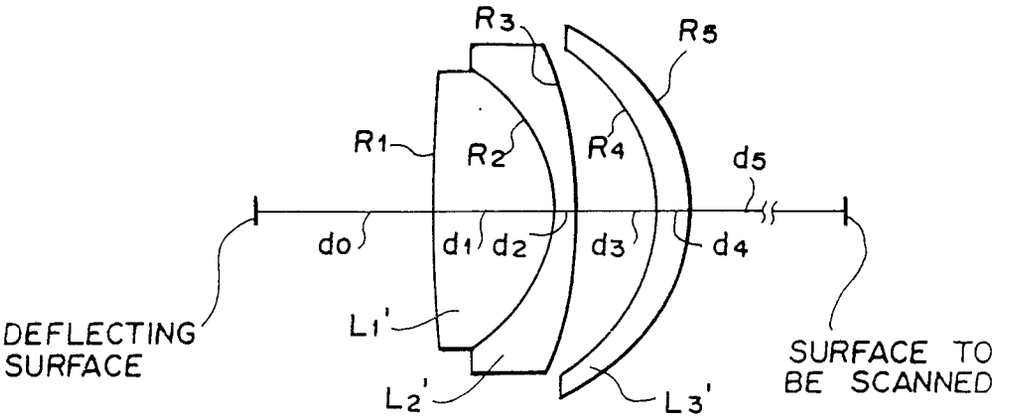


FIG.16B

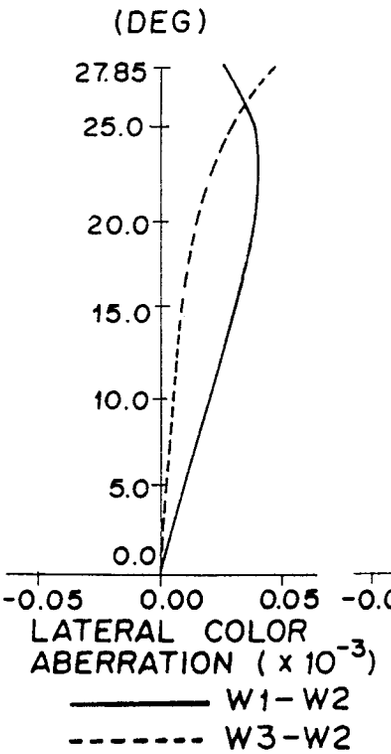


FIG.16C

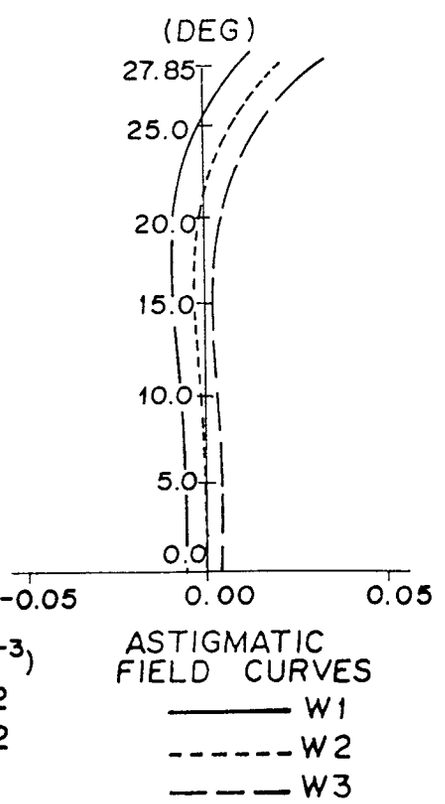


FIG.16D

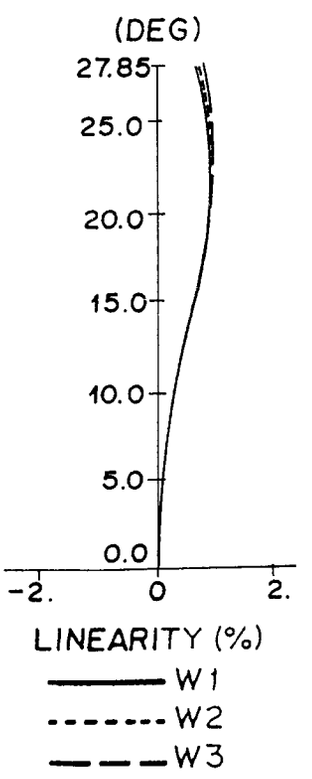


FIG.17A

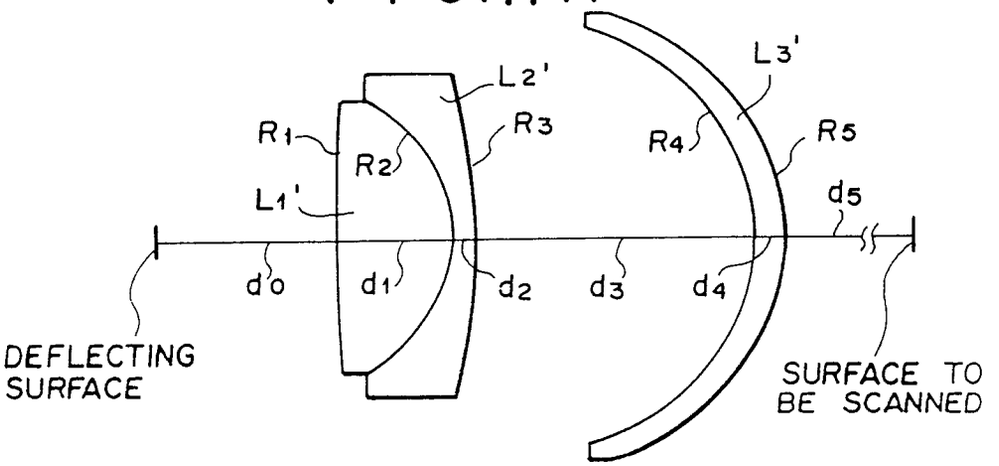


FIG.17B

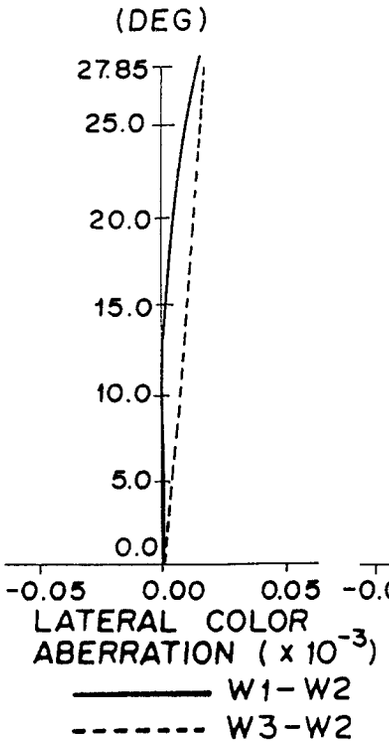


FIG.17C

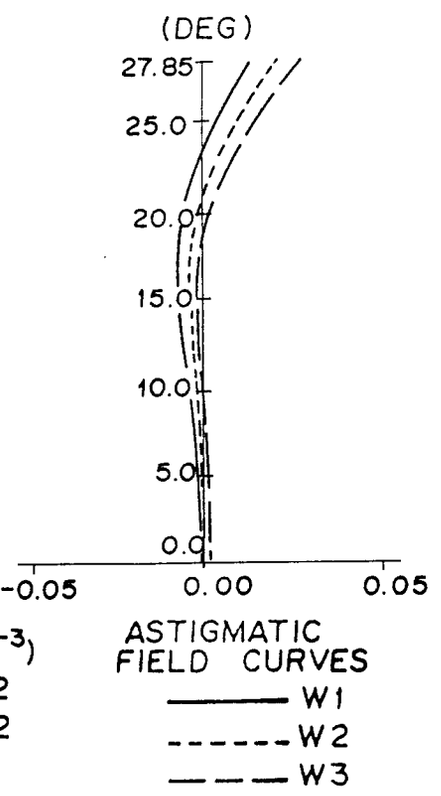


FIG.17D

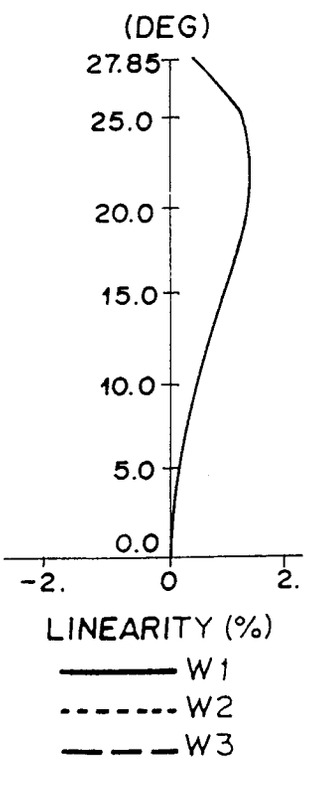


FIG.18A

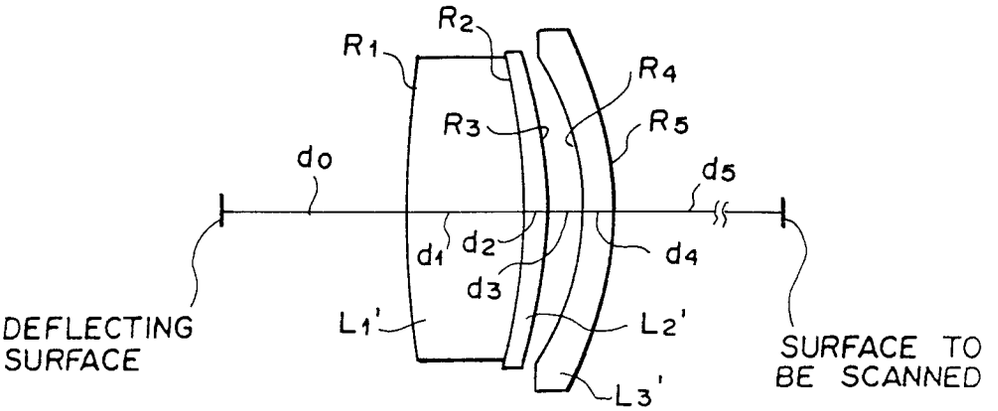


FIG.18B

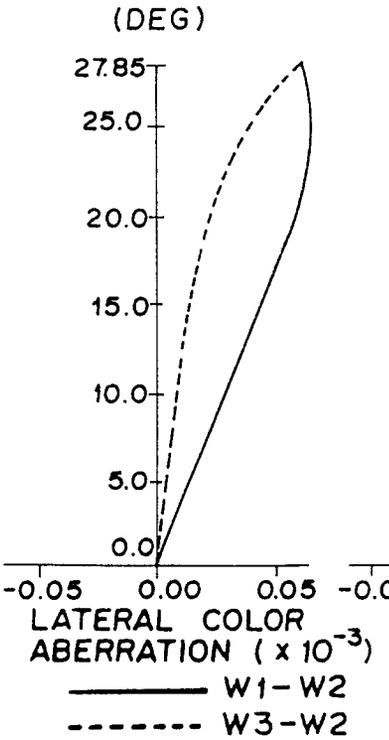


FIG.18C

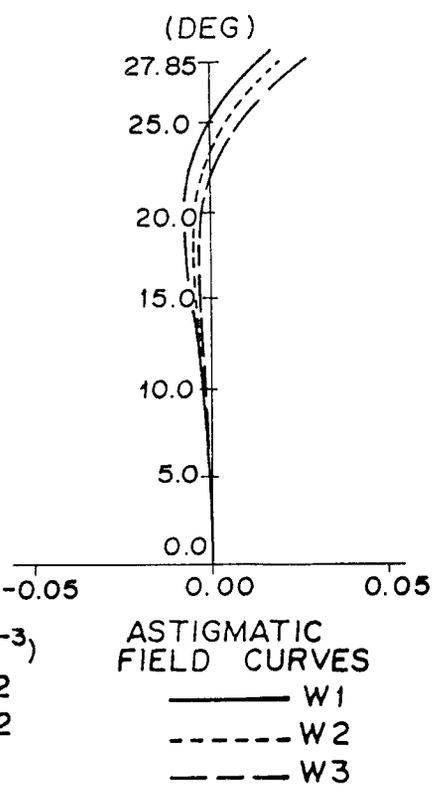


FIG.18D

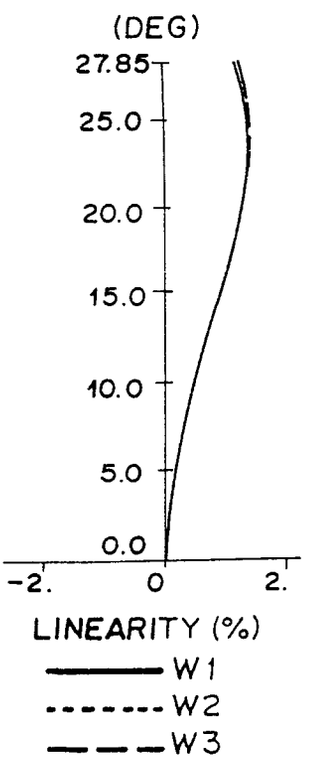


FIG.19A

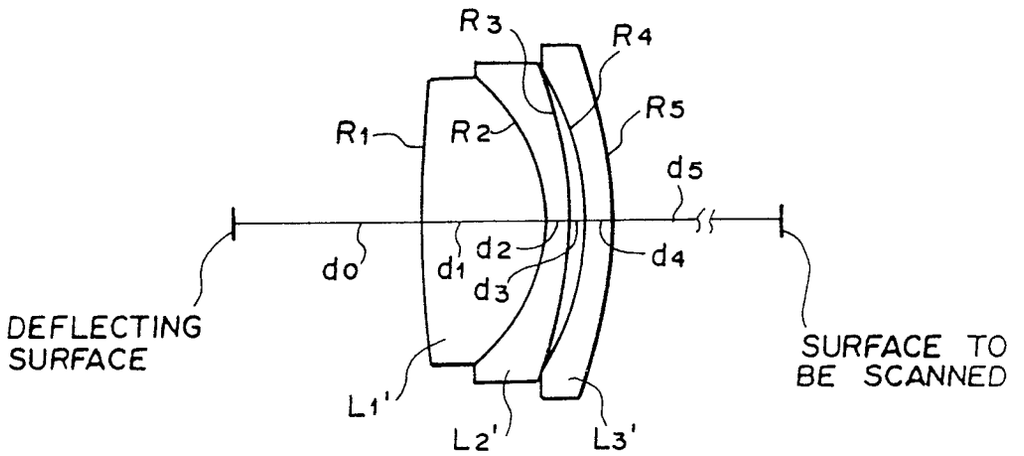


FIG.19B

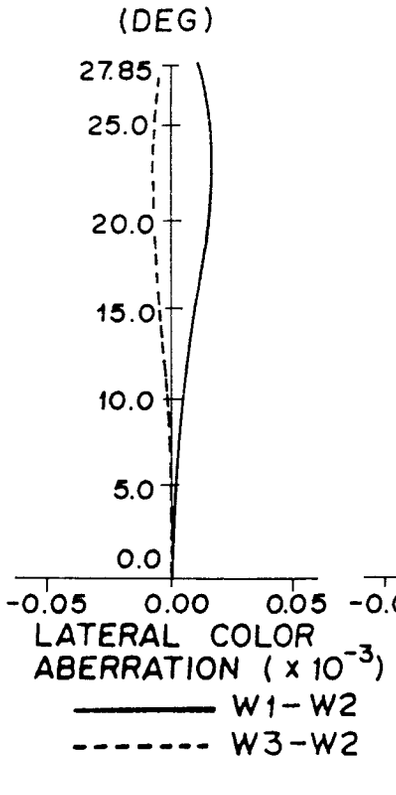


FIG.19C

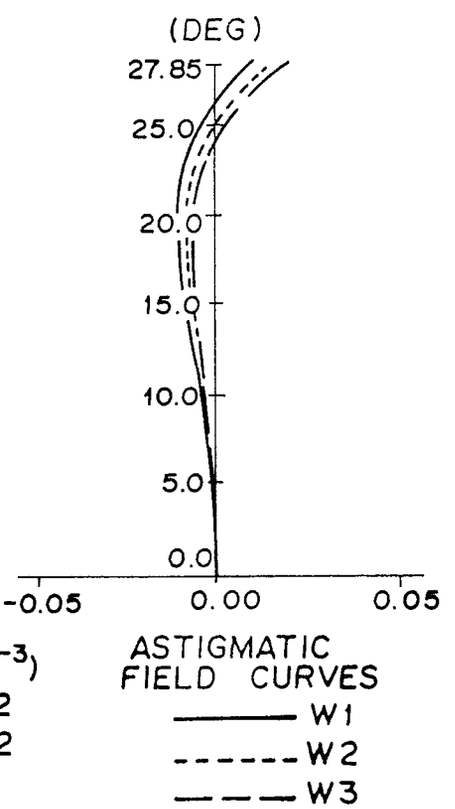


FIG.19D

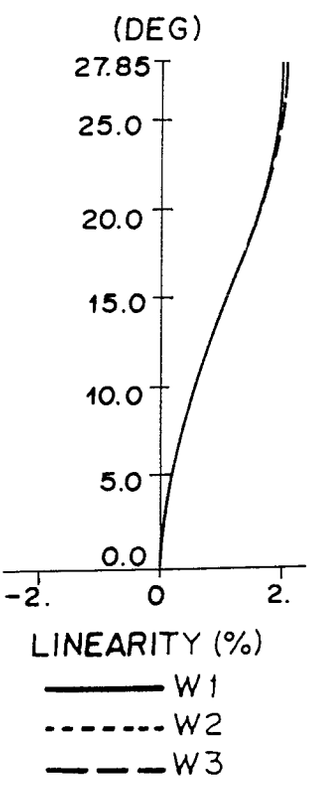


FIG.20A

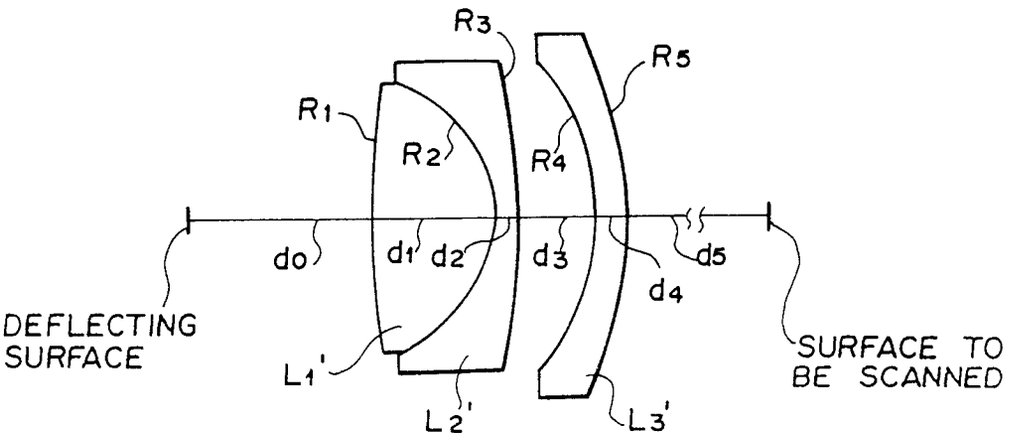


FIG.20B

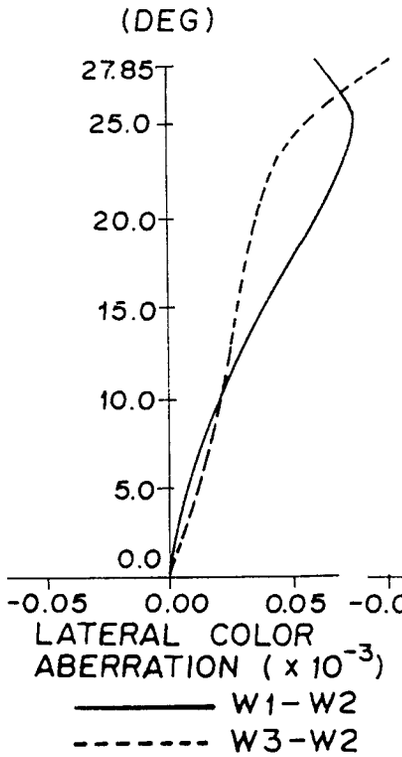


FIG.20C

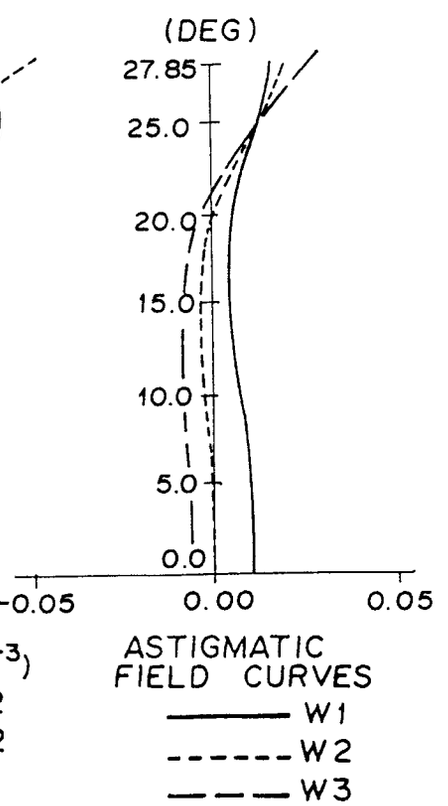


FIG.20D

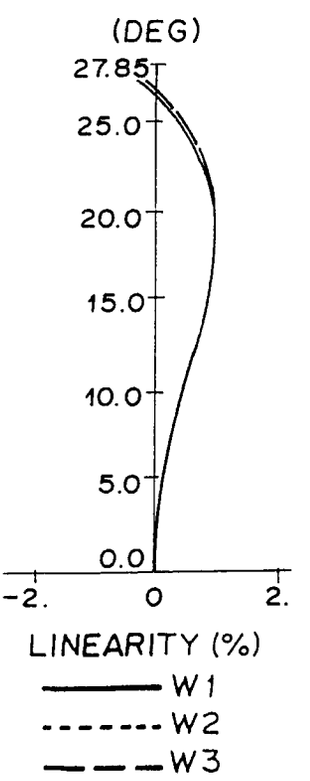


FIG.21A

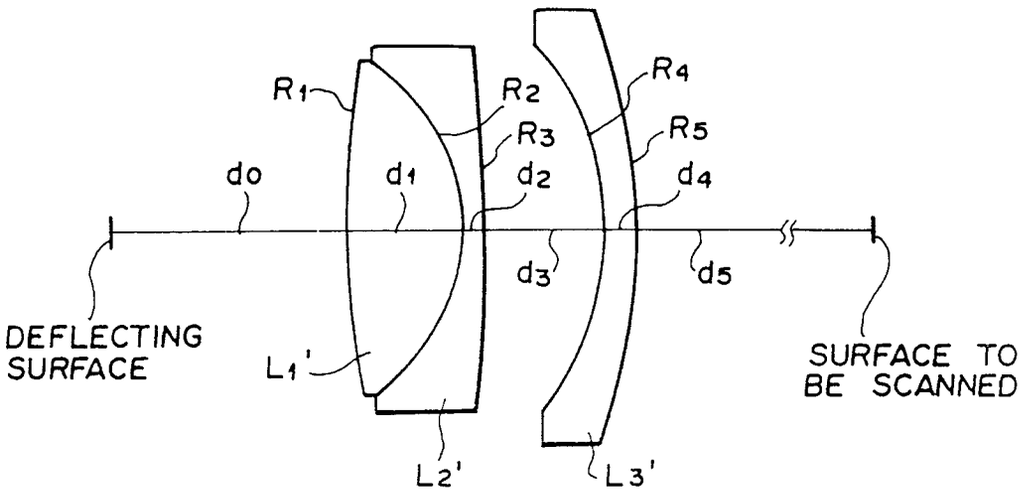


FIG.21B

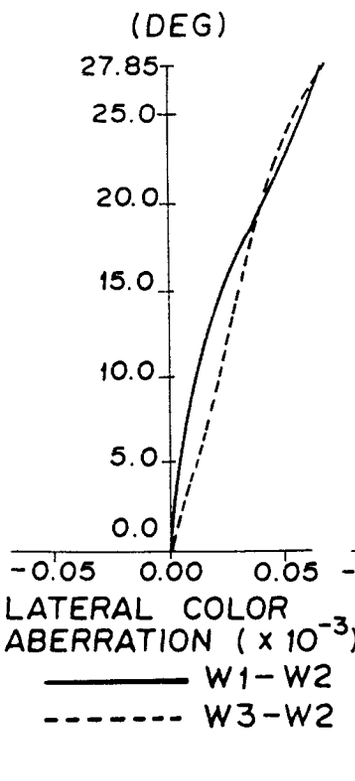


FIG.21C

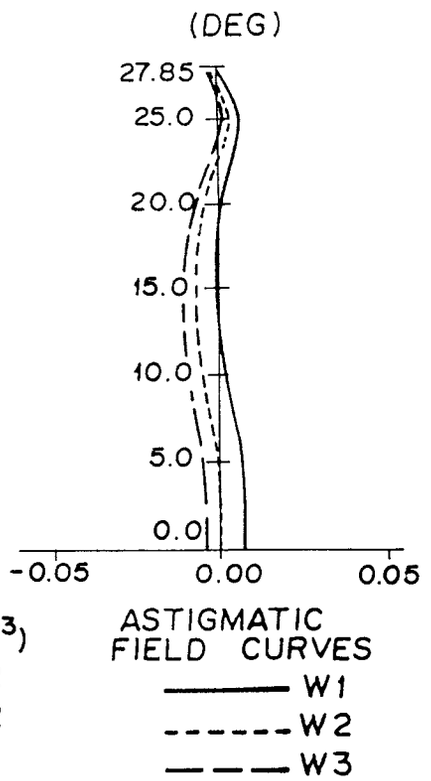


FIG.21D

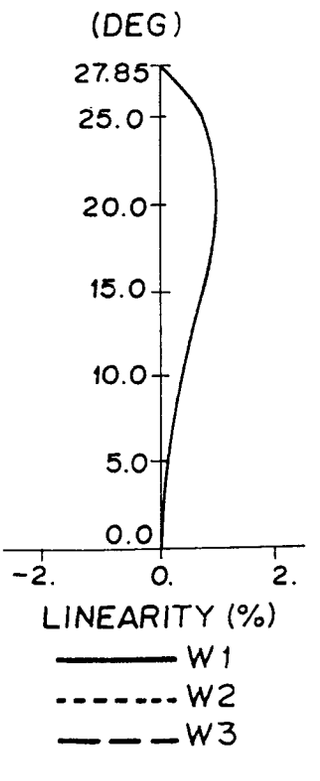


FIG.22A

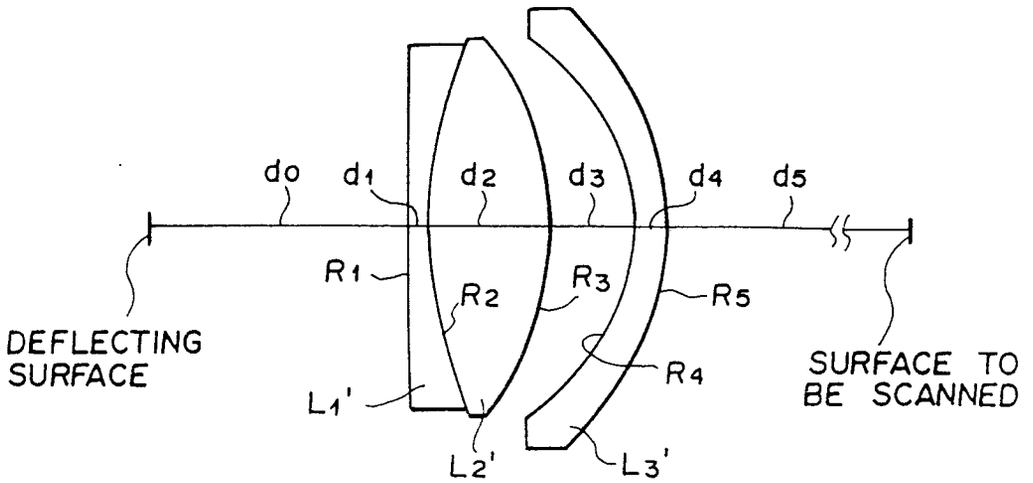


FIG.22B

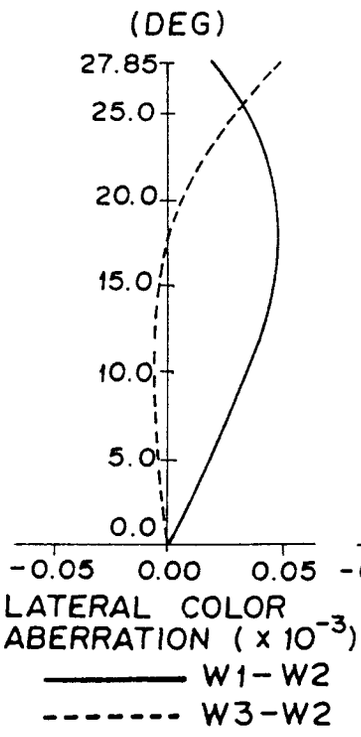


FIG.22C

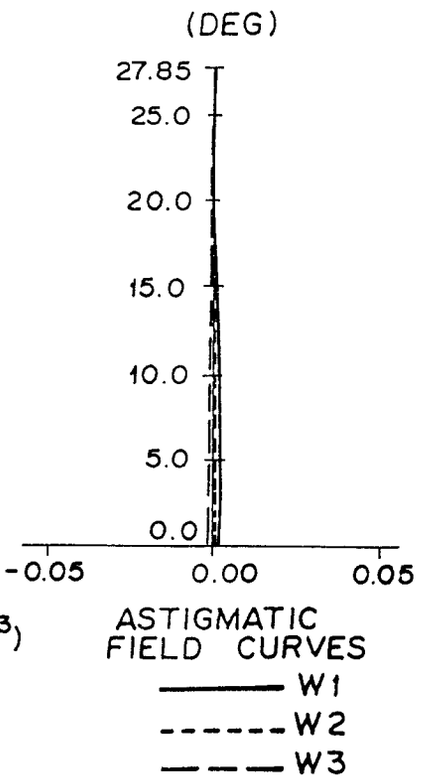


FIG.22D

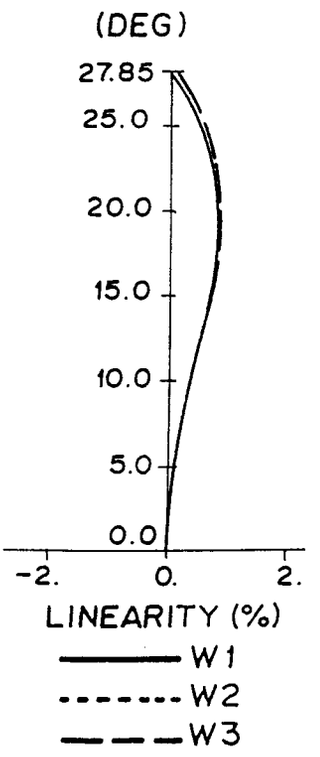


FIG.23A

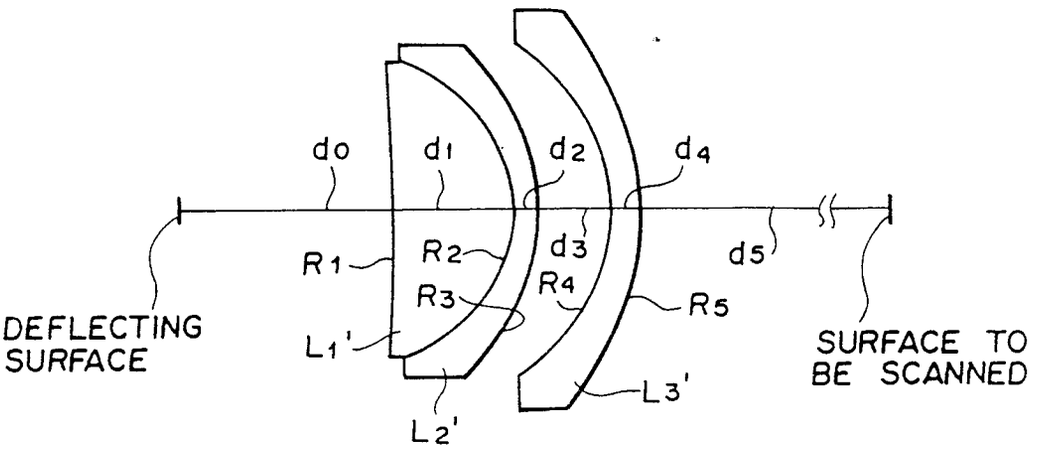


FIG.23B

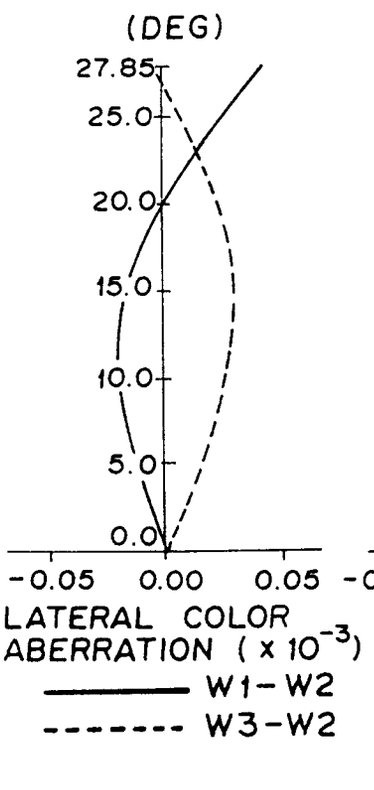


FIG.23C

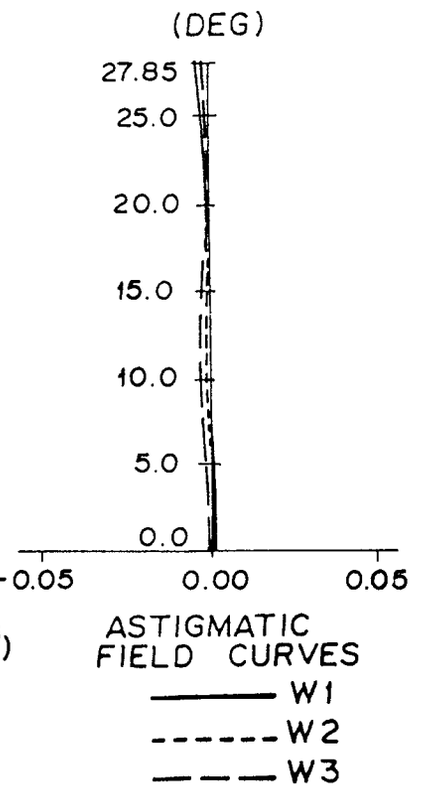


FIG.23D

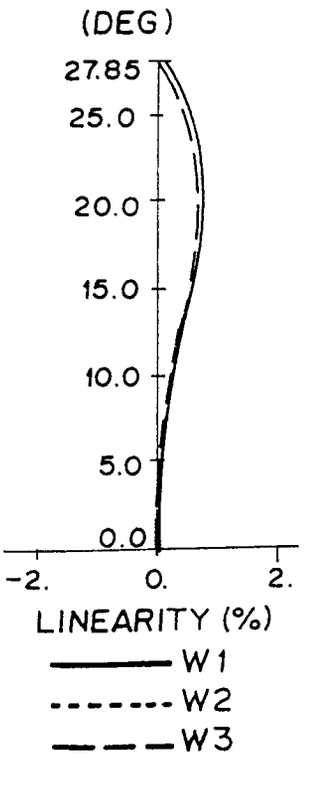


FIG.24A

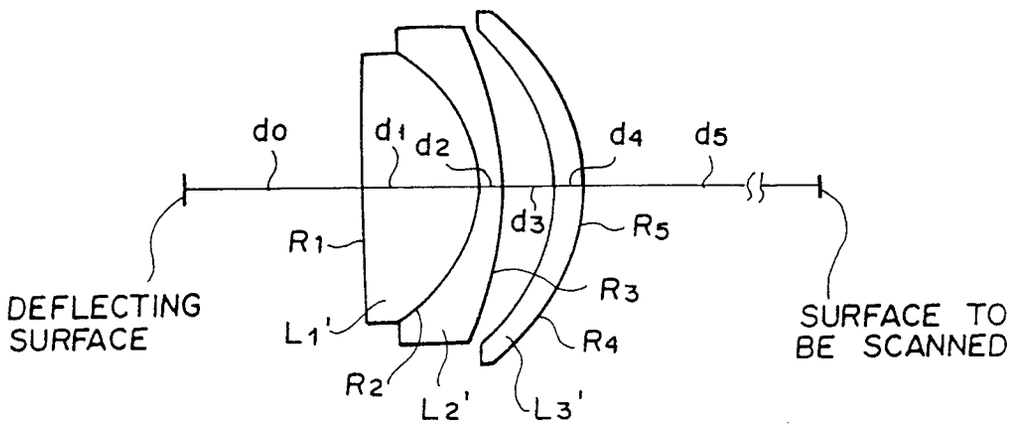


FIG.24B

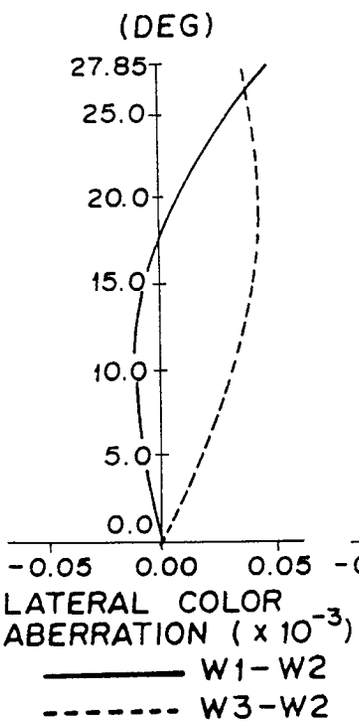


FIG.24C

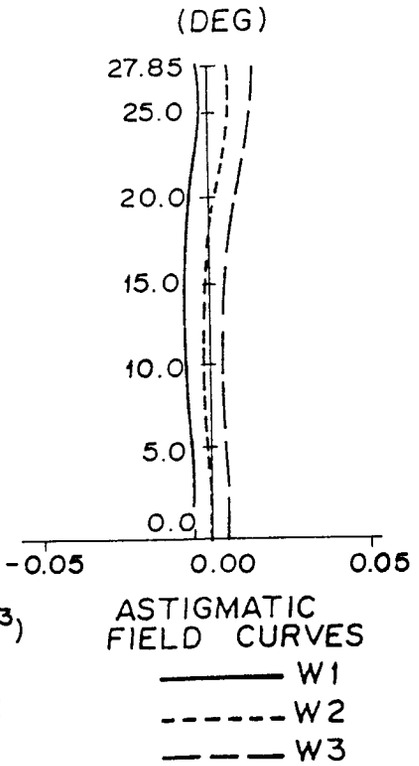


FIG.24D

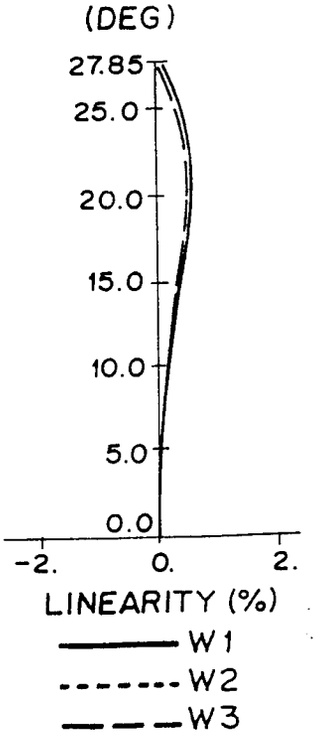


FIG.25A

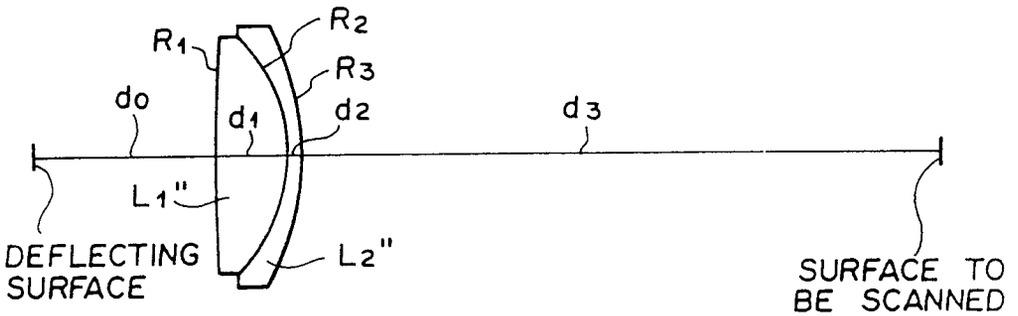


FIG.25B

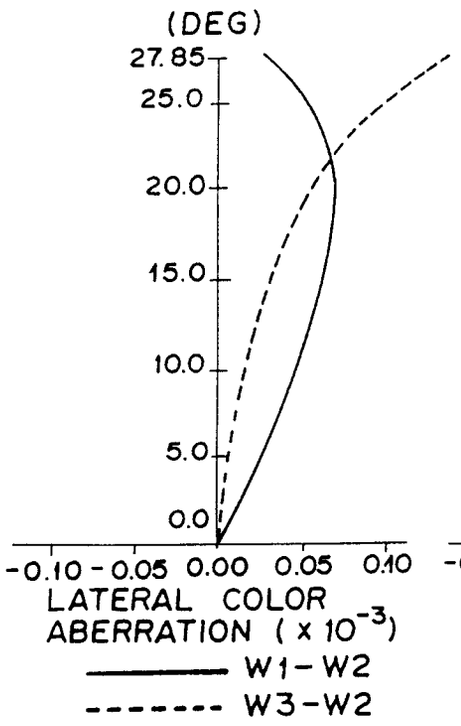


FIG.25C

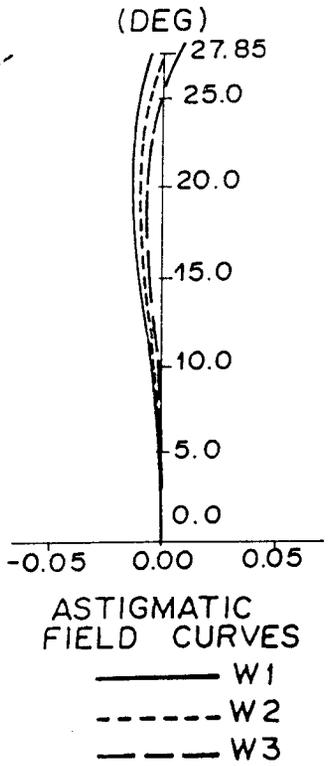


FIG.25D

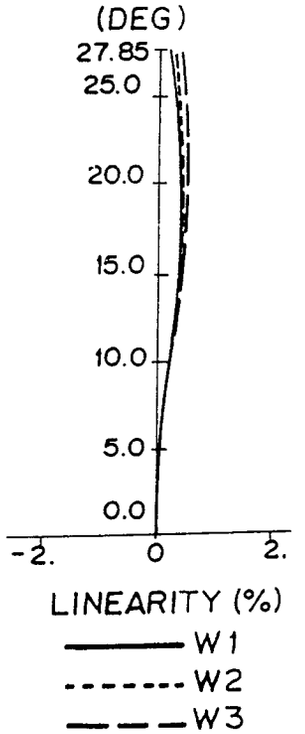


FIG.26A

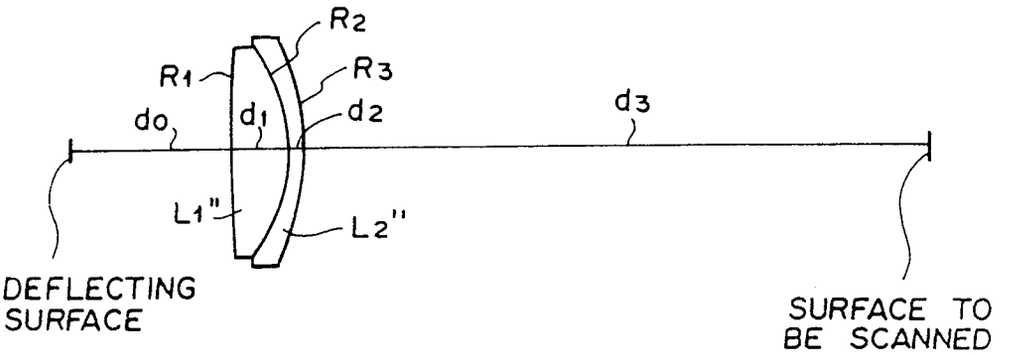


FIG.26B

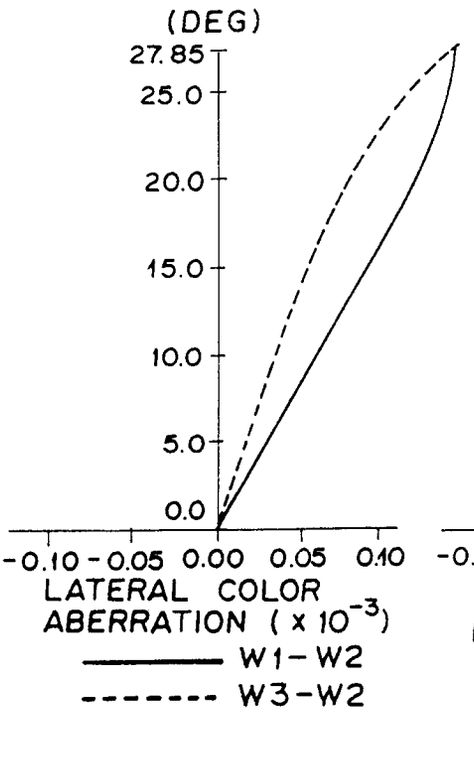


FIG.26C

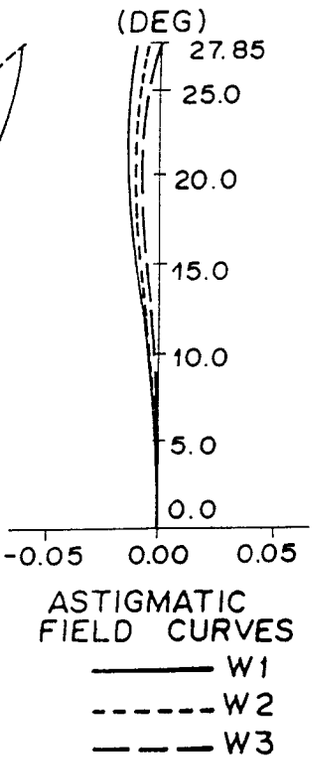


FIG.26D

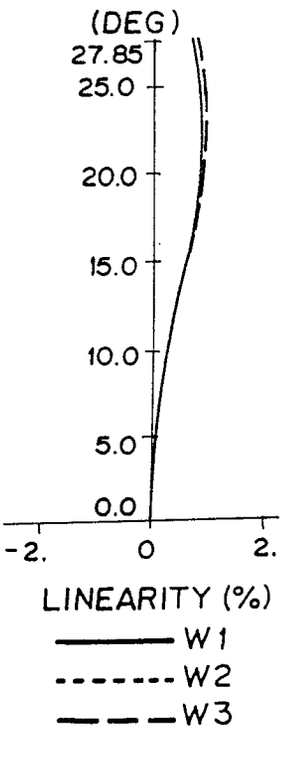


FIG.27A

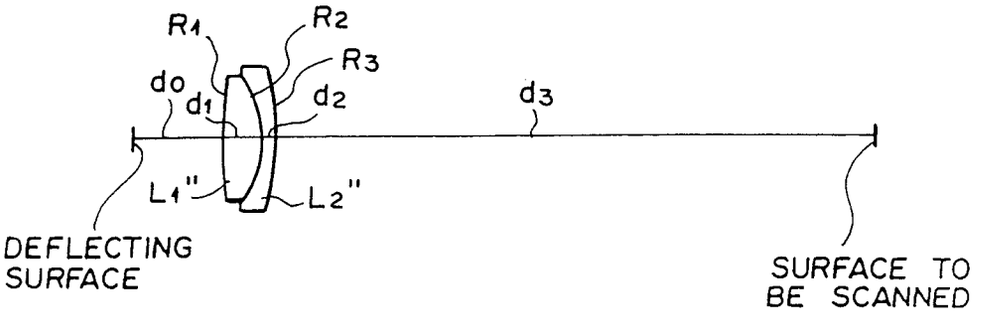


FIG.27B

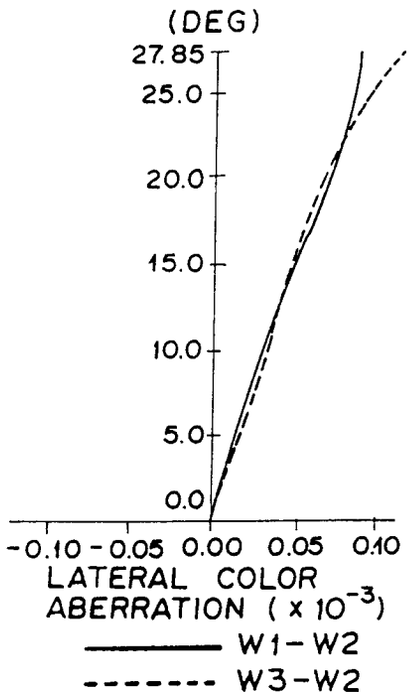


FIG.27C

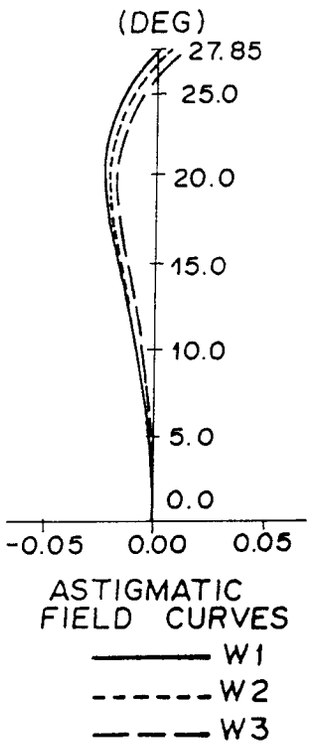


FIG.27D

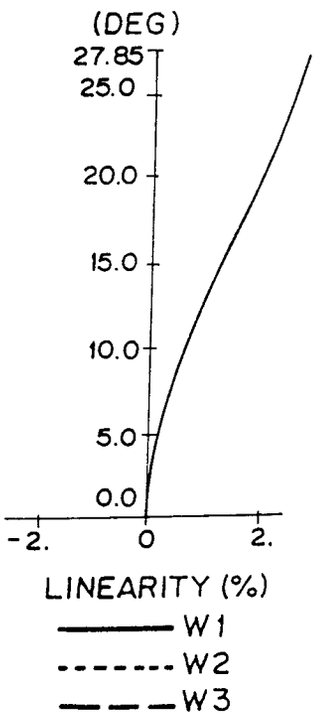


FIG.28A

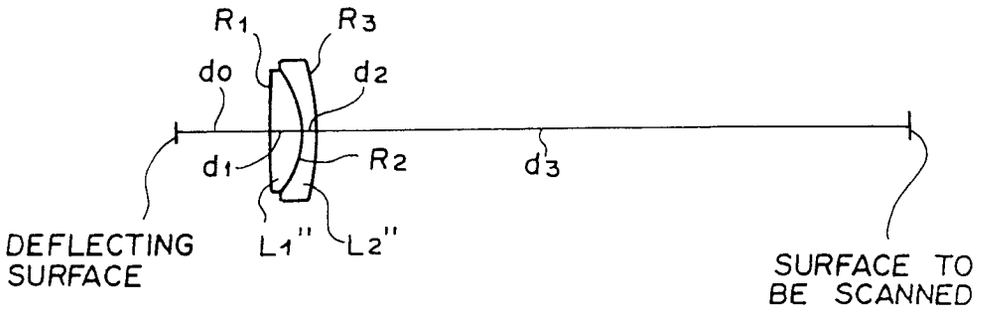


FIG.28B

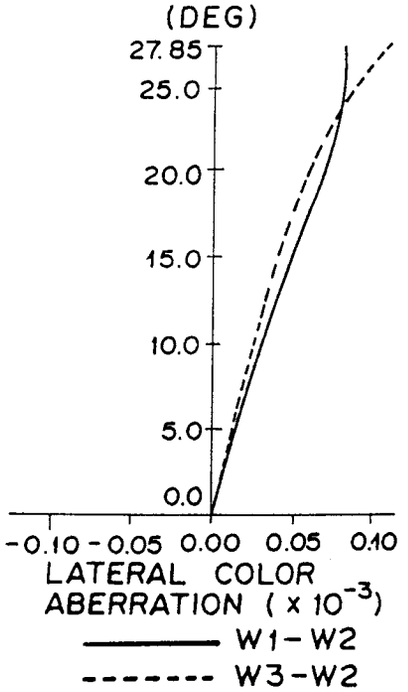


FIG.28C

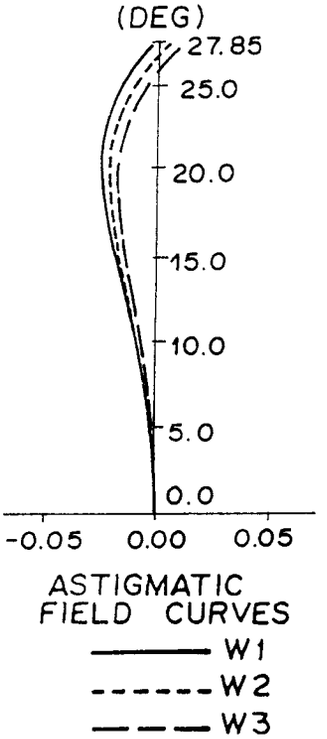


FIG.28D

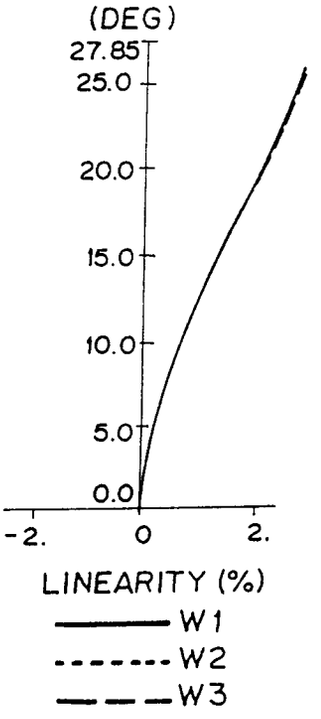


FIG.29A

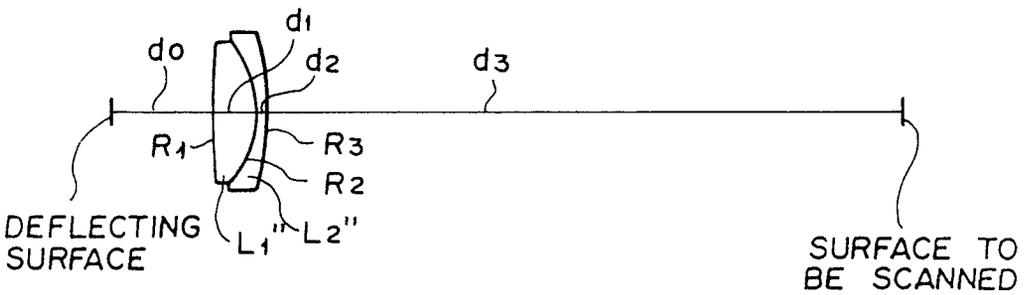


FIG.29B

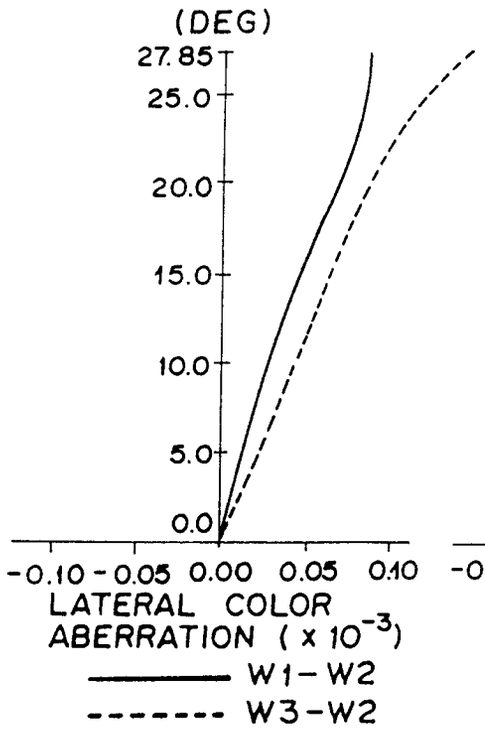


FIG.29C

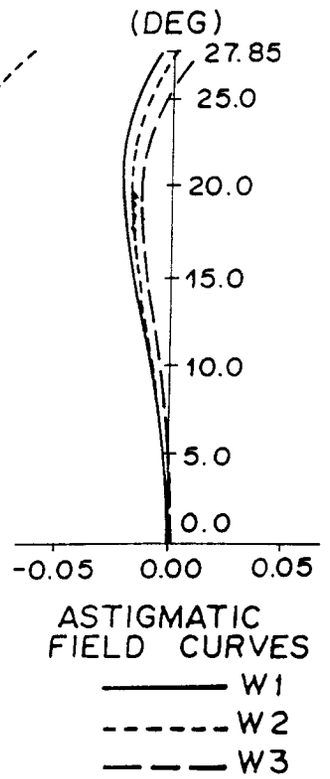


FIG.29D

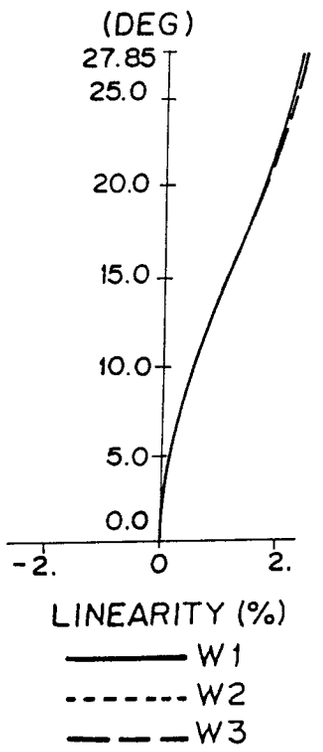


FIG.30A

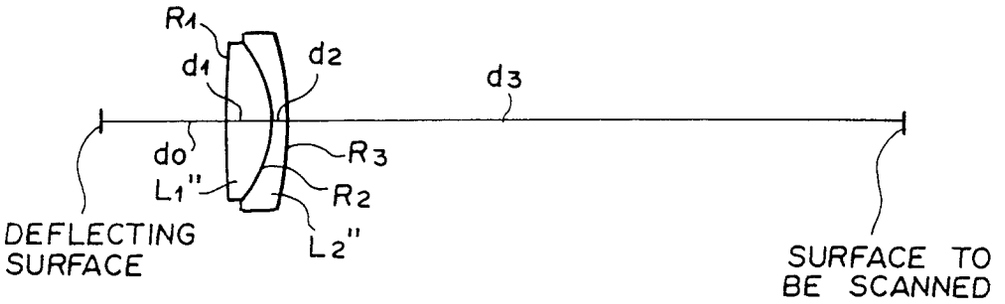


FIG.30B

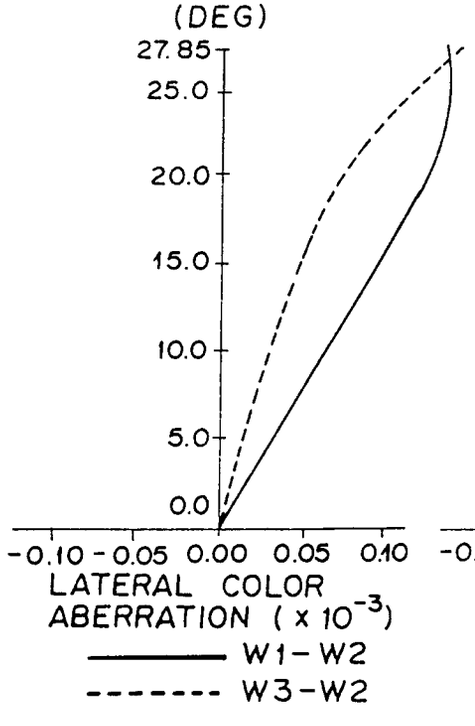


FIG.30C

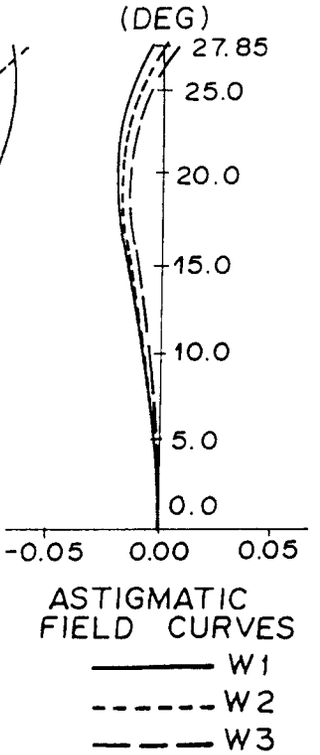


FIG.30D

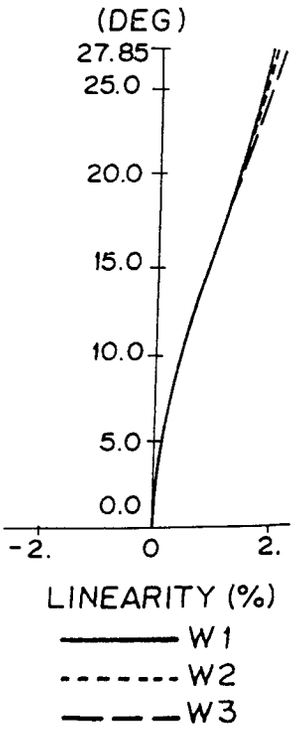


FIG.31A

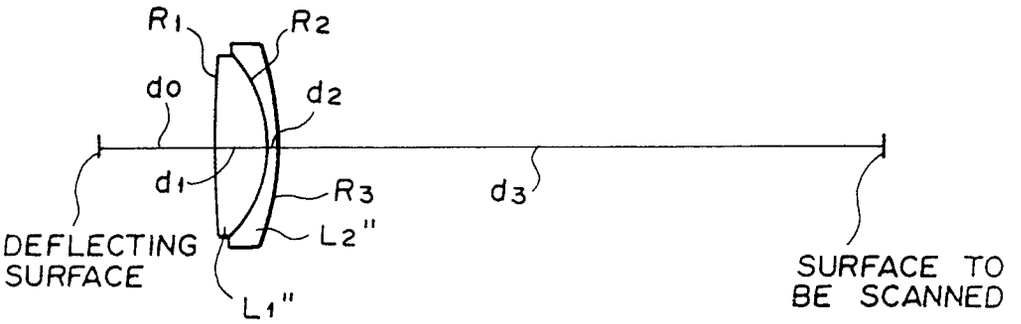


FIG.31B

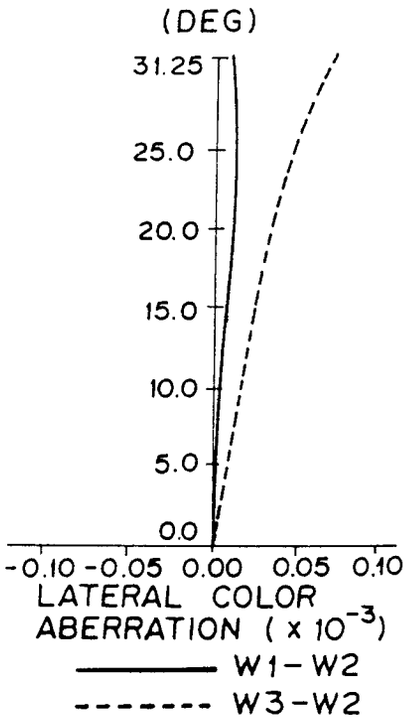


FIG.31C

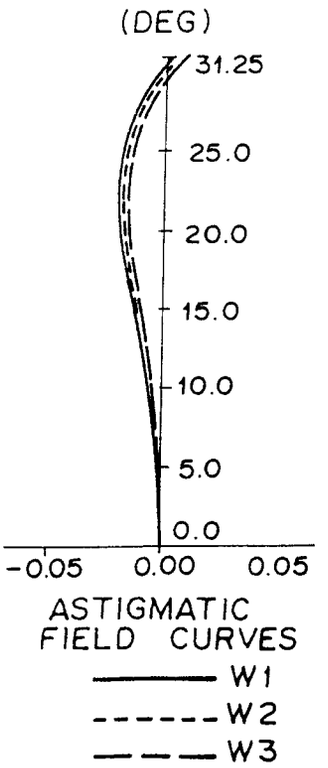


FIG.31D

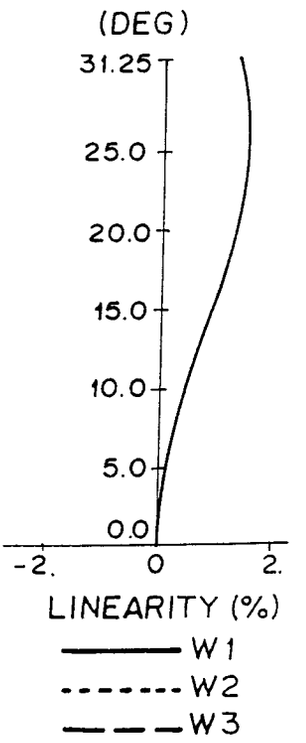


FIG.32A

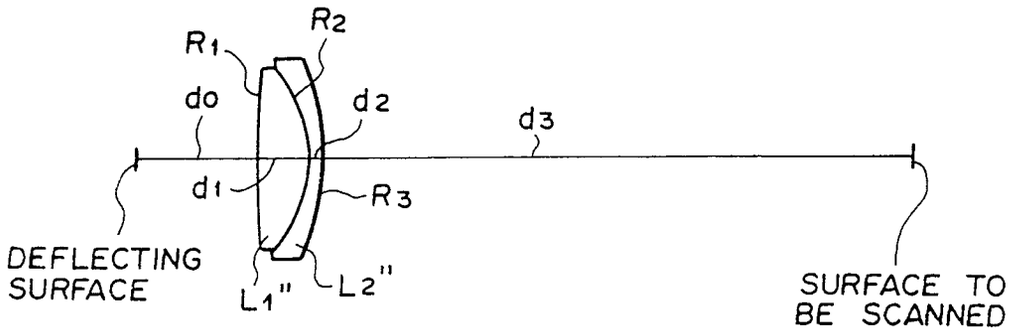


FIG.32B

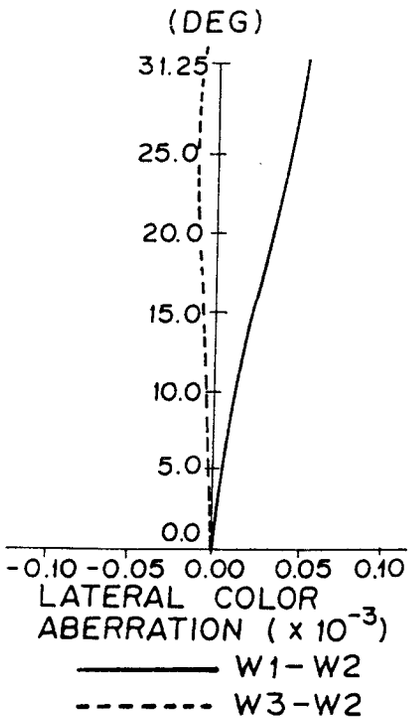


FIG.32C

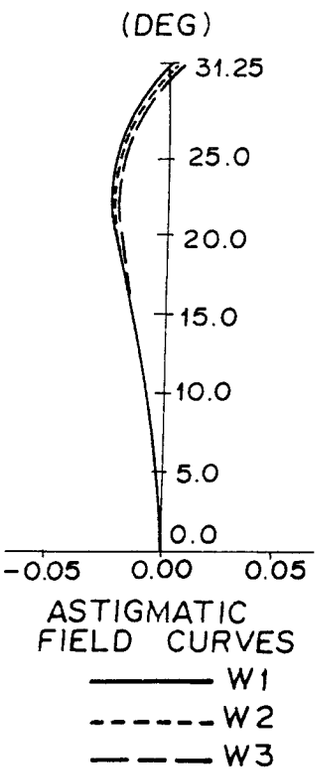


FIG.32D

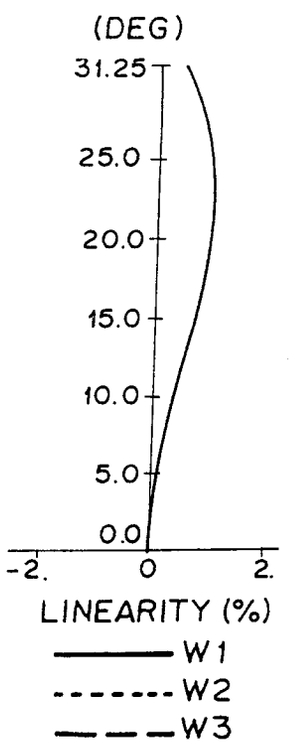


FIG.33A

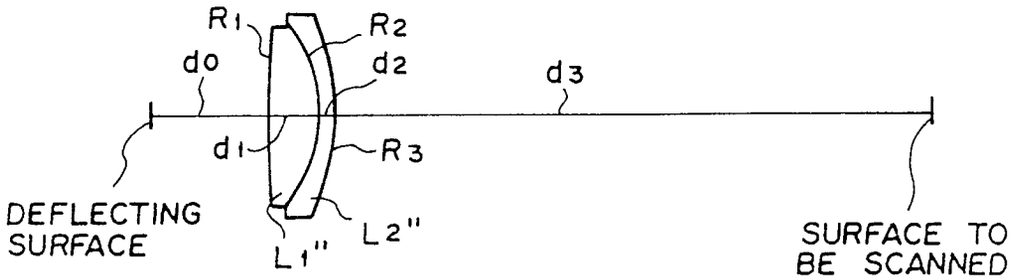


FIG.33B

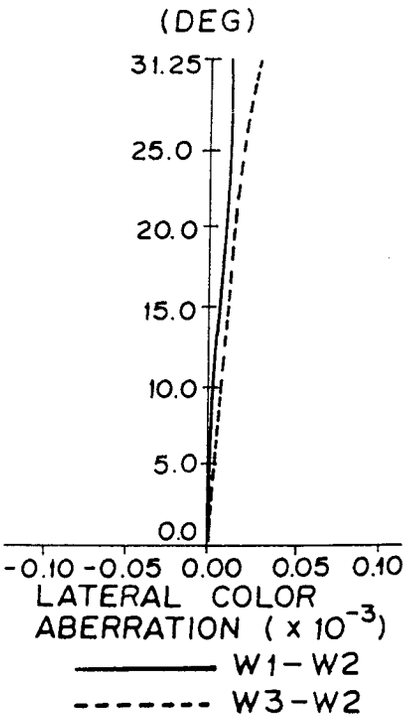


FIG.33C

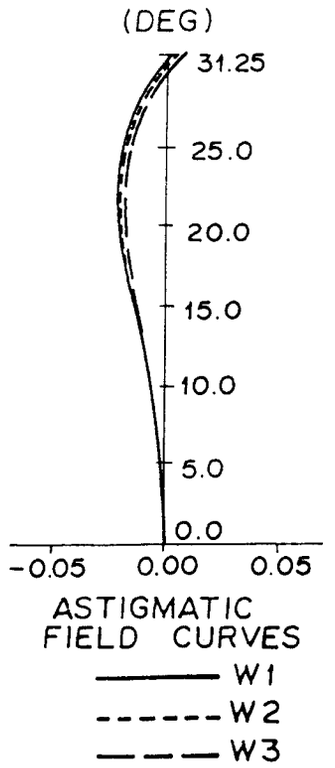


FIG.33D

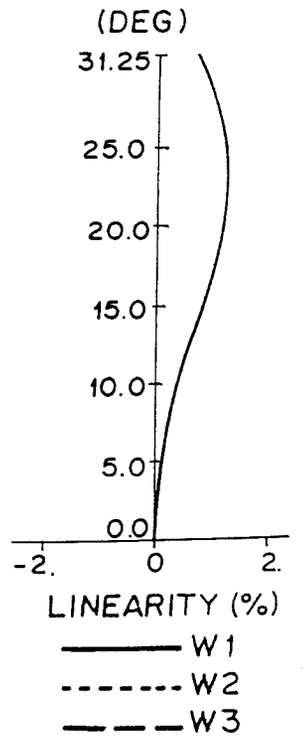


FIG.34A

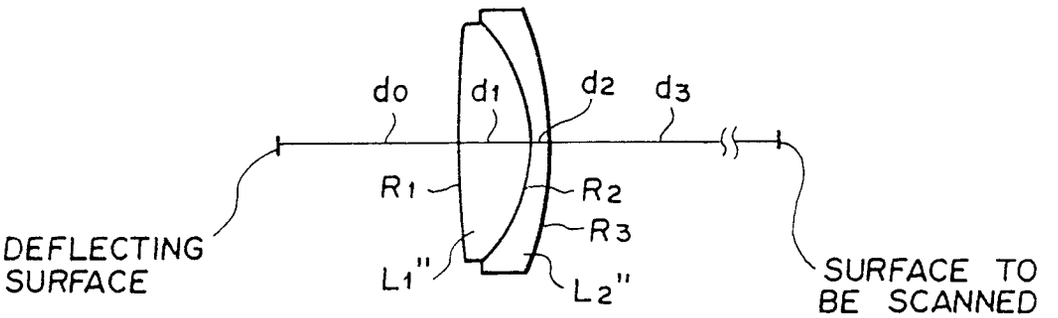


FIG.34B

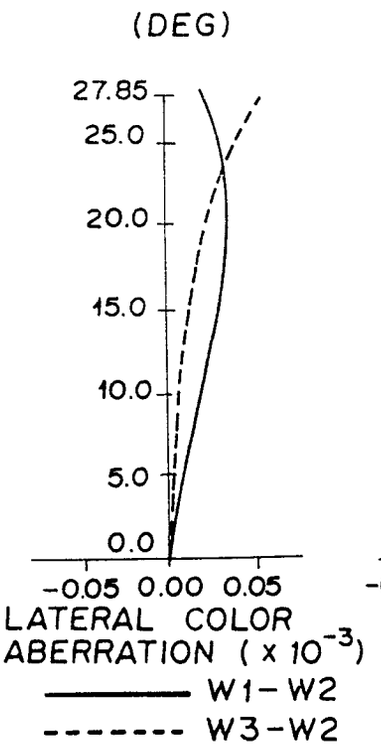


FIG.34C

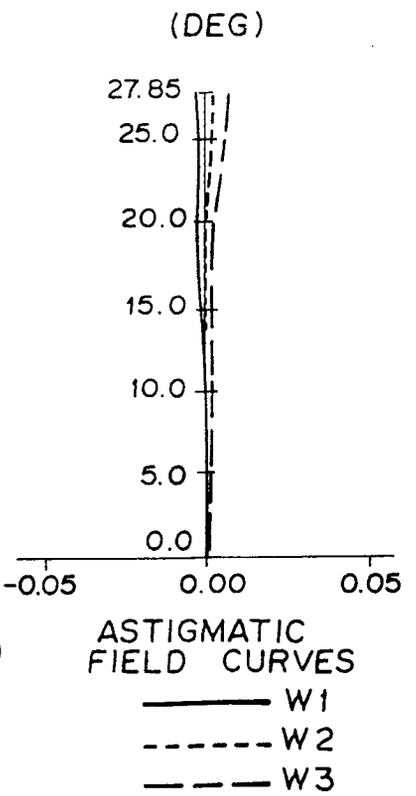


FIG.34D

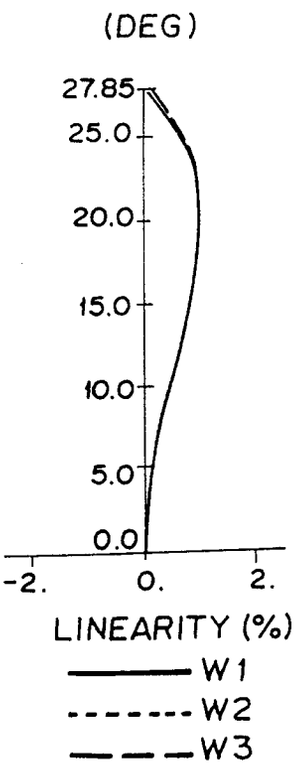


FIG.35A

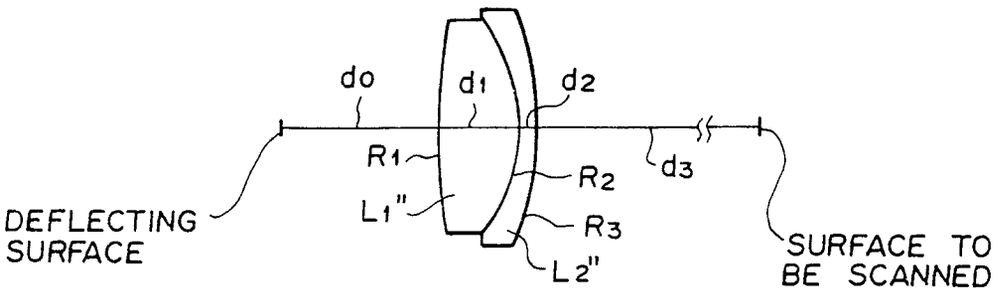


FIG.35B

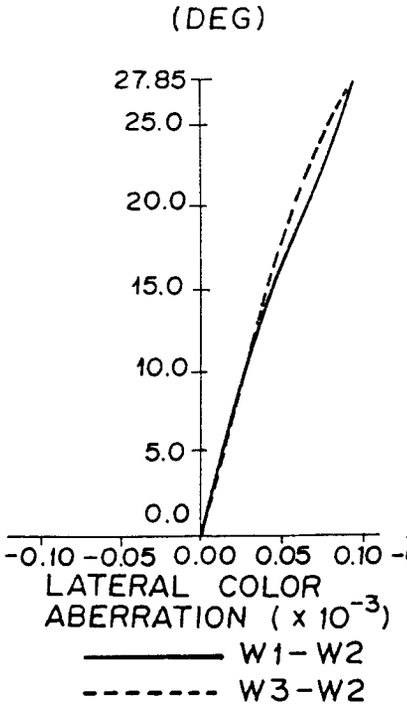


FIG.35C

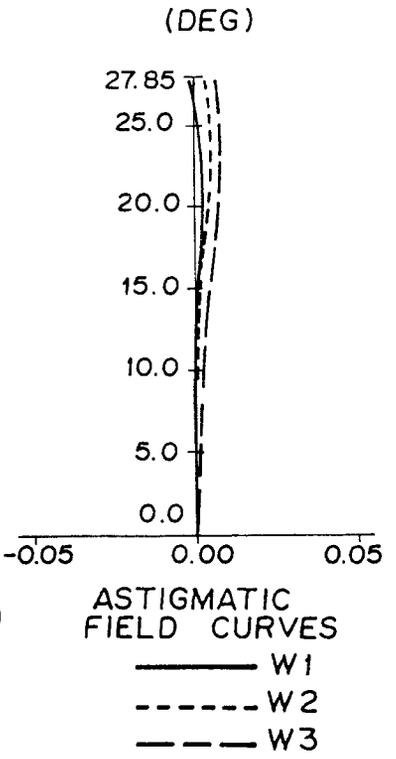


FIG.35D

